A THERMODYNAMIC ANALYSIS OF THE COMBINED STEAM TURBINE - GAS TURBINE POWER CYCLE

ROBERT GLENN MILLS

Prom. Nr. 2606

A Thermodynamic Analysis of the Combined Steam Turbine - Gas Turbine Power Cycle

THESIS

PRESENTED TO

THE SWISS FEDERAL INSTITUTE OF TECHNOLOGY, ZURICH

FOR THE DEGREE OF

DOCTOR OF TECHNICAL SCIENCES

BY

Robert Glenn Mills

Citizen of the United States of America

Accepted on the recommendation of

Prof. Dr. W. Traupel and Prof. Dr. G. Eichelberg

Zürich 1957 Hug & Söhne A. G., Zürich 4, Feldstraße 122

Contents

I. Introduction

I.1. Basic aim

Ever since the advent of the practical industrial gas turbine, engineers have been intrigued with the possibility of utilizing the large amounts of thermal energy normally wasted in the exhaust gases of the cycle. Even in the regenerative gas turbine cycle, huge quantities of combustion gases are exhausted at temperatures considerably above that of the surrounding atmosphere.

From time to time there have appeared in the literature various schemes for combining a steam cycle with the gas turbine cycle in such a manner as to utilize a sizable portion of this waste energy. The efficiencies claimed for these schemes are usually quite high in comparison with the usual gas turbine or steam cycles in use today. The published literature, however, appears to leave several questions only partially answered.

First, is there any basic thermodynamic reason why the combination steam turbine-gas turbine cycle should be superior in efficiency to either cycle taken separately?

Second, do any of the previously proposed schemes represent the optimum obtainable? The proposals are usually fairly concrete, with fixed temperatures and pressures for both the steam and gas turbine portions of the cycle. Are these combinations of temperature and pressure the best for the number and arrangement of components selected? Are there perhaps other arrangements of the same components which are more effective?

Third, can really high efficiencies actually be obtained *with a reasonable size and cost of plant*? Numerous theoretical cycles have been devised which are thermodynamically sound, but which cannot be reduced to workable machinery. Of those which are workable, some are not economically sound. For example, the Ericsson hot air engine ran well and at phenomenally high efficiency for its day; but it was so huge and expensive in comparison to its useful output that it was never of practical value.

This study is an investigation of the above questions.

I.2. Preliminary thermodynamic analysis

Let us initially consider the first question. What is the basic thermodynamic reason for the superiority (if any) of the combination steam turbine-gas turbine cycle?

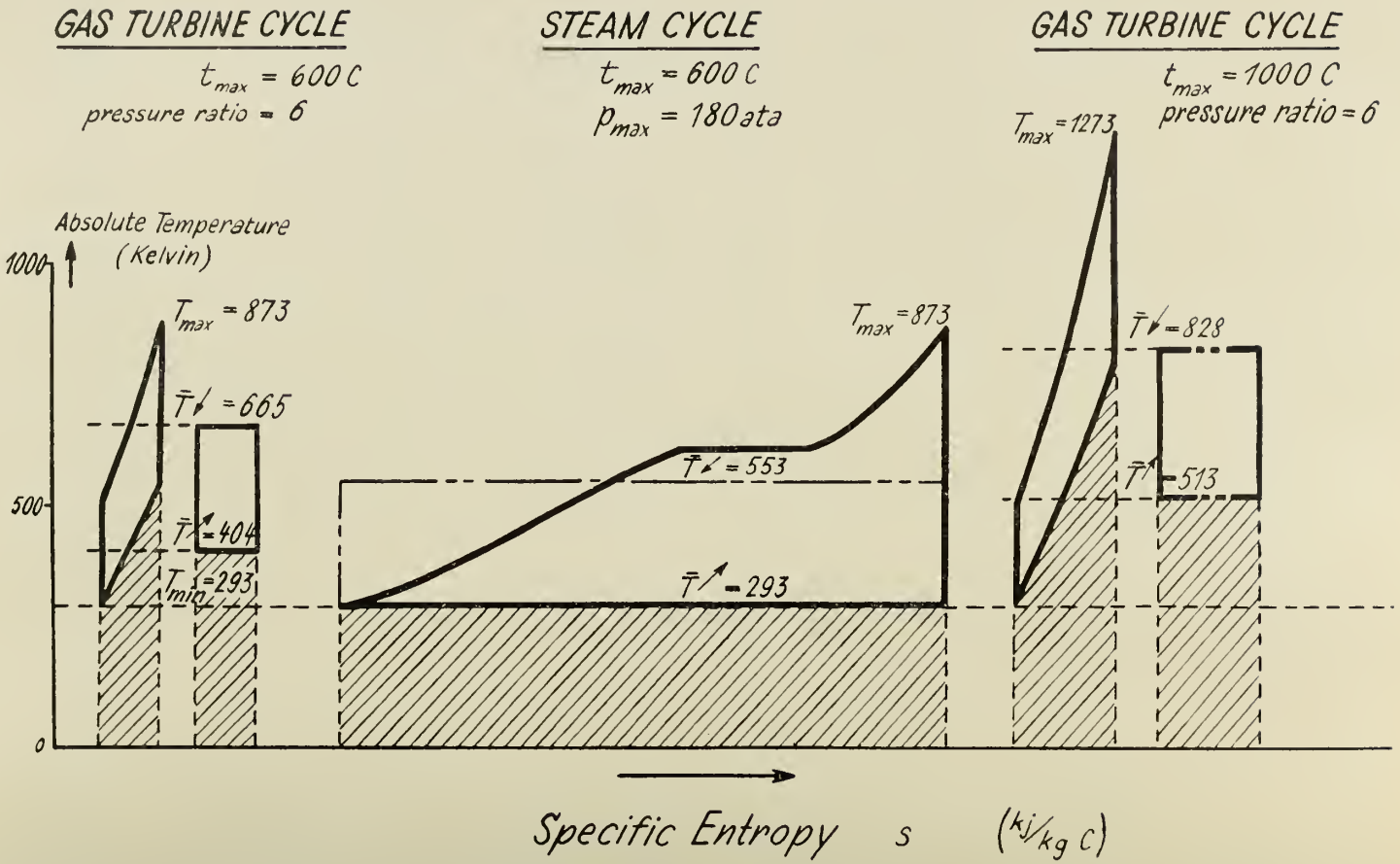

Fig. 1. Ideal gas turbine and steam cycles.

Figure 1 contains T-s representations of several ideal cycles. The first is a typical ideal gas turbine cycle — two isobars and two isentropics — operating between the limiting temperatures of 600 C and 20 C, for an assumed pressure ratio of 6. The mean temperature levels of heat supplied to and heat rejected by the cycle are also indicated. These are the effective temperatures in determining cycle efficiency. Alongside is illustrated a Carnot cycle operating between the same effective temperatures, and hence with the same efficiency (39%).

The mean temperature of heat transfer may be determined from the definition of entropy:

$$d s = \frac{d q_{rev}}{T} \tag{1.1}$$

or

$$\bar{T} = \frac{\int d q_{rev}}{\int d s} \tag{1.2}$$

where $d q_{rev}$ ≡ increment of heat reversibly transferred (kj/kg)
T ≡ absolute temperature at which the heat transfer occurs (C)
$d s$ ≡ increment of entropy (kj/kg C)

Next illustrated is a typical ideal steam (Rankine) cycle between the same temperature limits, together with its mean temperatures of heat supplied and heat rejected, and the corresponding Carnot cycle (efficiency = 47%).

The significant feature of these illustrations is that, even though the gas turbine and steam cycles operate between the same temperature limits, the average temperature at which heat is supplied to the gas turbine cycle is markedly higher than that of the steam cycle. Conversely, the mean temperature of heat rejection from the steam cycle is considerably lower than that of the gas turbine cycle.

The Carnot efficiency is

$$\eta_c \equiv \frac{T^{\swarrow} - T^{\nearrow}}{T^{\swarrow}} = 1 - \frac{T^{\nearrow}}{T^{\swarrow}}. \tag{1.3}$$

Therefore, for maximum efficiency we desire the mean temperature at which heat is supplied to be as high as possible (the gas turbine cycle), and the mean temperature at which heat is rejected to be as low as possible (steam cycle).

Herein lies the inherent advantage of the combined steam turbine-gas turbine cycle. In its simplest form, heat is supplied to the gas turbine portion of the combined cycle at a relatively high temperature level. The energy exhausted by the gas turbine is still at a high temperature level — high enough to allow it to be transferred to the steam portion of the cycle, which inherently receives heat at a low mean temperature. The heat finally rejected from the combined cycle leaves at the lowest possible temperature — that of the sink.

Another favorable feature is that in practice the upper temperature limit for the working fluid in a gas turbine is considerably above that of the steam cycle — currently about 200 C higher. Since the heat is transferred to the steam cycle through metal tube walls in the steam generator, it would appear that metallurgical considerations will severely limit development towards higher maximum temperatures for this cycle. For the gas turbine, however, blade cooling is rapidly nearing practicality, enhancing the possibility of much higher maximum cycle temperatures. This will also probably result in higher mean exhaust temperatures, as illustrated by the right hand cycles of figure 1.

If we reduce the pressure ratio of this last cycle to just under 4, we will slightly lower the mean temperature of heat supplied and raise the mean temperature at which heat is rejected. If the abcissa of the T-s diagram is changed from entropy per unit mass (s) to total entropy (S), and if we adjust the mass rates of flow so that the rate of flow in the gas turbine portion of the cycle is about $5^1/_3$ times that in the steam portion, we can represent one variation of the combined cycle as illustrated in figure 2. The mean temperature at which heat is supplied to the cycle is 792 K; and heat is rejected only at 293 K. This would indicate an ideal efficiency (for the corresponding Carnot cycle) of about 63% — considerably higher than for either cycle alone.

There is, however, an incidental loss in available energy in the transfer of energy from the gas turbine portion of the cycle to the steam portion, since the isobar of heat rejection of the former does not coincide with the isobar of heat supplied to the latter (figure 2). This transfer of heat across a finite temperature difference results in an increase in entropy, and hence in a loss in available energy. In the practical case, these isobars must have a finite separation at *all* points, since a finite temperature difference is required for heat transfer. This is the weakness of the combined cycle. If this separation can be kept small, the combined cycle is intrinsically better from an efficiency viewpoint than either of its component cycles, since it combines a high mean temperature for heat supplied to the cycle with a minimum temperature for heat rejected. If practical size and cost of heat transfer equipment require that this separation be very large, the combined cycle's inherent advantage may be nullified.

The evaluation of the cycle thus becomes one of engineering economics — of careful evaluation of all cycle losses on a practical engineering basis. To this end the following chapters are devoted.

I.3. Units and symbols

The Giorgi or meter-kilogram-second (MKS) system is undoubtedly the most convenient for this type of work, and has been used throughout the

COMBINED CYCLE

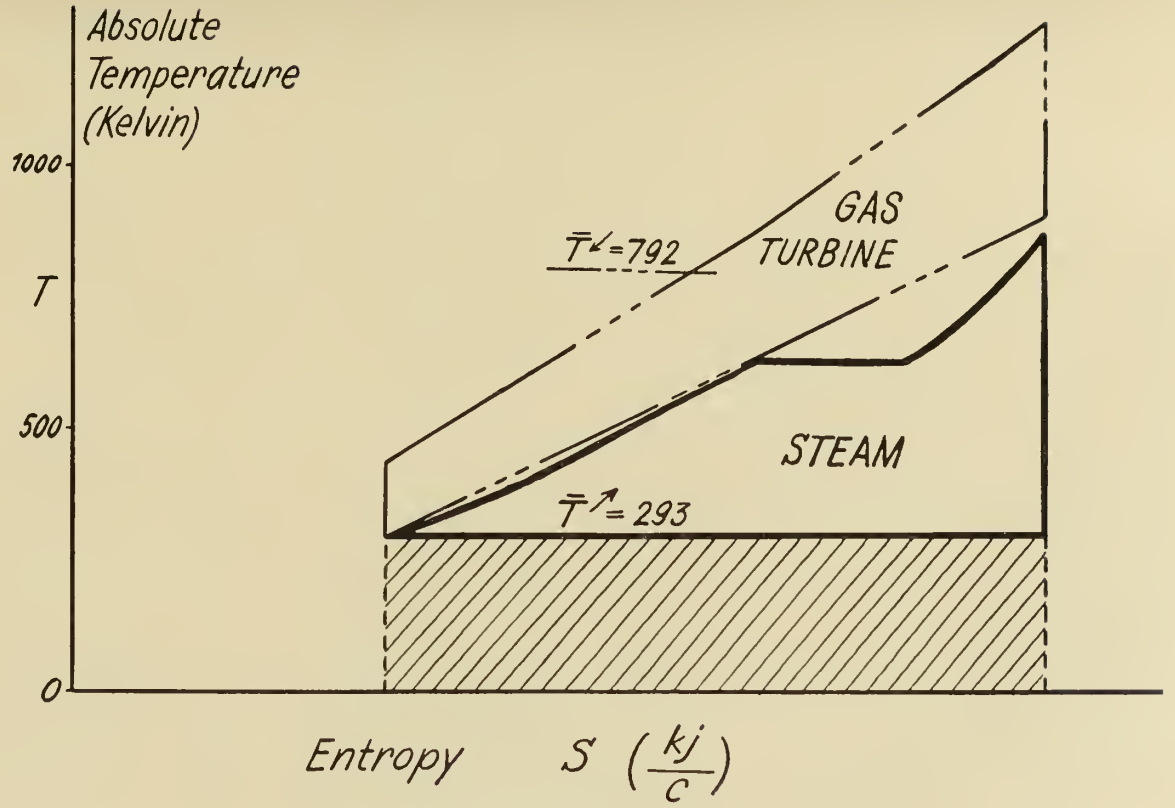

Fig. 2. Ideal combined cycle.

calculations, except where otherwise stated. The units used have been abbreviated as follows:

C	degrees Centigrade
K	degrees Centigrade absolute (Kelvin)
kg	kilogram
kj	kilojoule
KW	kilowatt (kj/sec)
m	meter
sec	second
ata	atmospheres of pressure, absolute (1 ata $= 1.013 \times 10^5$ kg/m sec^2)

The following symbols of general meaning have been used:

$=$ equals
$\equiv$ equals by definition
$\approx$ approximately equals
$\neq$ does not equal
$\sim$ proportional to

A dot over a quantity indicates the time rate of flow or change of that quantity. E. g., $\dot{m}_g$ indicates the mass rate of flow of combustion gases in kg/sec.

The mean value of a quantity is indicated by a dash over the symbol denoting that quantity. E. g., $\overline{T}$ indicates a mean absolute temperature.

Equations are numbered by chapters, and the numbers are enclosed in parentheses. E. g., (1.3) indicates the third equation of chapter I. The numbers in square brackets [ ] refer to the references listed in appendix C. All other symbols are defined as occurring. For convenience, a summary of these symbols may be found in appendix B.

II. Gas Turbine

II.1. General

For preliminary cycle calculations of a comparative nature, investigators of gas turbine or combined steam turbine-gas turbine cycles frequently assume a constant gas turbine efficiency. For more accurate calculations, intended to indicate quantitively what might be commercially obtainable in practical installations, certain refinements are necessary. Loss of working fluid through the labyrinth packings, loss of available energy due to incomplete conversion of turbomachinery exit velocity to pressure, and the influence of component pressure ratio — as expressed by the reheat factor — are examples of factors

which should be taken into consideration. More important still is the reduction in gas turbine efficiency (as opposed to overall cycle efficiency) occasioned by an increase in inlet temperature.

Early studies, on the basis of constant turbine efficiency, laid great stress on the advantages of higher turbine inlet temperatures. As the gas turbine developed, however, it became evident that practical considerations greatly limit the gains that formerly appeared so attractive. The loss of available energy occasioned by the necessity of turbine and blade cooling greatly reduces the cycle efficiency if ele vated turbine inlet temperatures are used — especially for the straight gas turbine cycle, in which this energy often cannot effectively be used elsewhere in the cycle. A higher temperature turbine also has greater expansion problems, especially if appreciable cooling is used. This necessitates larger blade clearances, with consequent deterioration of stage efficiency. The thermal expansion problems also press the turbine designer into greater use of highly loaded impulse blading, in lieu of the slightly more efficient reaction blading, to take advantage of the decrease in turbine size made possible by increasing the enthalpy drop per stage.

For this study, three separate turbine calculations are made. The simplest, for 700 C turbine inlet temperature, is based upon present day commercial practice for long life gas turbines. Hundreds of such turbines, in production by a dozen different firms, are in operation today.

For 850 C maximum temperature, a more liberal use of cooling air and a lower stage efficiency have been assumed. The results obtained by use of this turbine calculation may be considered as the upper limit of present day practice. Higher temperatures are in daily use for aircraft and small mobile or portable gas turbines, but only where efficiency or turbine life are secondary considerations. On the other hand, long life relatively high efficiency turbines with inlet temperatures in the vicinity of 800 C are now in commercial production [3]; and experimental long-life turbines with still higher temperatures are in operation.

An attempt has also been made to predict the probable results which may be obtained in the near future with a gas turbine inlet temperature of 1000 C. Many approaches to the problem of high inlet temperatures are being investigated — ceramic and ceramel blading, effusion cooling, spray cooling, and internal cooling of various types by air, water, and liquid metals — to mention a few. It appears that the internally cooled blade is the nearest to practical realization, since several actual turbines employing this solution have been built and operated at temperatures up to 1200 C. Data from these installations were used to calculate the 1000 C inlet temperature gas turbine in this study.

The turbines can be calculated by use of the properties of dry air; but it is perhaps more realistic to assume a combustion gas composition which is

near the average of the conditions encountered in the cycle calculations. Defining x as the mass ratio of "pure" (stoichiometric) combustion gas to the total combustion gas (stoichiometric combustion products plus excess air), it will be noted that x will be generally higher for the higher inlet temperature turbines. The following values of x are chosen as being near the mean of the conditions encountered in this study:

t_0	x
700 C	0.20
850 C	0.27
1000 C	0.34

Here t_0 is defined as the total gas temperature at the turbine inlet.

The gas properties are as recorded in the "*i-s* Tafel für Verbrennungsgase", developed by the Institut für Thermische Turbomaschinen, Eidgenössische Technische Hochschule, Zürich. The fuel used is 86% carbon, $12^1/_2$% hydrogen, $1^1/_2$% non-combustible components, with a lower heating value of 42,000 kj/kg. The basic data for the above table is [23].

It is emphasized, however, that the results of this work are valid within narrow limits for any type of fuel that can be burned in a gas turbine, whether it be natural gas, fuel oil, or coal. It is necessary only to correct for the efficiency of combustion (assumed to be 98% — see paragraph III.2); and in certain of the combined cycles (paragraph VIII), for the minimum value of excess air required to insure "complete" combustion.

II.2. Gas Turbine — Inlet Temperature 700 C

A uniform stage efficiency of 0.89 is assumed. Exit loss due to incomplete conversion of exit velocity to pressure (ζ_e) is, from experience data, taken to be 8.0 kj/kg. Mechanical losses for both compressor and gas turbine are assumed to be $1^1/_2$% of the specific internal gas turbine work (L_i), in units of kj/kg.

Let:

L_N ≡ net turbine shaft work (kj/kg)
m_a ≡ mass of air flowing through the gas turbine cycle (kg)
m_f ≡ mass of fuel (kg)
m_g ≡ mass of combustion gases flowing through the turbine (kg)
β ≡ loss of working fluid through labyrinth packing, expressed as percentage of m_g (dimensionless)
η_m ≡ mechanical efficiency (dimensionless)
Δi_T ≡ actual enthalpy drop in the turbine (kj/kg)

The turbine internal work (in kj) is

$$m_g(\Delta i_T - \zeta_e) \tag{2.1}$$

or, per kilogram air:

$$L_i = \frac{m_g}{m_a}(\Delta i_T - \zeta_e) \tag{2.2}$$

$$m_g = (m_a + m_f)(1-\beta) \tag{2.3}$$

$$L_i = \left(1 + \frac{m_f}{m_a}\right)(1-\beta)(\Delta i_T - \zeta_e) \tag{2.4}$$

In actual turbines, one finds that the packing losses can be held to a figure that approximates the additional mass added to the air stream by the burning of fuel. Equation (2.4) thus becomes

$$L_i = (\Delta i_T - \zeta_e) \tag{2.5}$$

and

$$L_N = \eta_m L_i \tag{2.6}$$

Let:

$\bar{c}_p$	$\equiv$	mean specific heat at constant pressure (kj/kg C)
p	$\equiv$	absolute pressure (kg/m sec^2)
R	$\equiv$	gas constant (m^2/sec^2 C)
T	$\equiv$	absolute temperature (C)
v	$\equiv$	specific volume (m^3/kg)
$(\Delta i_T)_s$	$\equiv$	isentropic turbine enthalpy drop (kj/kg)
η_i	$\equiv$	turbine internal efficiency (dimensionless)
η_p	$\equiv$	polytropic efficiency (dimensionless)
η_{st}	$\equiv$	efficiency of turbine stage (dimensionless)
κ	$\equiv$	isentropic exponent (dimensionless)
Π	$\equiv$	turbine pressure ratio (dimensionless)
Π_{st}	$\equiv$	stage pressure ratio (dimensionless)
$1+\rho$	$\equiv$	reheat factor (dimensionless)
Ψ_e	$\equiv$	$\left[1 - \left(\frac{1}{\Pi}\right)^{\frac{\kappa-1}{\kappa}}\right]$ (dimensionless)

Subscripts:

$_0$ refers to initial condition
$_e$ refers to condition at turbine exit
$_s$ refers to condition after isentropic expansion

From the definition of turbine internal efficiency:

$$\Delta i_T = \eta_i (\Delta i_T)_s \tag{2.7}$$

and from the definition of the mean specific heat at constant pressure:

$$(\Delta i_T)_s = \bar{c}_p (T_0 - T_s) = \bar{c}_p T_0 \left[1 - \frac{T_s}{T_0}\right] \tag{2.8}$$

The errors involved in treating the turbine gases as a perfect gas are insignificant, provided care is taken always to evaluate $\bar{c}_p$ and $\bar{\kappa}$ at the same

temperature. From the relationships $pv = RT$ and $pv^{\kappa} = \text{constant}$, for an isentropic expansion one derives

$$\frac{T_s}{T_0} = \left(\frac{p_e}{p_0}\right)^{\frac{\kappa-1}{\kappa}} \tag{2.9}$$

and

$$(\Delta i_T)_s = \bar{c}_p T_0 \left[1 - \left(\frac{p_e}{p_0}\right)^{\frac{\kappa-1}{\kappa}}\right] = \bar{c}_p T_0 \Psi_e \tag{2.10}$$

The curves of $\Psi_e = f(\Pi, \kappa)$ furnished in [47] were used to calculate $(\Delta i_T)_s$

By the definition of the reheat factor:

$$\eta_t = \eta_{st}(1+\rho) = \eta_p (1+\rho)_{\infty,\Pi}$$

As derived in appendix A:

$$(1+\rho) = \frac{(1+\rho)_{\infty,\Pi}}{(1+\rho)_{\infty,\Pi_{st}}} \tag{a.59}$$

whence

$$\eta_p = \frac{\eta_{st}}{(1+\rho)_{\infty,\Pi_{st}}} \tag{2.11}$$

where $(1+\rho)_{\infty,\Pi}$ is the reheat factor for a turbine with essentially an infinite number of stages, operating through a total pressure ratio Π. $(1+\rho)_{\infty,\Pi_{st}}$ is the same for a total pressure ratio of Π_{st}. For an uncooled turbine:

$$(1+\rho)_{\infty,\Pi} = \frac{1}{\eta_p}\left[\frac{1-\left(\frac{1}{\Pi}\right)^{\frac{n-1}{n}}}{1-\left(\frac{1}{\Pi}\right)^{\frac{\kappa-1}{\kappa}}}\right] \tag{a.45}$$

and $(1+\rho)_{\infty,\Pi_{st}}$ is calculated from the same formula substituting Π_{st} for Π. (See appendix A.)

The stage pressure ratio is estimated by use of a wheel speed $u \approx 200$ m/s, and a turbine velocity ratio

$$\nu \equiv \frac{u}{\sqrt{2\Delta i_s}} = 0.65 \tag{2.12}$$

II.3. Gas Turbine — Inlet Temperature 850 C

By the generous use of air for root cooling and for film cooling of the turbine discs and walls, and by the use of either air or water to cool the initial stator blading, long life gas turbines with inlet temperatures approaching 850 C are possible. There will, however, be additional losses, due to (a) by-passing of the earlier stages by some of the cooling air, the volume of which will be considerably larger than in the 700 C turbine, (b) greater leakage losses through the necessarily larger clearances, (c) use of impulse blading rather than the slightly more efficient reaction blading, and (d) other smallsacrifices

in efficiency which may be necessary to ease construction problems or save costly materials in a turbine designed for such a high inlet temperature.

Accordingly this turbine's overall thermodynamic characteristics are calculated in two parts. The first portion, from a total gas temperature of 850 C to 700 C, is assumed to have an internal efficiency of 0.86. The 850 C initial temperature is calculated as the temperature that would be obtained if the cooling air and hot gases mixed thoroughly before entering the turbine. Thus the main gas stream leaving the combustion chamber will actually be at a temperature somewhat greater than 850 C.

Since more fuel is required to attain the 850 C initial temperature, an $x = 0.27$ is assumed. For impulse blading, $\nu = 0.5$ is used. In all other respects this first portion is calculated as was the turbine for $t_0 = 700$ C.

For the second portion, from a total gas temperature of 700 C to exit, exactly the same assumptions and procedure are used as for the complete turbine with $t_0 = 700$ C; except that $x = 0.27$ is used.

II.4. Gas Turbine — Inlet Temperature 1000 C

a) *Development of basic equations for heat transferred in cooling*

Definitions (see also figure 3):

b ≡ blade chord (m)
c_n ≡ axial component of gas velocity (m/sec)
D_i, D_m, D_0 ≡ inner, mean, outer diameter of the blade rows (m)
F_b ≡ total heat transfer surface for a blade row (m^2)
F_{I} ≡ heat transfer surface of the blading proper (m^2)
F_{II} ≡ heat transfer surface of the cylindrical housing and rotor surfaces between the blade roots and blade tips (m^2)
F_{III} ≡ heat transfer surface of the cylindrical housing and rotor surfaces in the clearance space between the blade rows (m^2)
h_g ≡ mean gas side heat transfer coefficient (kj/C sec m^2)
l ≡ blade length (m)
$\dot{m}_g$ ≡ mass rate of gas flow (kg/sec)
$\dot{Q}$ ≡ heat transferred per unit time (kj/sec)
q ≡ heat transferred in cooling process, per unit mass of gas (kj/kg)
$\bar{t}_g$ ≡ mean total gas temperature (C)
$\bar{t}_w$ ≡ mean wall temperature (C)
α ≡ direction of gas velocity relative to fixed blades (^{0})
β ≡ direction of gas velocity relative to moving blades (^{0})
δ_a ≡ axial clearance between blade rows (m)
π ≡ 3.14159
τ ≡ blade pitch (m)
Y ≡ ratio of blade perimeter to blade chord (dimensionless)

Indices:

0 ≡ conditions at stage entrance
1 ≡ conditions between rotor and stator blade rows
2 ≡ conditions at rotor blading (stage) exit
′ ≡ belonging to stationary blade row (nozzles)
″ ≡ belonging to moving blade row (buckets)

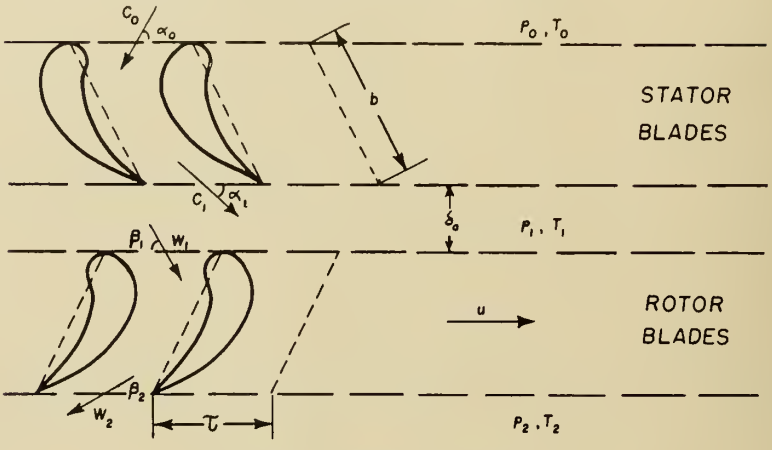

Fig. 3. Blading symbols.

For a single blade row, the heat transferred from the gas stream to the blades is

$$\dot{Q} = h_g F_b (\bar{t}_g - \bar{t}_w) \tag{2.13}$$

Here the mean gas side heat transfer coefficient (h_g) contains not only the convective heat transfer, but also any minor heat transfer by radiation from the gas stream to the metal surfaces concerned. In turn

$$F_b \equiv F_{\mathrm{I}} + F_{\mathrm{II}} + F_{\mathrm{III}} \tag{2.14}$$

We can express the surface of the blading in terms of blade length and chord by

$$\begin{aligned} F_{\mathrm{I}} &= \text{constant} \times b \times l \times \text{number of blades} \\ &= \Upsilon b l \left(\frac{\pi D_m}{\tau} \right) \end{aligned} \tag{2.15}$$

Let us now consider the outer and inner boundaries of the passage between two rotor blades. The inner boundary is a portion of the rotor, and the gas stream flows by this surface and past the blade surfaces with the relative velocity w. The surface between the blade tips may be either moving (if shrouding is used) or stationary. Shrouded blading is assumed, and the gas thus sweeps past all boundaries with the same velocity.

The shrouding also extends a certain distance into the axial clearance space both before and after the rotor blades. The heat transfer is calculated as though the shrouding extended over the entire axial clearance space following the blade row, and did not extend at all into the clearance space preceding the row. This simplifying assumption should have negligible effect on the accuracy of the calculation of the total heat transferred in the cooling process. Similarly, all boundary surfaces of the stator blading and of the following axial clearance space are assumed to be stationary.

These assumptions have been made to keep the calculations from becoming unnecessarily complicated. It is to be noted that the ratio $F_{\mathrm{I}}:F_{\mathrm{II}}:F_{\mathrm{III}}$ would be approximately the same as if no shrouding were used; and that, in the mean, approximately the same total areas would be swept by gases at approximately the same temperatures and velocities. Therefore, any inaccuracies introduced by these simplifying assumptions are considered smaller than the inaccuracies of the basic heat transfer data.

By laying out representative blade profiles, one can see that the area F_{II} for the section of the stator row through D_m can be approximated by multiplying the blade perimeter by $\frac{\tau \sin \alpha_1}{2}$ (see, e. g., figure 3). The sum of the areas of the inner and outer boundary surfaces will be approximately twice that of the area F_{II} at a section through D_m, or

$$F_{\mathrm{II}} = (\Upsilon b \tau \sin \alpha_1)\left(\frac{\pi D_m}{\tau}\right) \tag{2.16}$$

(For the rotor blading, $\sin \beta_2$ is to be substituted for $\sin \alpha_1$.)

The bounding cylindrical surfaces in the clearance spaces following each blade row will be approximated by

$$F_{\mathrm{III}} = \pi \delta_a (D_a + D_i) = 2\pi \delta_a D_m \tag{2.17}$$

Finally

$$F_b = F_{\mathrm{I}} + F_{\mathrm{II}} + F_{\mathrm{III}} = \pi D_m l \left[\Upsilon\left(\frac{b}{\tau} + \frac{b}{l}\sin \alpha_1\right) + 2\frac{\delta_a}{l}\right] \tag{2.18}$$

The flow rate of the combustion gases, in kg/sec, is

$$\dot{m}_g = \frac{\pi D_m l c_n}{v} \tag{2.19}$$

Combining (2.13), (2.18), and (2.19) to obtain the heat transferred per kilogram of working fluid:

$$q = \frac{\dot{Q}}{\dot{m}_g} = \frac{h_g F_b (\bar{t}_g - \bar{t}_w)}{\pi D_m l (c_n/v)} = \frac{v}{c_n}\left[\Upsilon\left(\frac{b}{\tau} + \frac{b}{l}\sin \alpha_1\right) + 2\frac{\delta_a}{l}\right] h_g (\bar{t}_g - \bar{t}_w) \tag{2.20}$$

The expression in square brackets is dependent only on the geometry of the turbine and blading. Later expressions can be simplified by setting

$$\Omega \equiv \left[Y \left(\frac{b}{\tau} + \frac{b}{l} \sin \alpha_1 \right) + 2 \frac{\delta_a}{l} \right] \tag{2.21}$$

whereupon (2.20) becomes

$$q = \frac{v}{c_n} \Omega h_g (\bar{t}_g - \bar{t}_w) \tag{2.22}$$

The mean gas side heat transfer coefficient for the surfaces concerned must be experimentally determined. It is generally expressed in the literature in terms of the dimensionless Nusselt number (Nu). Nu is known to be a function of the Reynolds number (Re), and is generally approximately proportional to the cube root of the Prandtl number (Pr) [8], [28].

In contrast to the effect of Prandtl number, no single-valued relationship between Nu and Re, valid for all turbines and cascades, appears to have yet been established. The location of the transition point from laminar to turbulent flow appears to be particularly important. With like Reynolds number, this transition will vary with different profiles; and will be affected by the amount of turbulence before the blading, by deviation of gas flow from the optimum angle of attack, and by other conditions in the turbine or cascade.

If the boundary layer is fully laminar, $\mathrm{Nu} \sim \mathrm{Re}^{0.5}$. If it is fully turbulent, $\mathrm{Nu} \sim \mathrm{Re}^{0.8}$ [33]. Experimentally measured values on actual blading lie somewhere between the above. Since the flow in a turbine is usually somewhat more turbulent than in a wind tunnel cascade, the turbines generally show a markedly higher Nusselt number.

On the basis of cascade measurements, it might also appear that impulse blading has a higher Nu than has reaction blading for the same Reynolds number. Nevertheless, some reaction bladings have a higher heat transfer coefficient than some impulse bladings. Further, since the published results are as yet rather meager, no definite conclusions in this respect appear advisable.

Therefore, for either impulse or reaction blading, the following relationship has been selected for use in estimating the heat transferred in cooling the high temperature gas turbine:

$$\mathrm{Nu} = 0.113\, \mathrm{Re}^{0.7}\, \mathrm{Pr}^{1/3} \tag{2.23}$$

or for Pr constant at 0.7:

$$\mathrm{Nu} = 0.1\, \mathrm{Re}^{0.7} \tag{2.24}$$

This relationship is well within the region of the various published results correlated by Smith [42], [43], and Ellerbrock [8]. In addition, it is approximately that of the almost identical results reported on independent investigations of actual turbines by the U. S. National Advisory Committee on Aeronautics [8], and by the British National Gas Turbine Establishment [33].

Actually, for a purely thermodynamic investigation of the combined steam turbine-gas turbine cycle, the exact determination of the cooling heat trans-

ferred is not nearly so important as for the gas turbine cycle alone. In the straight gas turbine cycle, wherein it is frequently impractical to utilize the heat of cooling elsewhere in the cycle, this energy may be lost. In the combined cycle a significant percentage of the available energy of the cooling heat is converted to useful work in the steam portion of the cycle. Thus any errors in calculating the cooling heat have much reduced effect on the calculated overall efficiency.

In calculating Nu, Re and Pr, an attempt must be made to select a characteristic length l and to so evaluate the gas properties and measure the relative velocity that the resulting values best correlate with the experimental data. It is interesting to note that although Smith [42], [43], Ellerbrock [8], and Ainley [33] have each made different selections in this regard, the resulting relationships between Nu and Re are not much different. Therefore, the definitions of Ainley [33] are used:

$$\mathrm{Nu} = \frac{h_g b}{\lambda} \tag{2.25}$$

For the stator blading:

$$\mathrm{Re} \equiv \frac{b c_1 \gamma}{\mu} = \frac{b c_1}{\mu v} = \frac{b c_n}{\mu v \sin \alpha_1} \tag{2.26}$$

(since, from figure 3, $c_n = c_1 \sin \alpha_1 = w_2 \sin \beta_2$)

Similarly for the rotor blading,

$$\mathrm{Re} \equiv \frac{b w_2}{\mu v} = \frac{b c_n}{\mu v \sin \beta_2} \tag{2.27}$$

$$\mathrm{Pr} \equiv \frac{c_p \mu}{\lambda} \tag{2.28}$$

Symbols in the above, not previously defined:

c_1 ≡ exit velocity from nozzle (stationary) blading (m/sec)
w_2 ≡ relative exit velocity from buckets (moving blading) (m/sec)
γ ≡ density (kg/m^3)
λ ≡ thermal conductivity (kj/m C sec)
μ ≡ viscosity (kg/m sec)

The gas properties λ and μ are to be evaluated at the average wall temperature ($\bar{t}_w$). The density (or specific volume) is to be evaluated at the mean of the blading entrance and exit pressures, and at the mean of the wall temperature and the total temperature of the gas stream.

Since the heat transfer takes place through the boundary layer, the gas temperature (t_g) to be used in the calculations should be that sensed by the outer surface of the boundary layer. Since the boundary layer is practically at rest (in relationship to the blade wall) this will be in the neighborhood of

the total temperature — i. e., the temperature existing after the kinetic energy of the gas stream has been fully converted to thermal energy. The proper gas temperature may be approximated [47] for an "uncooled" turbine by

$$t_g = t + \sqrt{\mathrm{Pr}}\,\frac{w^2}{2\,c_p} \tag{2.29}$$

where $t \equiv$ mean temperature of the gas stream without correction for gas velocity

In correlating the experimental data from the high temperature cooled turbine [33], it was found that negligible error was introduced by utilizing the local total temperature $\left(t + \frac{w^2}{2\,c_p} \equiv t^*\right)$ at each point on the blade surface, and this procedure has been followed in these calculations. Thus the arithmetic mean total temperature for the stator blading is

$$\bar{t}_g{}' = \frac{t_0{}^* + t_1{}^*}{2} = \frac{t_0{}^* + (t_0{}^* - q'/c_p)}{2} = t_0{}^* - \frac{q'}{2\,c_p} \tag{2.30}$$

similarly

$$\bar{t}_g{}'' = t_1{}^* - \frac{q''}{2\,c_p} \tag{2.31}$$

Combining (2.25) with (2.22):

$$q = \frac{v\,\lambda}{c_n\,b}\,\Omega\,(\bar{t}_g - \bar{t}_w)\,\mathrm{Nu} \tag{2.32}$$

and introducing the chosen Nu-Re relationship (2.24):

$$q = 0.1\,\frac{v\,\lambda}{c_n\,b}\,\Omega\,(\bar{t}_g - \bar{t}_w)\,\mathrm{Re}^{0.7} \tag{2.33}$$

Substituting the definition of Re, (2.26) or (2.27), and Ω (2.21):

$$q = 0.1\,\frac{\lambda}{(\mu \sin \alpha_1)^{0.7}}\left(\frac{v}{b\,c_n}\right)^{0.3}\left[Y\left(\frac{b}{\tau} + \frac{b}{l}\sin\alpha_1\right) + 2\,\frac{\delta_a}{l}\right](\bar{t}_g - \bar{t}_w) \tag{2.34}$$

(As previously, in this and in the following heat transfer equations, for the rotor blading $\sin\beta_2$ is to be substituted for $\sin\alpha_1$.)

b) *Dimensionless representations of heat transfer*

In equation (2.34), all the normally independently variable design parameters are explicitly represented. It is also of interest, however, to transform the heat transfer equation to enable direct determination of the influence of variation of certain commonly used dimensionless parameters.

Multiplying (2.33) by $\frac{b\,c_n\,\bar{c}_p}{v\,\lambda\sin\alpha_1}$,

dividing by the identical expression Re × Pr, and setting Pr ≈ 0.7 as before:

$$q = 0.143 \frac{\Omega}{\sin \alpha_1} \frac{\bar{c}_p (\bar{t}_g - \bar{t}_w)}{\mathrm{Re}^{0.3}} \tag{2.35}$$

The cooling factor (ξ) is defined by

$$\xi \equiv \frac{q}{\Delta i_s}, \tag{2.36}$$

where $\Delta i_s \equiv$ isentropic enthalpy drop for the stage or the blade row under consideration (kj/kg). ξ_p is similarly defined as the cooling factor for an infinitesimal stage.

Following the reasoning leading to equation (2.10), for the nozzle blading:

$$\Delta i_s' = \bar{c}_p T_0 \left[1 - \left(\frac{p_1}{p_0} \right)^{\frac{\kappa-1}{\kappa}} \right] \tag{2.37}$$

and

$$\xi' = \frac{0.143 \Omega}{(\mathrm{Re}')^{0.3} \sin \alpha_1} \frac{(\bar{t}_g' - \bar{t}_w')}{T_0 \left[1 - \left(\frac{p_1}{p_0} \right)^{\frac{\kappa-1}{\kappa}} \right]} \tag{2.38}$$

similarly for the buckets:

$$\xi'' = \frac{0.143 \Omega}{(\mathrm{Re}'')^{0.3} \sin \beta_2} \frac{(\bar{t}_g'' - \bar{t}_w'')}{T_1 \left[1 - \left(\frac{p_2}{p_1} \right)^{\frac{\kappa-1}{\kappa}} \right]} \tag{2.39}$$

If, in the argument leading to equations (2.9) and (2.10), instead of the previously assumed isentropic expansion we substitute the polytropic expansion represented by $p v^n =$ constant, we arrive at

$$\Delta i' = \bar{c}_p T_0 \left[1 - \left(\frac{p_1}{p_0} \right)^{\frac{n-1}{n}} \right] \tag{2.40}$$

As developed in appendix A, the reciprocal of equation (a. 28), for the cooled turbine stage:

$$\frac{n-1}{n} = (\eta_p + \xi_p) \left(\frac{\kappa - 1}{\kappa} \right) \tag{2.41}$$

Or for the nozzle blading alone:

$$\left(\frac{n-1}{n} \right)' = (\eta_p' + \xi_p') \left(\frac{\kappa - 1}{\kappa} \right), \tag{2.42}$$

where the polytropic efficiency for the blading (η_p') is defined as for the uncooled turbine. The entire isentropic enthalpy drop is the algebraic sum of the increase in kinetic energy of the gas molecules $\left(\frac{c_1^2 - c_0^2}{2} \right)$, heat transferred in cooling (q'), and energy dissipated by friction.

Denoting the gas velocities entering and leaving the stator blading by c_0 and c_1 respectively, the useful energy is the increase of kinetic energy of the gas stream:

$$\frac{c_1^2 - c_0^2}{2} = \eta_s' \Delta i_s' \tag{2.43}$$

The friction energy is

$$p'_f = (1 - \eta_s') \Delta i_s' \tag{2.44}$$

And the cooling heat is

$$q' = \xi' \Delta i_s' \tag{2.36}$$

The mean blade speed (u) may be dimensionlessly expressed by the Crocco number.

$$\mathrm{Cr}' \equiv \frac{u}{\sqrt{2 c_p T_0}} \tag{2.45}$$

$$\mathrm{Cr}'' \equiv \frac{u}{\sqrt{2 c_p T_1}} \tag{2.46}$$

whence

$$(\mathrm{Cr}'')^2 = (\mathrm{Cr}')^2 \frac{T_0}{T_1} = (\mathrm{Cr}')^2 \Pi^{\frac{\kappa-1}{\kappa}(\eta_p' + \xi_p')} \tag{2.47}$$

From the foregoing equations we can express the enthalpy drop in the stator dimensionlessly by

$$\frac{\Delta i'}{u^2/2} = \frac{1}{(\mathrm{Cr}')^2} \left[1 - \left(\frac{p_1}{p_0} \right)^{\frac{\kappa-1}{\kappa}(\eta_p' + \xi_p')} \right] \tag{2.48}$$

with a similar expression for $\frac{\Delta i''}{u^2/2}$.

It is sometimes desired to express the heat of cooling (q) dimensionlessly in terms of wheel speed (u) rather than the isentropic enthalpy drop (Δi_s). In this case, from the definition of ξ (2.36):

$$\frac{q}{u^2/2} = \frac{\Delta i_s}{u^2/2} \xi \tag{2.49}$$

The work (L) of the stage is equal to the mean rotor blade peripheral velocity (u), multiplied by the change in the peripheral component of the absolute velocities entering and leaving the moving blades. Denoting the peripheral components by the subscript u, and the absolute velocities entering and leaving the rotor blades by c_1 and c_2,

$$L = u (c_{u_1} - c_{u_2}) \tag{2.50}$$

Expressing the velocities in a dimensionless form by deviding by u

$$\left(\text{e. g., } C_1 \equiv \frac{c_1}{u} \right), \text{ we have}$$

$$L = u^2 (C_{u_1} - C_{u_2}) \tag{2.51}$$

or, defining: $(C_{u_1} - C_{u_2}) \equiv \Delta C_u$

$$L = 2(\Delta C_u)\frac{u^2}{2} \tag{2.52}$$

Also, by definition, $$L \equiv \eta_{st} \Delta i_s \tag{2.53}$$

Combining: $$\eta_{st} \Delta i_s = 2 \Delta C_u \frac{u^2}{2} \tag{2.54}$$

Or, as long as η_{st} and the velocity triangle remain unchanged

$$\frac{\Delta i_s}{u^2/2} = \frac{2 \Delta C_u}{\eta_{st}} = \text{constant} \tag{2.55}$$

whence, from (2.49), $$\frac{q}{u^2/2} = \xi \times \text{constant} \tag{2.56}$$

Similar reasoning holds for q' and q'' in relation to ξ' and ξ'', as calculated by equations (2.38) and (2.39).

If desired, we can express ξ $\left(\text{and hence } \frac{q}{u^2/2}\right)$ directly in terms of the Crocco number. From equations (2.37) and (2.43):

$$\Delta i_s' = c_p T_0 \left[1 - \left(\frac{p_1}{p_0}\right)^{\frac{\kappa-1}{\kappa}}\right] = \frac{c_1^2 - c_0^2}{2 \eta_s'} \tag{2.57}$$

Substituting (2.45), and $C_0 \equiv \frac{c_0}{u}$ and $C_1 \equiv \frac{c_1}{u}$

$$\frac{u^2/2}{(\mathrm{Cr}')^2}\left[1 - \left(\frac{p_1}{p_0}\right)^{\frac{\kappa-1}{\kappa}}\right] = \frac{u^2/2\,(C_1^2 - C_0^2)}{\eta_s'} \tag{2.58}$$

or $$\left[1 - \left(\frac{p_1}{p_0}\right)^{\frac{\kappa-1}{\kappa}}\right] = \frac{(\mathrm{Cr}')^2 (C_1^2 - C_0^2)}{\eta_s'} \tag{2.59}$$

Substituting in (2.38):

$$\xi' = \frac{0.143 \Omega \eta_s' (\bar{t}_g' - \bar{t}_w')}{(\mathrm{Re}')^{0.3} (\mathrm{Cr}')^2 (C_1^2 - C_0^2) T_0 \sin \alpha_1} \tag{2.60}$$

Similarly

$$\xi'' = \frac{0.143 \Omega \eta_s'' (\bar{t}_g'' - \bar{t}_w'')}{(\mathrm{Re}'')^{0.3} (\mathrm{Cr}'')^2 (W_2^2 - W_1^2) T_1 \sin \beta_2} \tag{2.61}$$

To evaluate the above equations numerically, certain assumptions must be made as to turbine size and geometry — particularly as regards the velocity triangle.

Let:

r_k ≡ kinematic reaction ≡ $\frac{\Delta i''}{\Delta i' + \Delta i''}$ (dimensionless)

C_n ≡ axial component of gas flow (dimensionless)

W ≡ gas velocity relative to moving blading (dimensionless)

The meanings of all symbols are made clearer by use of figure 4. The small letters denote velocities in meters/second. The capital letters denote the same velocities expressed dimensionlessly by dividing by u. For simplicity of calculation, u and the velocity triangle are assumed constant throughout the water cooled portion of the turbine; i. e., from a total gas temperature of 1000 C at inlet until the total temperature has dropped to 700 C. At this point the water-cooled turbine is terminated, and a separate "uncooled" turbine identical to that calculated in paragraph II.2 is assumed.

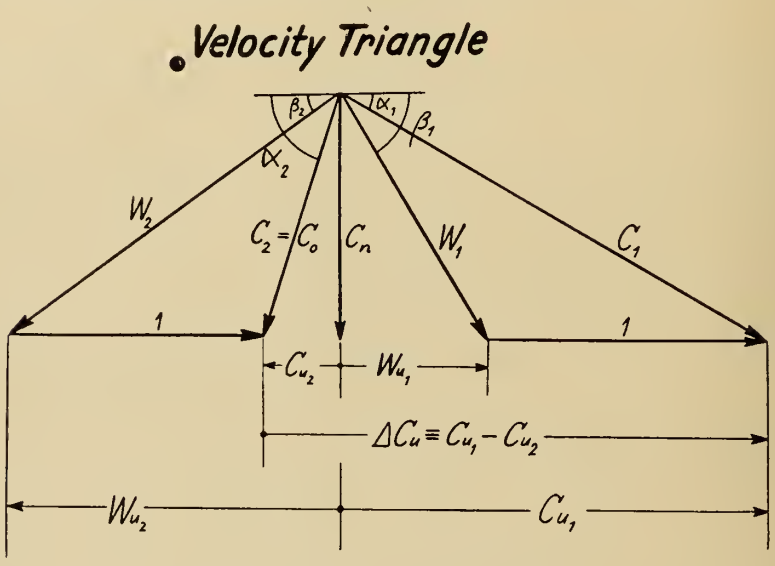

Fig. 4. Turbine velocity triangle.

For the impulse turbine the following velocity triangle is assumed:

$$r_k = 0.2; \quad \Delta C_u = 1.8; \quad C_n = 0.55$$

For the reaction turbine:

$$r_k = 0.5; \quad \Delta C_u = 1.2; \quad C_n = 0.55$$

$$r_k \equiv \frac{\Delta i''}{\Delta i' + \Delta i''} = \frac{\frac{W_2^2 - W_1^2}{2}}{\frac{C_1^2 - C_0^2}{2} + \frac{W_2^2 - W_1^2}{2}} = \frac{W_2^2 - W_1^2}{C_1^2 - C_0^2 + W_2^2 - W_1^2} = \frac{W_{u_2}^2 - W_{u_1}^2}{C_{u_1}^2 - C_{u_2}^2 + W_{u_2}^2 - W_{u_1}^2} \tag{2.62}$$

From the velocity triangle (figure 4):

$$W_{u_1} = C_{u_1} - 1 \tag{2.63}$$

$$W_{u_2} = C_{u_2} - 1 \tag{2.64}$$

Whence $$r_k = 1 - \frac{C_{u_1} + C_{u_2}}{2} \tag{2.65}$$

From the above the following are calculated:

	r_k	ΔC_u	C_n	C_{u_1}	C_1	C_{u_2}	$C_2 = C_0$	$\frac{C_1^2 - C_0^2}{2}$
Impulse	0.2	1.8	0.55	1.7	1.787	−0.1	0.559	1.440
Reaction	0.5	1.2	0.55	1.1	1.230	−0.1	0.559	0.600

	W_{u_1}	W_1	W_{u_2}	W_2	$\frac{W_2^2 - W_1^2}{2}$	α_1	$\alpha_2 = \alpha_0$
Impulse	0.7	0.890	−1.1	1.230	0.360	17° 58′	79° 42′
Reaction	0.1	0.559	−1.1	1.230	0.600	26° 34′	79° 42′

	β_1	β_2	$\sin\alpha_1$	$\sin\beta_2$	$(\sin\alpha_1)^{0.7}$	$(\sin\beta_2)^{0.7}$	$L = u^2 \Delta C_u$
Impulse	38° 9′	26° 34′	0.3078	0.4472	0.438	0.569	$1.8\,u^2$
Reaction	79° 42′	26° 34′	0.4472	0.4472	0.569	0.569	$1.2\,u^2$

Several modern thick (because of the necessity of providing adequate space for cooling holes) profiles were selected, and perimeters and chords were measured to determine typical values of Y. For a flat plate with no camber $Y = 2$; but as can be seen from the below table, even for very thick profiles with large camber, Y does not show a large variation.

For a given α_0 and α_1 (or β_1 and β_2), there exists a narrow region within which the ratio of blade length to blade pitch (b/τ) produces the lowest losses. These most favorable ratios have been determined by extensive tests; the below values are those reproduced in [47]:

	Y	b/τ
Impulse nozzles	2.5	1.42
Impulse buckets	2.67	1.56
Reaction blading	2.33	1.35

Before each blade row a certain axial clearance (δ_a) is required to allow disturbances from the preceding row to be smoothed out somewhat before impingement on the blades following. In general $\delta_a/b \approx 0.3$. $\delta_a/l = b/l \times \delta_a/b$.

Whence $$\delta_a/l = 0.3\, b/l \tag{2.66}$$

b/l in turn is arbitrarily taken equal to 0.5 for the first row of stationary blading. For succeeding rows one calculates as follows:

From continuity considerations:

$$\dot{m}_g = \frac{D_m \pi l c_n}{v} = \frac{\pi D_m l c_n p}{R T} = \text{constant} \tag{2.67}$$

throughout the turbine, neglecting the small amount of gland leakage to the outer atmosphere.

Therefore

$$\frac{\frac{D'm\,l'\,c_n'\,p'}{R'\,T'}}{\frac{D_m\,l\,c_n\,p}{R\,T}} = 1$$

If u is held constant throughout the turbine, D_m is constant and, for constant b:

$$\frac{l'}{l} = \frac{\left(\frac{b}{l}\right)}{\left(\frac{b}{l}\right)'} = \frac{\overline{p}}{\overline{p}'}\,\frac{\overline{T}'}{\overline{T}} \tag{2.68}$$

One also needs an absolute value of b, which is of course proportional to the size of the turbine. Fortunately this value enters into the heat transfer equations — (2.34), (2.35), (2.38), (2.39), (2.60) and (2.61) — only to the power 0.3. Its direct influence is thereby greatly reduced, and selection of a typical value will not too greatly impair the accuracy of the calculations as applied to other turbine sizes. $b = 50$ mm is therefore selected.

Due to the paucity of experience data, one is upon somewhat uncertain ground when it comes to assuming an average wall temperature (t_w). This will depend in great measure on the rate of heat removal from the inside of the blade. A successful cooling system will maintain a fairly even wall temperature at the highest practicable level which is consistent with metallurgical requirements.

On the basis of the data published for water cooled blading by *Smith* [42], and upon the experiences of *Schmidt* [40], [43], the average wall temperature has been taken at 500 C for the rotor and the rotor blading, and at 700 C for the more lightly loaded stationary blading and stator.

With this difference in temperature between stationary and rotating parts, some heat will be transferred to the rotor and rotor blading by radiation from the hotter stationary metal. However, on the basis of the calculations of *Brown* [2] and *Smith* [42], for the temperatures selected the radiant heat transfer will be negligible in comparison with the convective heat transfer.

The calculations in this work, although based upon average wall temperatures attained by the use of water cooled blades, will hold equally well for other types of blade cooling — provided these wall temperatures can be maintained and provided that the heat of cooling is eventually utilized in the generation of steam for the steam portion of the combined cycle.

The methods which appear to be closest to practical realization are:

1) *Schmidt*'s natural convection method [40], [43]. The radial holes in the blades are closed at the outer end and open to a "steam drum" in the rotor's center. Blade speed is such that the water in the blades is near critical pressure. The method thus takes advantage of the very large changes in specific volume at small temperature differences in the vicinity of the critical point, and of the high centrifugal force field produced by the rapidly rotating rotor and

blading, to induce very high circulation velocities and hence high heattransfer rates in the blade internal cooling holes. Very pure water is required to prevent scale and the build up of sludge and deposits in the outer ends of the holes. Two experimental units have been built, and a commercial machine is soon to be in operation.

2) The "thermal syphon" method [4]. The cavities within the blade are completely enclosed, and when cool contain about 2% by volume of the cooling liquid (generally water or a low boiling point metal). The blades are cooled at the roots, where cooling is mechanically much simpler, by a separate coolant (e. g., by the water which is the working medium in the steam cycle). The liquid in the cavity flows outward, wetting the internal walls and cooling them as it evaporates. The vapor recondenses at the cooled root, and repeats the cycle. Aside from simplifying the mechanical problems of cooling, the method has the advantage that no foreign matter can enter the cooling cavity — thus obviating in-service difficulties due to stoppage of blade cooling passages or decrease in heat transfer rates caused by deposit build-up.

3) Direct cooling by circulating liquids through internal blade passages. Liquid metals have exceedingly high heat transfer coefficients [1]. A great deal of research on this method of cooling is being done in connection with production of power by atomic energy. This research is producing experience data and handling procedures which will enable rapid application of this cooling method to the field of gas turbine blade cooling.

The first numerical calculations are made at constant Reynolds number, to determine the effect of varying Crocco number and the type of blading (impulse *vs* reaction). Equations (2.60) and (2.61) are solved for both blading types on the basis of the previously listed assumptions, a Reynolds number of 4×10^5, and a varying Crocco number. The results are reproduced in figure 5. The same equations are then solved for impulse blading alone, with varying Reynolds number. The Reynolds number effect is thus illustrated by figure 6.

From these figures is evident that a high Crocco number (i. e., blade speed) is advantageous from a cooling loss standpoint. A higher blade speed also makes possible higher gas velocities, which means higher Reynolds number; which, from figure 6, also reduces the heat transfer per kilogram of working fluid. Finally, since for a given velocity triangle

$$L = u^2 \Delta C_u \tag{2.52}$$

the work per stage is increased by increasing the Crocco number. This makes a smaller turbine, and simplifies the mechanical problems engendered by the relatively great temperature differences existing in a water cooled turbine.

The limit is, of course, the mechanical strength of the blades at the temperatures involved, and of their attachments to the rotor. Using present long life gas turbine practice as a guide, a mean blade speed of 200 m/sec is selected.

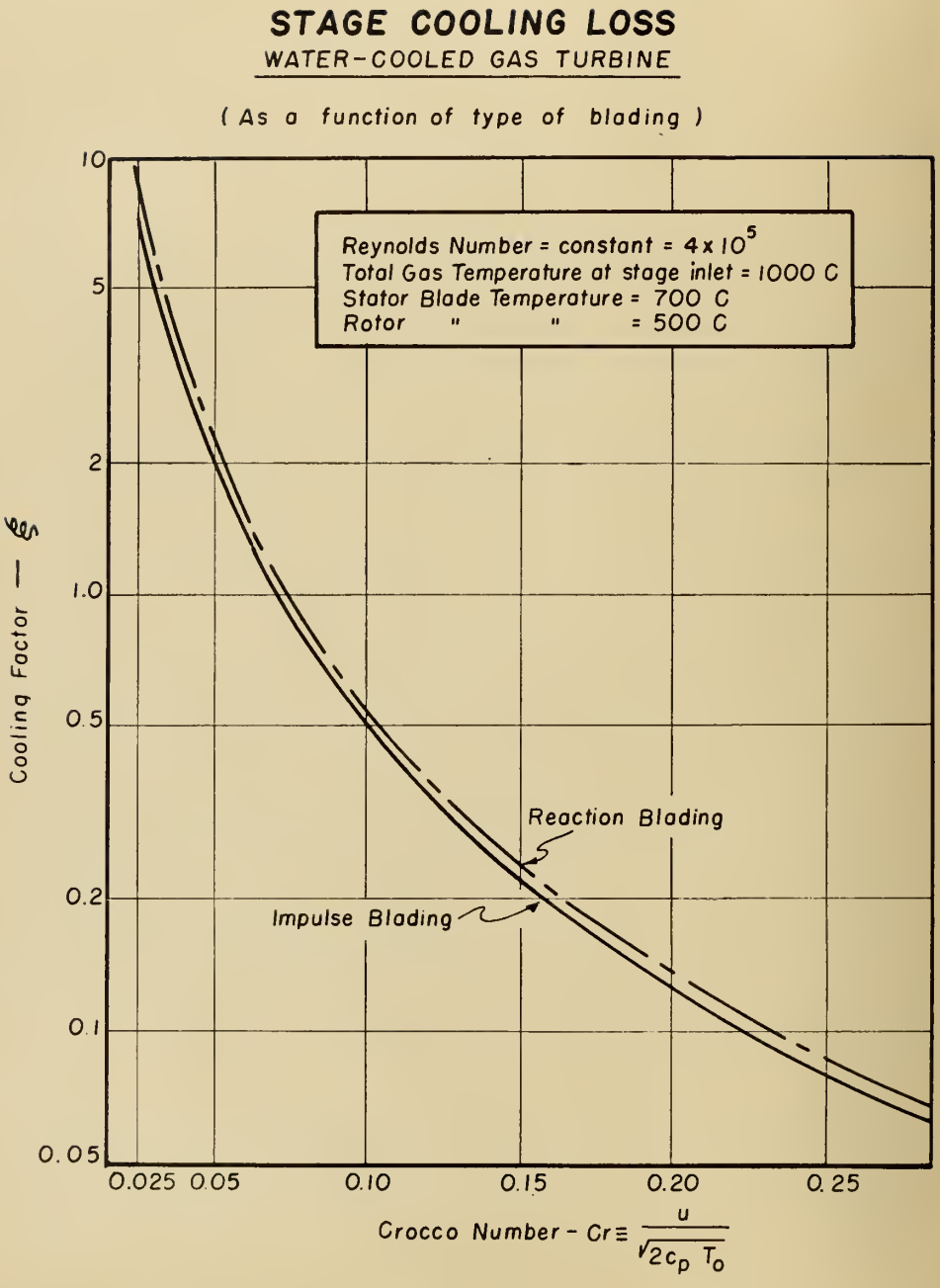

Fig. 5. Gas turbine stage cooling loss (by type of blading).

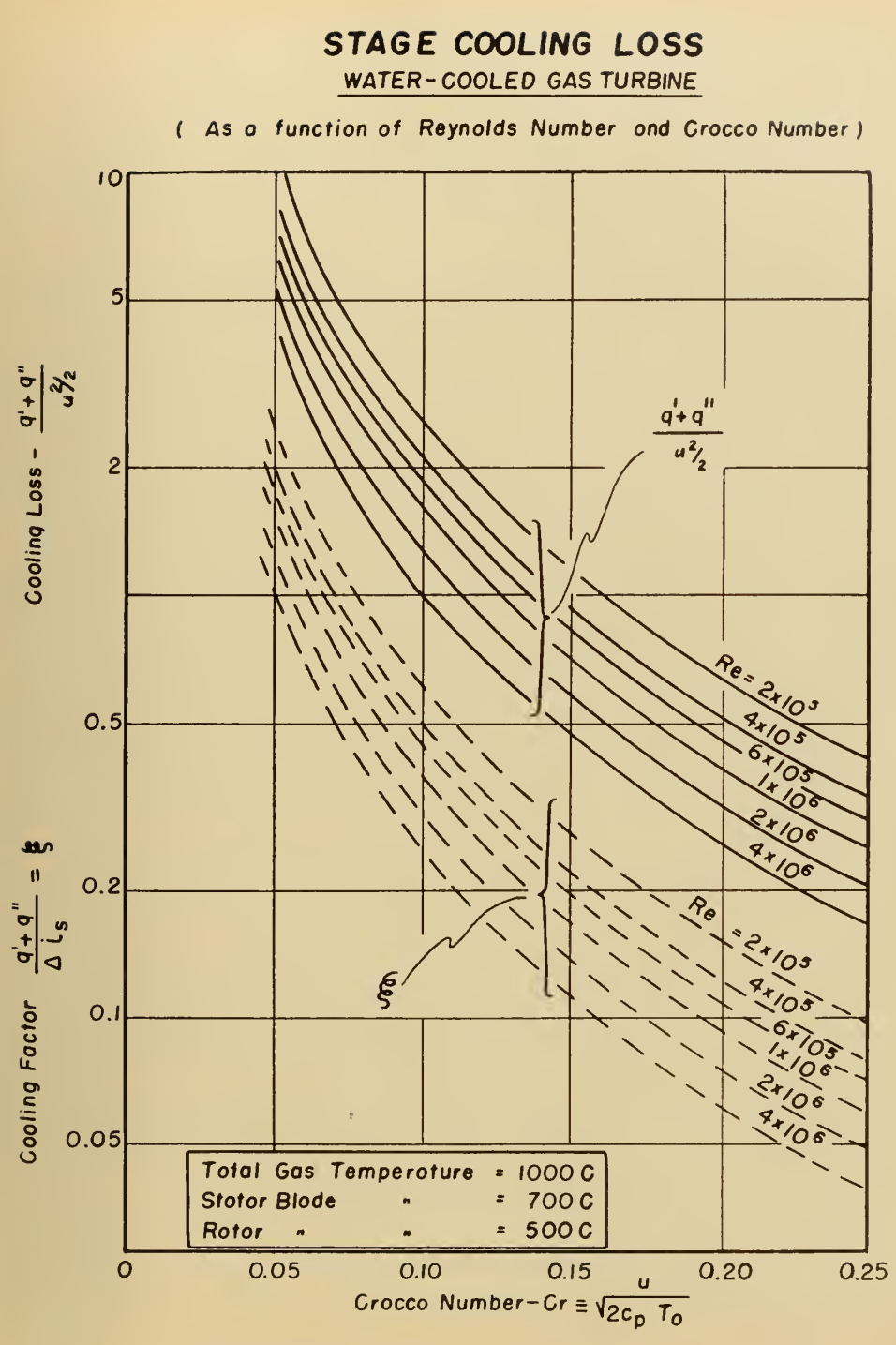

Fig. 6. Gas turbine stage cooling loss (by Reynolds and Crocco numbers).

Figure 5 would also indicate a slight advantage for the impulse turbine. Since gas velocities are higher for impulse blading, the Reynolds number would also be higher, thus (from figure 6) somewhat increasing this advantage. However, as future blade profiles are developed with heat transfer considerations in mind, the lower velocities of the reaction blading may make possible retention of laminar flow over a relatively greater portion of the profile, thus offsetting the above advantages.

Inconclusive though these considerations may be, use of impulse blading will in any case result in fewer stages, and hence a smaller turbine. At high temperatures this is likely to be an overriding advantage, and all further calculations have therefore been carried out for this type of blading.

In calculating the complete turbine, one notes that Ω, Re, Cr, q and ξ vary with each blade row. It is therefore more convenient to carry through the heat transfer computations by the use of equation (2.34). Holding the turbine initial temperature constant at 1000 C, various initial pressures are selected, and the calculations carried out blade row by blade row — terminating when the total gas temperature drops to 700 C. Here an exit loss (ζ_e) is assumed as previously; and expansion from the exit pressure to atmospheric pressure is accomplished in a separate "uncooled" turbine.

The results of these calculations, giving q and ξ as a function of turbine inlet pressure, are reproduced as figure 7.

The calculations of net turbine work and other characteristics of the turbine are similar to those for the lower temperature turbines.

Curves of net work (L_N) and exit temperature of the combustion gases for all three turbines are reproduced as figures 8 and 9.

III. Other Gas Turbine Cycle Components

III.1. Compressor and Intercoolers

The compressor is calculated as an axial flow compressor with a stage efficiency (η_{st}) of 90%. The temperature of the air at compressor entrance is 20 C. The air is assumed to be cooled to 35 C in the intercoolers. An exit loss of 2.5 kj/kg (includes also any incidental pressure drop at entrance) is assumed.

Since the working medium is air, the data from Keenan and Kaye's "Gas Tables" [23] may be used directly. The isentropic enthalpy rise is a simple calculation from the tabulations of this reference.

Since the axial compressor enjoys a relatively low pressure rise per stage, the correction for a finite number of stages is insignificant, and the polytropic efficiency (η_p) is approximately equal to the stage efficiency (η_{st}). Thus the reheat factor, derived in a manner similar to that in appendix A.1 for a turbine is

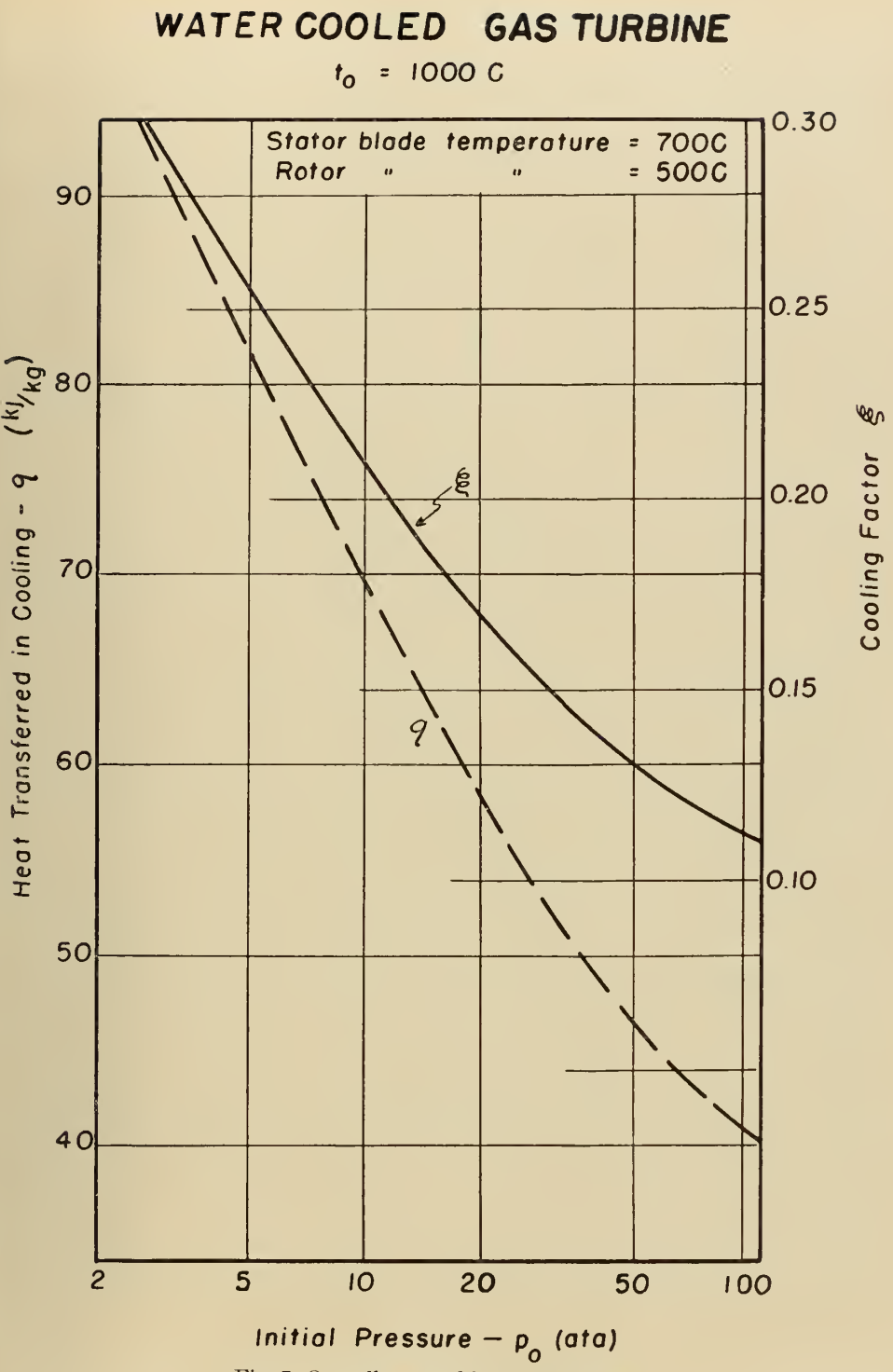

Fig. 7. Overall gas turbine cooling losses.

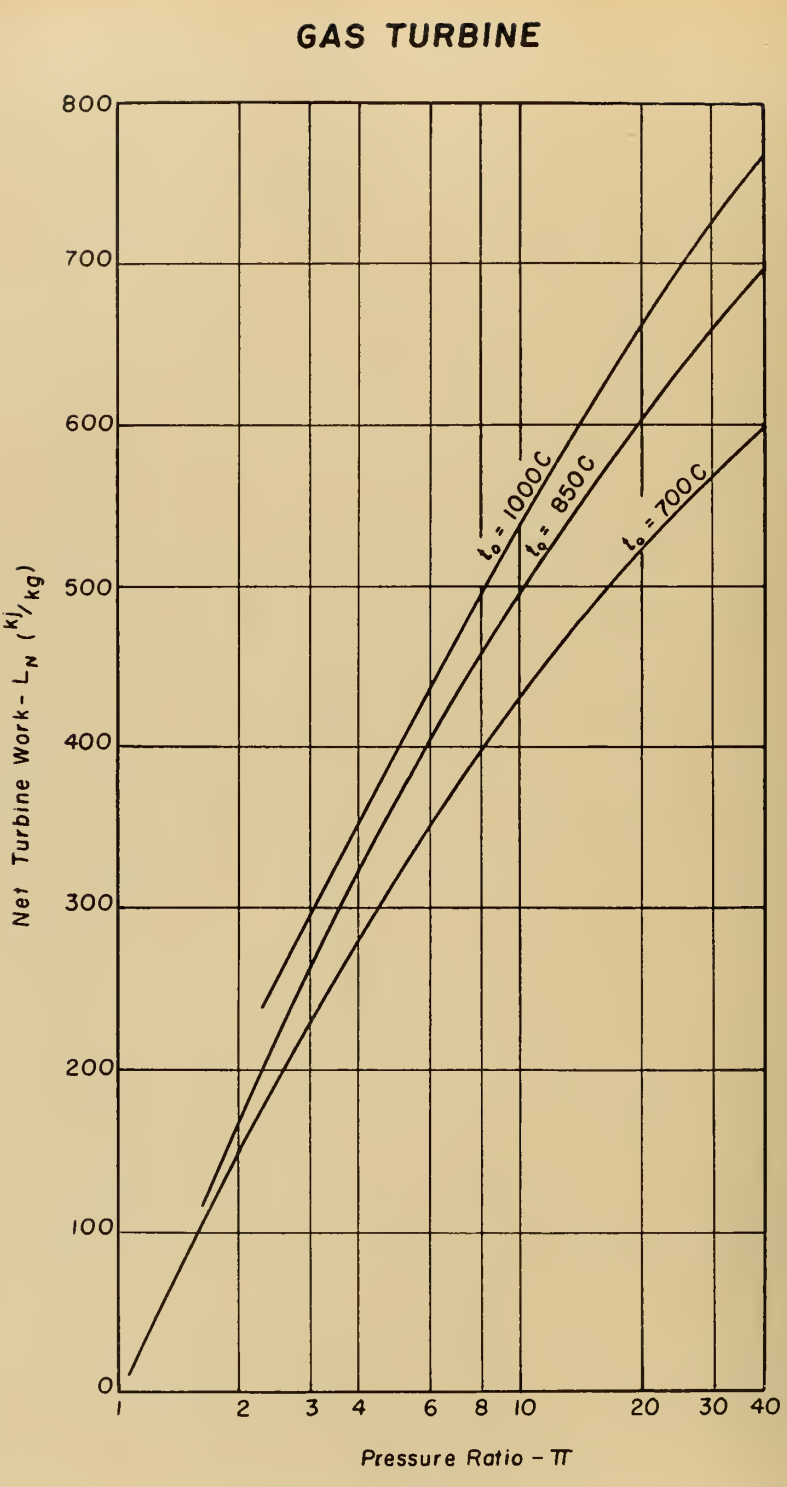

Fig. 8. Net gas turbine work.

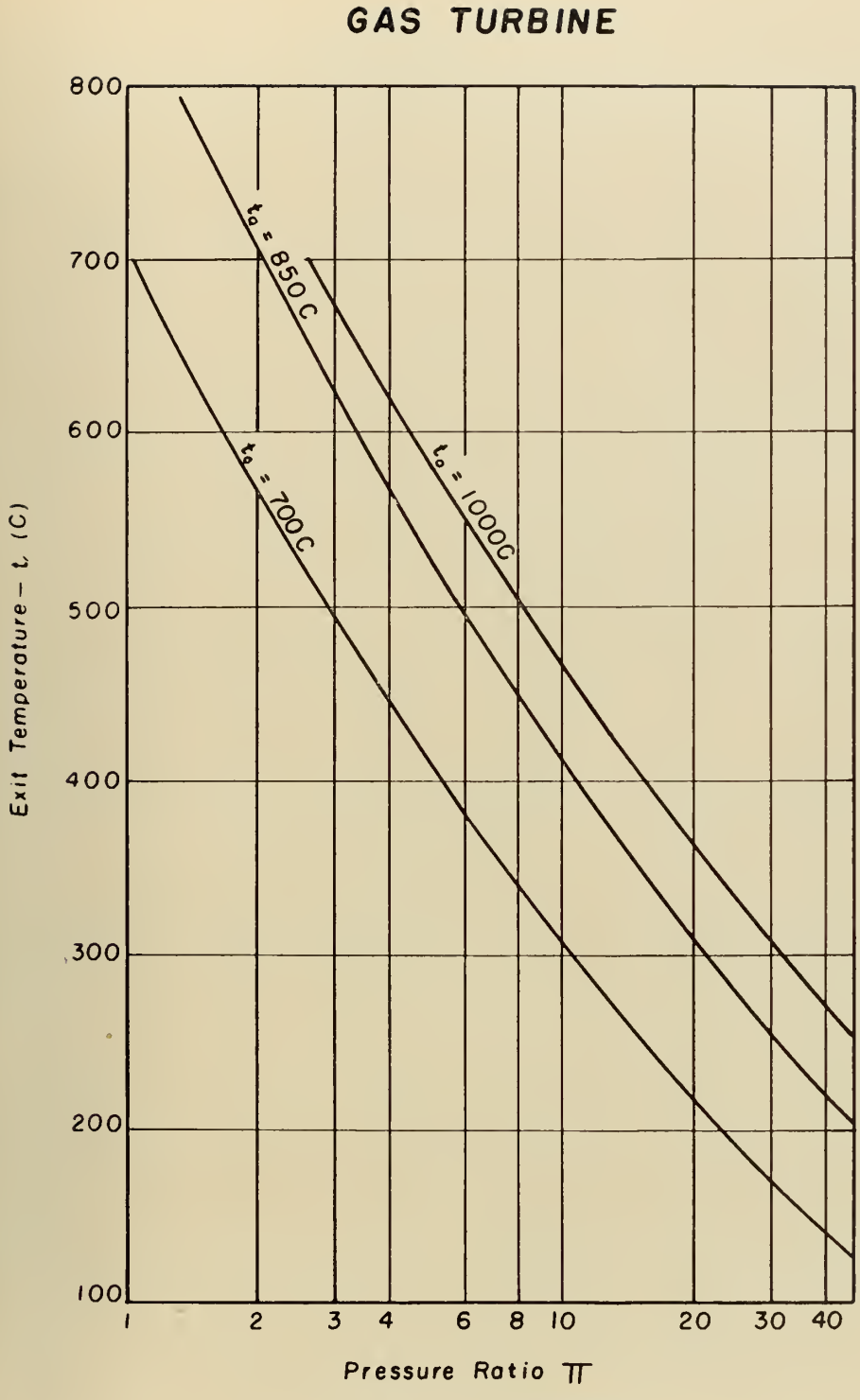

Fig. 9. Gas turbine exit temperature.

$$(1+\rho)_\infty = \eta_{st} \frac{(\Pi^{\frac{n-1}{n}} - 1)}{(\Pi^{\frac{\kappa-1}{k}} - 1)} \tag{3.1}$$

wherein

$$n = \frac{\kappa}{\kappa - \frac{1}{\eta_{st}}(\kappa - 1)} \tag{3.2}$$

The compressor isentropic efficiency $(\eta_C)_s$ is then

$$\frac{\eta_{st}}{(1+\rho)_\infty}.$$

Symbol definitions are the same as in the preceding chapter.

Let:

Δi_C ≡ total enthalpy rise in compressor (kj/kg)
$(\Delta i_C)_s$ ≡ isentropic enthalpy rise in compressor (kj/kg)
L_C ≡ compressor work (kj/kg)
ζ_e ≡ exit loss (kj/kg)

The indicated compressor work is equal to the actual enthalpy rise, or

$$\Delta i_C = \frac{(\Delta i_C)_s}{(\eta_C)_s} \tag{3.3}$$

Since the mechanical losses of the compressor (bearing friction, etc.) have been lumped with the gas turbine mechanical losses,

$$L_C = \Delta i_C + \zeta_e \tag{3.4}$$

The compressor with intercoolers is calculated as a series of normal compressors — the first with an entrance temperature of 20 C, and the following compressors with an entrance temperature of 35 C. An exit loss is assumed for each compressor. In addition a pressure loss of 2% $\left(\frac{\Delta p}{p} = 0.02\right)$ is assumed for each intercooler.

Practical design considerations presently limit the pressure ratio (Π) to between 6 and 10 for a non-cooled compressor on a single shaft. Above these pressure ratios two compressors in series, operating at different shaft speeds, must be used; and an exit loss assumed for each. For compressors of $\Pi < 6$, a single exit loss of 2.5 kj/kg is included in the calculations. For $\Pi > 10$, an additional exit loss at mid-pressure is assumed. These losses are quite small; therefore, to avoid discontinuities, the "no intercooler" curve of figure 10 for $6 < \Pi < 10$ is simply faired in between these limiting points.

The curves of compressor work as a function of overall pressure ratio, for 0, 1, 2 and 3 intercoolers, are reproduced as figure 10.

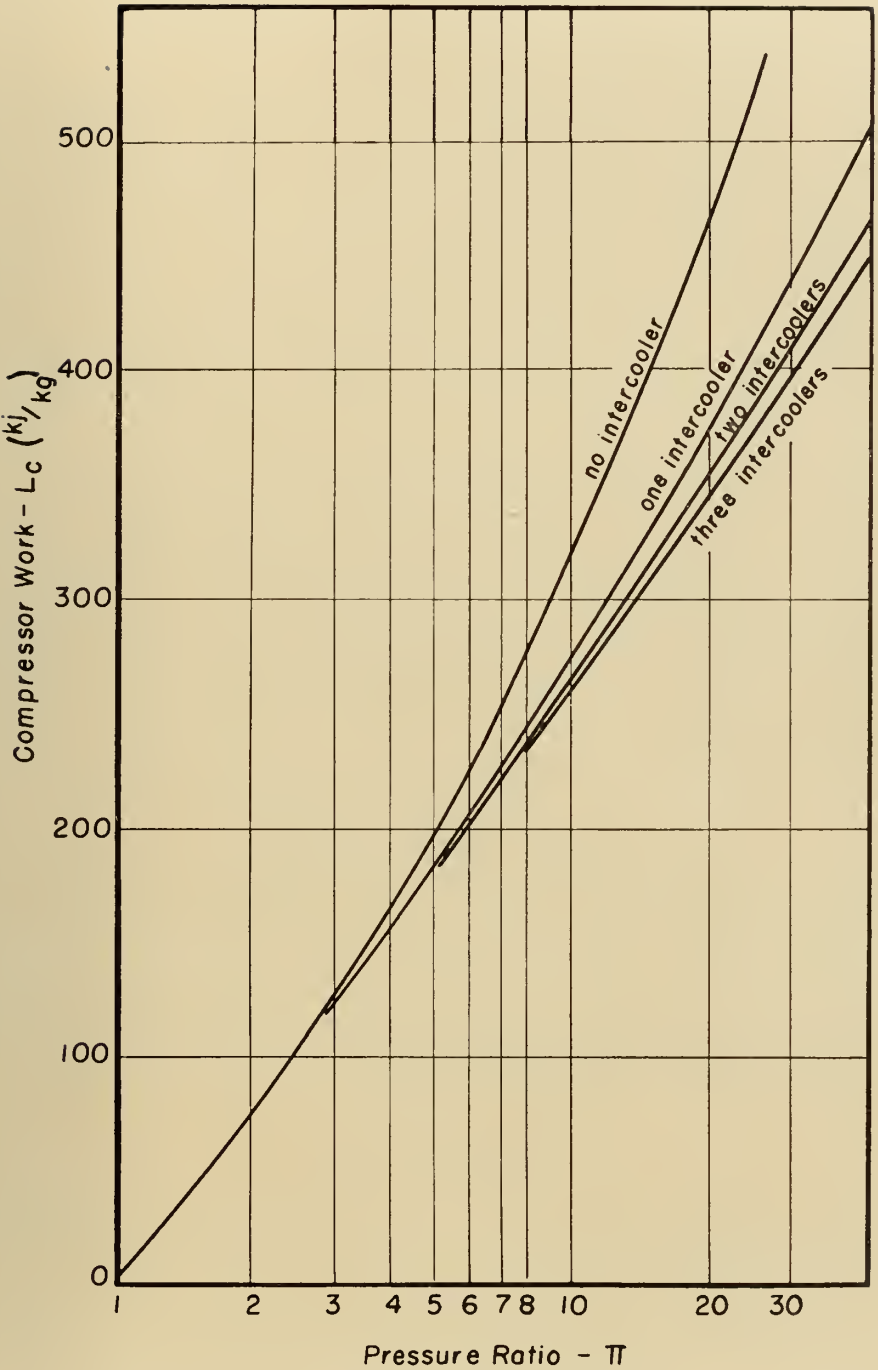

Fig. 10. Compressor work.

Although higher pressure ratios have sometimes occasionally been used in the later cycle calculations to yield a smooth curve, it is to be noted that the great changes in specific volume impose severe design difficulties for plants with pressure ratios of greater than 20 to 25.

It is sometimes suggested for the combined steam turbine – gas turbine cycle that efficiency could be improved by utilizing the heat discarded in the intercooler to partially pre-heat the steam generator feed water. This gain is further analyzed in chapter VIII; but it is perhaps interesting here to consider the effect of this innovation on the size of the intercooler.

To illustrate, let us take a compressor of overall pressure ratio = 10, with a single intercooler at mid-pressure. The air temperature at intercooler inlet is thus about 160 C. Assuming a cooling water inlet temperature of 20 C, and an air exit temperature of 35 C, we have a minimum temperature difference of 15 C, which has been found by experience to be economically feasible.

If we allow for 5 C rise in cooling water temperature, the logarithmic mean temperature difference between water and air is 54 C. If, on the other hand, we use the steam cycle condensate as a coolant, a 5 C temperature rise is of little value. If we maintain a constant temperature difference of 15 C between air and coolant throughout the intercooler, we can heat the condensate to a temperature of 145 C. But since the heat transfer surface is inversely proportional to the mean temperature difference, we have increased the size of the intercooler by the ratio $\frac{54}{15}$, or about three and a half times. This larg increase in intercooler size must be weighed against the thermodynamic gains discussed in chapter VIII.

III.2. Combustion Chamber

In accordance with common practice for industrial gas turbines, a first law efficiency of 98% is assumed for the combustion chamber. A pressure loss of 2% $\left(\frac{\Delta p}{p} = 0.02\right)$ is assumed. As these are commonly attained values, and as there is not much chance of appreciable improvement for commercial equipment, for the purposes of cycle analysis no further refinements in the combustion chamber calculations are required.

III.3. Regenerator

Since a regenerative gas turbine cycle with a good regenerator effectiveness has certain marked advantages over the simple cycle, particularly in efficiency, the gas turbine regenerator has been the subject of intensive analysis. The main aim has been to reduce the tremendous bulk and weight normally associated with this piece of equipment. For the cycle analysis however,

regardless of bulk, the required characteristics are the regenerator effectiveness (η_R) and the gas side and air side pressure drops.

For a regenerator of fixed size and physical configuration these characteristics are not independent. The gas velocity is dependent primarily upon the pressure drop; and higher velocities produce higher heat transfer rates and consequently more favorable η_R. The heat transfer rate is also better by higher gas density (higher absolute pressure); and, of course, by cleaner surfaces. The above gives rise to the possibility of finding an optimum balance between air side pressure drop, gas side pressure drop, and heat transfer surface arrangement to obtain the best overall heat transfer coefficient (k), and hence the best η_R for a given investment in cost.

Let us consider the above variables have been so adjusted as to give an optimum k. We will hold k constant and investigate briefly the effect of η_R on regenerator size.

Let:

c_p ≡ specific heat at constant pressure (kj/kg C)
F ≡ gas side heat transfer surface (m^2)
i ≡ enthalpy (kj/kg)
k ≡ heat transmission coefficient, gas to air (kj/sec C m^2)
L_N ≡ net specific work of the cycle, per kilogram gas flow (kj/kg)
$\dot{m}_a$, $\dot{m}_g$ ≡ air, respectively gas, flow (kg/sec)
N ≡ net power output of the cycle (kj/sec = KW)
$\dot{Q}$ ≡ heat flow (kj/sec)
t ≡ temperature (C)
Δt ≡ temperature difference, gas to air (C)
η_R ≡ regenerator effectiveness ≡ $\frac{i_5 - i_6}{i_5 - i_2}$ (dimensionless)
Θ ≡ dimensionless temperature difference ≡ $\frac{t_5 - t_6}{\Delta t}$

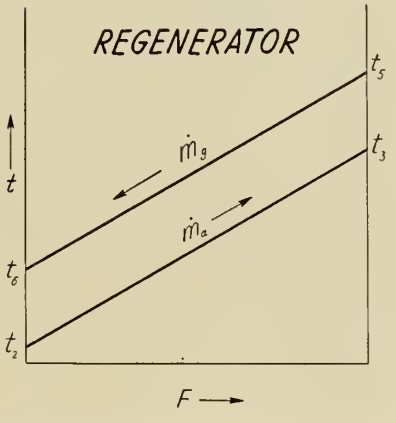

Fig. 11. Regenerator heat transfer diagram.

Subscripts (refer figure 11):

2 ≡ condition of air entering regenerator
3 ≡ condition of air leaving regenerator
5 ≡ condition of combustion gases entering regenerator
6 ≡ condition of combustion gases leaving regenerator

$$\dot{Q} = k\,F\,(\Delta t) = (i_5 - i_6)\,\dot{m}_g = \bar{c}_{p_g}(t_5 - t_6)\,\dot{m}_g \tag{3.5}$$

$$\frac{F}{\dot{m}_g} = \frac{c_{p_g}(t_5 - t_6)}{k\,\Delta t} = \frac{\bar{c}_{p_g}}{k}\Theta \tag{3.6}$$

$$N = \dot{m}_g\,L_N \tag{3.7}$$

$$\frac{F}{N} = \frac{c_p}{k\,L_N}\Theta \tag{3.8}$$

For $\dot{m}_g \bar{c}_{p_g} \approx \dot{m}_a \bar{c}_{p_a}$

$$\Delta t = (t_5 - t_3) = (t_6 - t_2) \tag{3.9}$$

$$\eta_R \equiv \frac{t_5 - t_6}{t_6 - t_2} = \frac{t_3 - t_2}{t_5 - t_2} \tag{3.10}$$

$$\Theta \equiv \frac{t_5 - t_6}{\Delta t} = \frac{t_5 - t_6}{t_6 - t_2} = \frac{\dfrac{t_5 - t_6}{t_5 - t_2}}{\dfrac{t_5 - t_2}{t_5 - t_2} - \dfrac{t_5 - t_6}{t_5 - t_2}} = \frac{\eta_R}{1 - \eta_R} \tag{3.11}$$

$$\text{or } \frac{F}{N} = \frac{\bar{c}_p}{k\,L_N}\left(\frac{\eta_R}{1 - \eta_R}\right) \tag{3.12}$$

L_N and N do not vary appreciably with small changes in η_R. If we assume k held constant, it is evident that for small η_R a slight increase η_R does not involve much increase in heat transfer surface $\left(\text{expressed in } \frac{\text{m}^2}{\text{KW}}\right)$. As η_R approaches unity, however, a slight increase in η_R requires a very large increase in regenerator size. We thus have a very stringent economic limit on the value of η_R.

The heat transmission coefficient (k), which we have here held constant, actually varies with the fluid velocity past the heat transfer surfaces. This is in turn dependent on the pressure drop. Pressure drop is also dependent on regenerator size, and also influences the specific work output (L_N). These may be related in various ways, and different variables held constant to investigate their individual effects and to determine an optimum arrangement. The resulting (and more exact) expressions will be considerable more complicated than equation equation (3.12); but the general conclusion is the same. In the final analysis, the selected value of η_R will also involve economic considerations of fixed versus operating costs, load factor, etc.

With these factors in mind, regenerative gas turbine cycles for industrial use under high load factor generally have a regenerator effectiveness and

pressure drops in the neighborhood of the below values, which are selected for use in this study:

$$\eta_R = 0.75$$

$$\frac{\Delta p}{p} \text{ (gas side)} = 0.03$$

$$\frac{\Delta p}{p} \text{ (air side)} = 0.02$$

IV. Gas Turbine Cycle

IV.1. Cycle calculations

With calculations and selections of the characteristics of all gas turbine components completed, it is readily possible to calculate the characteristics of the gas turbine cycles alone, prior to combination with the steam cycle. This is valuable, not only for comparison with the combination cycle; but also for comparison with other analyses of the gas turbine cycle, some of which consider more of the great number of arrangements and variations of components than is here practicable (e. g., wet compression, reheating, comprex, thermopressor, free piston compressor, etc.). Diagrams of the cycles calculated are reproduced as figures 12 and 13. The simple gas turbine cycle, consisting of compressor, turbine and combustion chamber, is labeled cycle I. The arabic numerals following (e. g., I 1, I 2, I 3) indicate the number of stages of intercooling in the compression process. Addition of the letter "a" (e. g., cycle Ia) indicates the addition of a regenerator.

The following symbols have been used in the cycle diagrams:

C ≡ Compressor
CC ≡ Combustion chamber
GT ≡ Gas turbine
R ≡ Regenerator

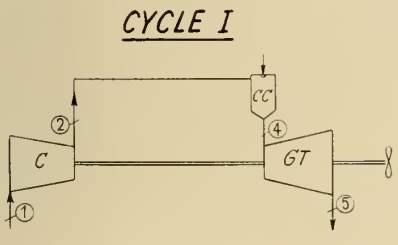

Fig. 12. Cycle I diagram.

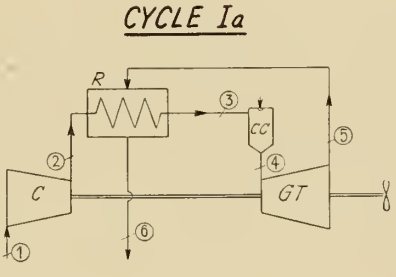

Fig. 13. Cycle Ia diagram.

In this chapter (and in chapter VIII) only open cycle arrangements have been analyzed. A corresponding closed cycle could be analyzed for any of these arrangements; but the efficiencies at full load would be about the same. Because of the usually higher working fluid pressures in the various heat exchangers at full load, more favorable overall heat transfer coefficients would allow selection of a higher effectiveness for each of these units. Against this, however, must be balanced the additional losses encountered in the air heater and in the air pre-cooler. For this reason the open and closed cycles show similar efficiencies at full load (the point analyzed in this work); and any advantages or disadvantages of the closed cycle will lie in part load economy, space and weight requirements, ease of control, lower maintenance costs, etc.

The pressure drops indicated in chapter III for the individual components are intended to include the connecting piping. The net effect of the pressure drops is to reduce the pressure ratio available to the gas turbine, in comparison with that generated by the compressor.

The only cycle loss not previously accounted for in the individual components is the incidental loss of heat by radiation and convection from the high temperature components to the surroundings. This will vary with the number of components and their sizes, and with the maximum cycle temperature. If we assume a mean value of this loss equal to 2% of the heat released in the combustion chamber, we account in part for the temperature effect. As the loss is not too large, we can neglect the variation from this mean caused by variation in size of equipment.

In all other respects the cycle calculations are simple and straightforward; therefore no detailed elaboration is presented.

IV.2. Results

The results of the simple gas turbine cycle without regenerator are presented in figure 14; those with regenerator, in figure 15. As is expected, intercooling yields some improvement in cycle efficiency, especially in the cycle with a regenerator. Intercooling also pushes the point of maximum efficiency towards the higher pressure ratios.

Assuming that the most advantageous intercooling is always used, we can plot a single efficiency curve for each inlet temperature for each cycle. These are plotted for comparison in figure 16.

The use of a regenerator causes a marked increase in cycle efficiency, and decreases the pressure ratio at which this occurs. Although not illustrated, use of a regenerator causes a slight decrease in specific work; whereas use of intercooling or increase in cycle maximum temperature causes comparatively large increases in specific work.

Worthy of note is that the 1000 C cycle does not show the favorable effi-

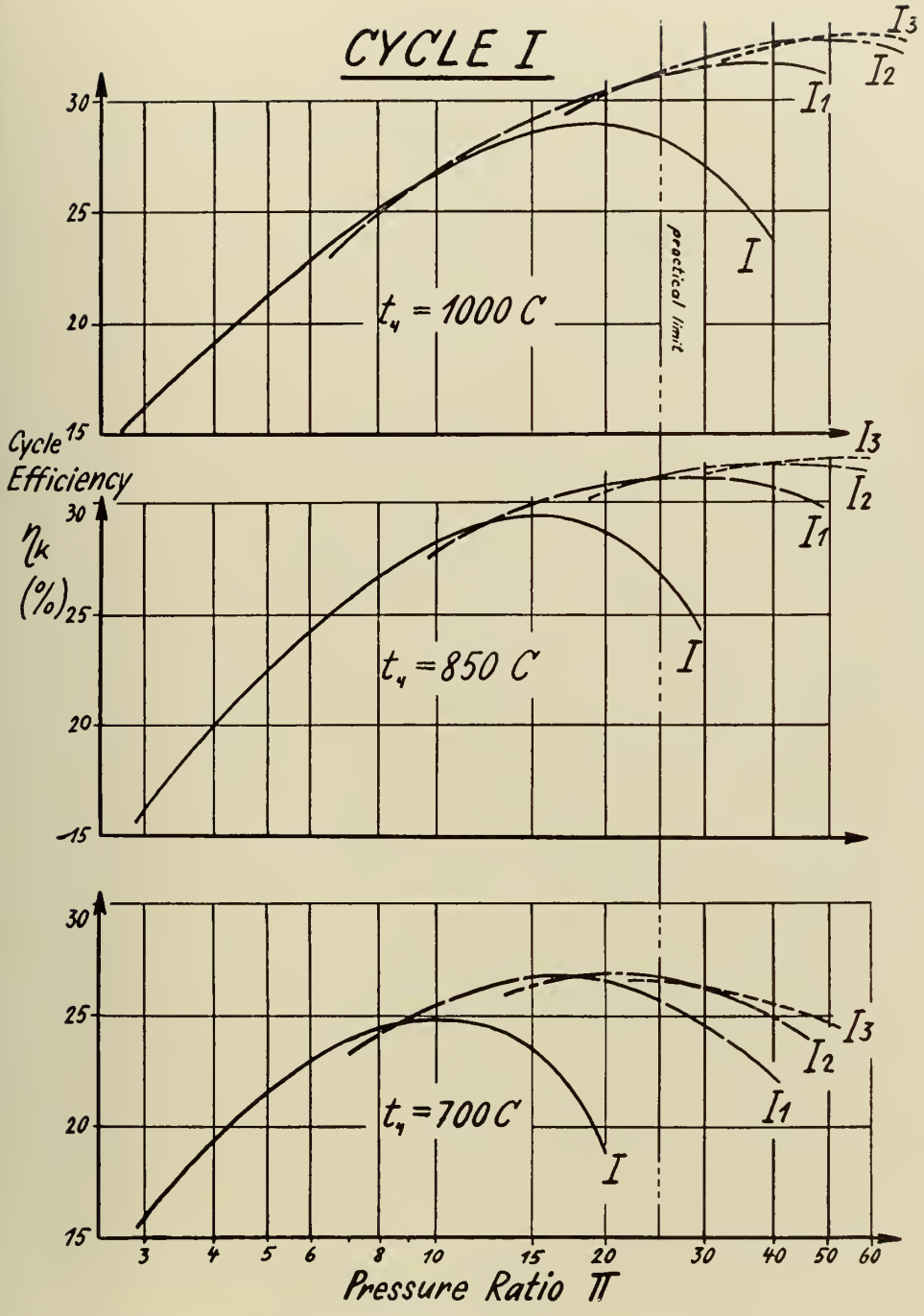

Fig. 14. Cycle I efficiency curves.

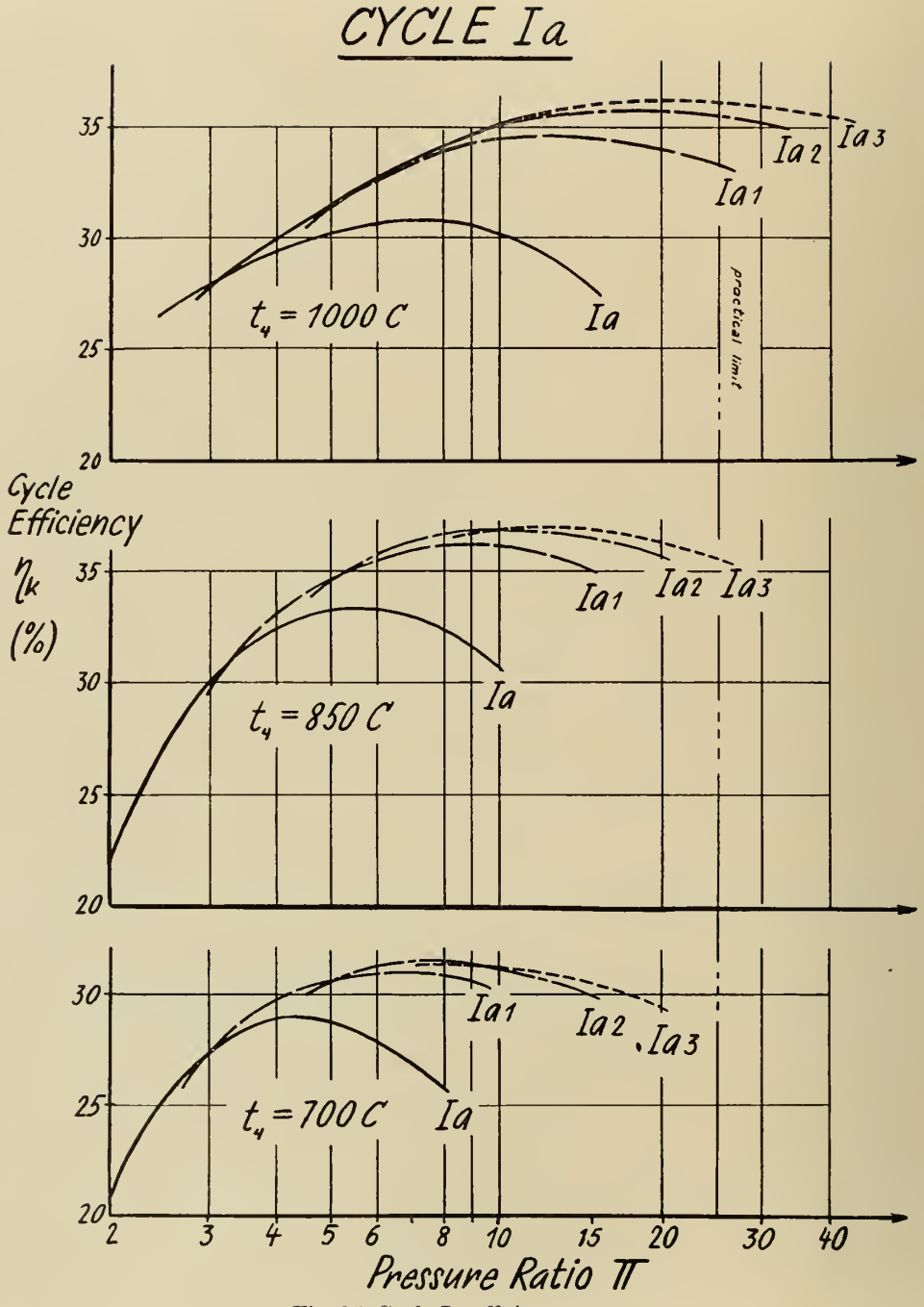

Fig. 15. Cycle Ia efficiency curves.

COMPARISON OF CYCLES AT VARIOUS MAXIMUM TEMPERATURES

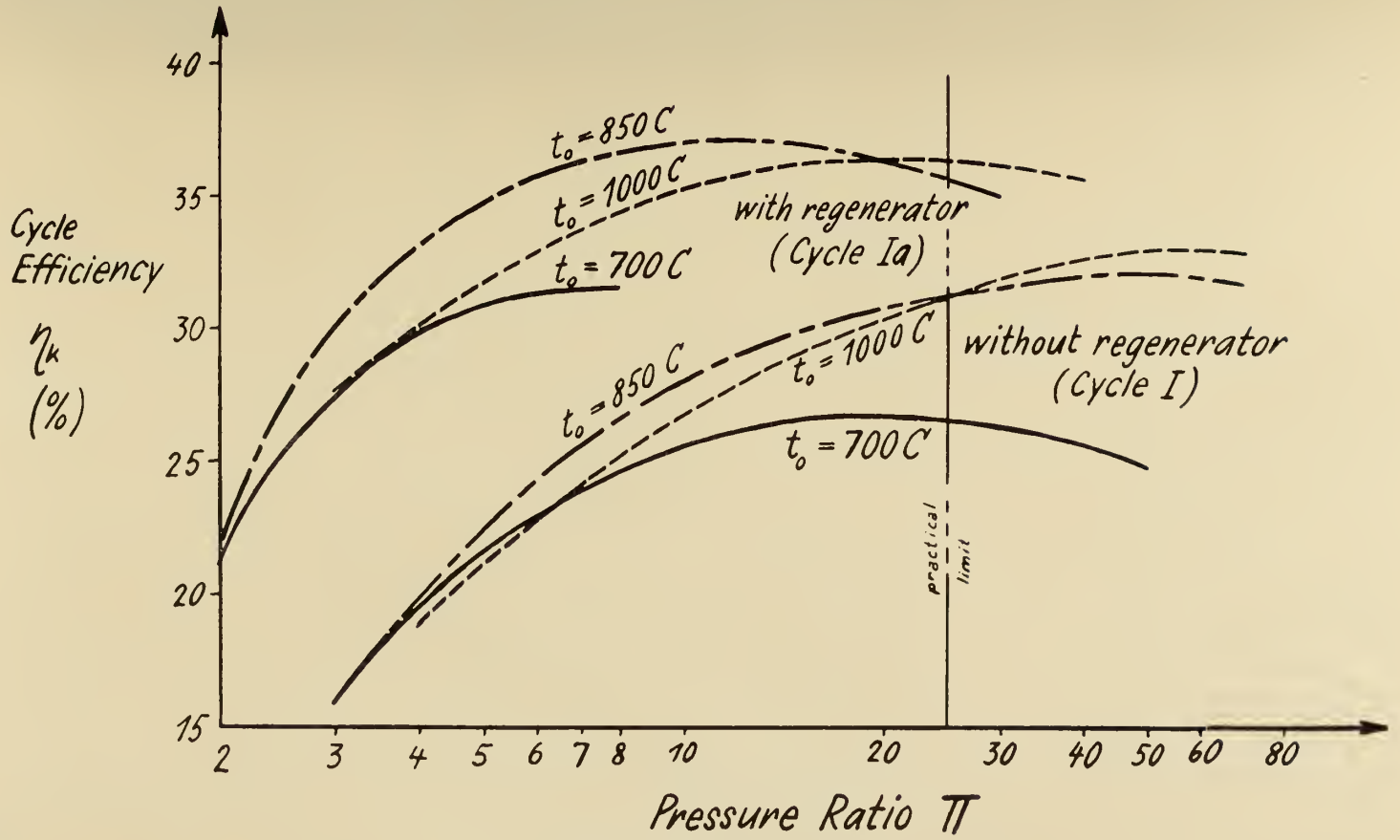

Fig. 16. Comparison of gas turbine cycles.

ciencies that one has been led to expect for higher temperatures. This is partly because a cooled turbine compares poorly with an uncooled unit as regards turbine efficiency. Further, the 850 C turbine is air-cooled. Once the cooling air has been heated, this "heat of cooling" is available to the remainder of the turbine for partial conversion to useful work. The 1000 C turbine, on the other hand, has been calculated with water-cooling. Any heat removed in cooling is lost to the gas turbine cycle. If we could assume that this heat were utilized in an efficient steam cycle, the efficiency curve of the 1000 C cycle would be at all points superior to the lower temperature curves.

V. Steam Turbine

V.1. The Standard Turbine Series

The main problem here involved is the selection of a standard series of turbines, of commercially obtainable efficiencies, which will permit consistently comparable reflection of advantages and disadvantages of various steam inlet pressures and temperatures.

Other investigators of the combined steam turbine-gas turbine cycle have generally chosen a constant turbine efficiency, e. g., [29], [30], [31], [35], [50]. This has the advantage of simplicity; but it can tend to confuse the final results, particularly when the steam turbine furnishes a large portion of the useful power. On the one hand, large turbines which operate at high inlet pressures and temperatures may have overall efficiencies as high as 88%. On the other hand, even a well designed turbine intended to utilize saturated steam at very low inlet pressure might have an efficiency of 75% or less. This latter is a case quite likely to be encountered for a steam cycle which utilizes primarily the exhaust heat of a gas turbine.

The method chosen to reduce inconsistencies to an acceptable level is to determine the overall characteristics of a series of steam turbines based on the following economically obtainable parameters:

a) For inlet temperatures of 450 C and above, the first or control stage is a Curtis (two-row impulse) stage with an arbitrarily selected internal efficiency of 70%. For inlet temperatures of less than 450 C, the control stage is a single row impulse stage, and its calculation is combined with that for the intermediate pressure stages.

b) For the intermediate pressure turbine stages (i. e., between the exit of the Curtis stage and the point where the steam condition curve crosses the saturation line on the Mollier diagram, for turbine inlet temperatures of 450 C or more) a uniform internal stage efficiency of 88% is used. For lower inlet temperatures, as discussed in paragraph V.3, inlet pressures

are correspondingly lower. Thus, for temperatures less than 450 C, volume rates of steam flow are high enough to preclude partial admission for full power operation for reasonably large turbines; and an average internal stage efficiency of 88% for *all* stages operating on superheated steam may safely be assumed.

c) For the low pressure part of the turbine (i. e., under the saturation curve), the decrease in stage efficiency is approximated by multiplying 88% by a factor equal to the quality of the steam.

d) Gland seal steam loss, dummy (balancing) piston loss, etc., amount to a loss of 2% of total steam after passage through the control stage.

e) Final stage steam exit velocity is 200 meters/second, which corresponds to a leaving loss of 20 kj/kg.

f) Miscellaneous mechanical losses amount to 1% of total turbine power.

g) Condenser pressure is 0.05 ata.

h) Pressure loss in throttle and inlet piping equals 10% of boiler pressure.

Calculation method (refer to figure 17)

The calculations are based on the Mollier diagram [25], extended to 700 C by the data of [10]. Steam condition curves and internal turbine efficiencies have been calculated for a large number of turbines, to ensure coverage of all practical inlet conditions.

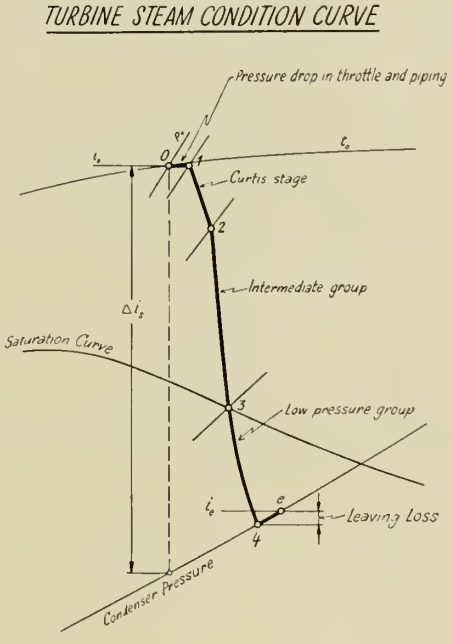

Fig. 17. Steam turbine condition curve.

The Curtis stage, where applicable, is calculated on the basis of an internal efficiency of 70%, a wheel speed of 150 m/s, and a velocity ratio $\left(\nu = \frac{u}{\sqrt{2\,\Delta i_s}}\right)$ of 0.25.

The intermediate stages are handled as a group, with an assumed average stage efficiency of 88%. Initial steam condition is determined by the exit condition from the Curtis stage. An estimated condition curve is drawn on the Mollier diagram to allow an initial estimate of the total pressure ratio Π for this group of stages, and to enable an initial determination from [24] of the mean isentropic exponent κ. The polytropic exponent n is determined by:

$$\frac{n-1}{n} = \eta_p \frac{\kappa - 1}{\kappa} \tag{a.28}$$

The reheat factor $(1+\rho)$ is calculated from the formula:

$$(1+\rho) = \frac{(1+\rho)_{\infty,\Pi}}{(1+\rho)_{\infty,\Pi_{st}}} \tag{a.59}$$

where

$$(1+\rho)_{\infty,\Pi} = \frac{1}{\eta_p} \frac{1-\left(\frac{1}{\Pi}\right)^{\frac{n-1}{n}}}{1-\left(\frac{1}{\Pi}\right)^{\frac{\kappa-1}{\kappa}}} \tag{a.45}$$

and is defined as the reheat factor for a turbine with infinitely small stages of efficiency $\eta_{st} = \eta_p$, operating through the pressure ratio Π. $(1+\rho)_{\infty,\Pi_{st}}$ is calculated from the same formula, substituting the average stage pressure ratio Π_{st} for Π.

This latter correction is always small, and a very rough estimate of Π_{st} will suffice. Π_{st} is therefore estimated by use of a mean wheel speed of 200 m/s and $\nu = 0.65$. In almost all cases the error introduced by assuming an infinite number of stages is insignificant. If the error in assuming infinitesimal stages is appreciable, the η_p corresponding to an initially assumed η_{st} may be calculated from

$$\eta_p = \frac{\eta_{st}}{(1+\rho)_{\infty,\Pi_{st}}} \tag{2.11}$$

The overall internal efficiency of the intermediate pressure group is then the product of the internal stage efficiency and the reheat factor. The corrected condition curve is drawn on the Mollier diagram, and the initially estimated values of Π and κ adjusted as required.

For the low pressure group a stage efficiency of $\eta_{st} = 0.88\,\bar{X}$ is assumed, where $\bar{X} \equiv$ mean quality of the steam for the stage. This correction factor is introduced to approximate the losses caused by impingement of droplets of moisture against the rotor blades, and the loss of working fluid through the dewatering apparatus.

STEAM TURBINE – INTERNAL EFFICIENCY

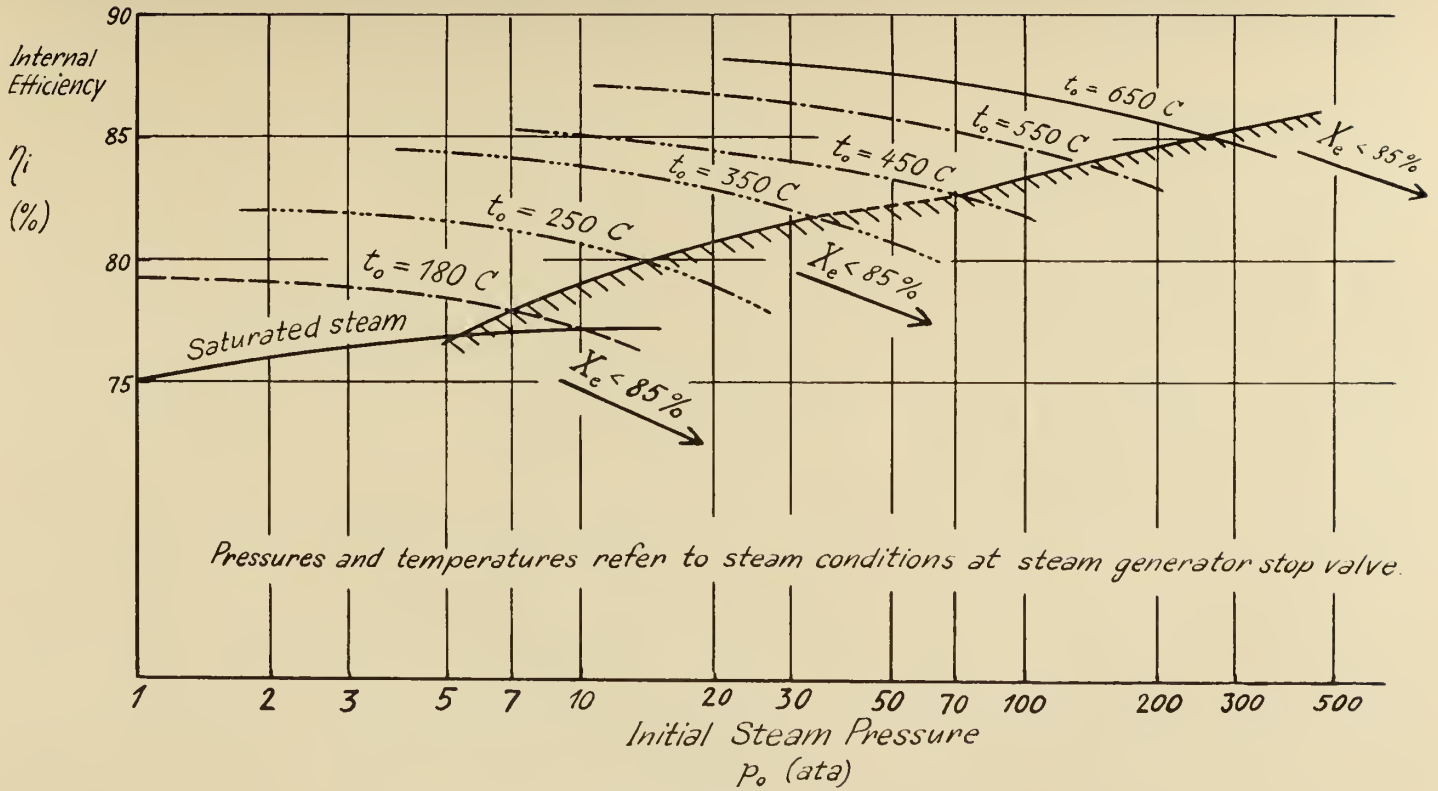

Fig. 18. Steam turbine efficiencies.

To facilitate the construction of the condition curves, the slopes of the curves for various pressures and moisture contents are calculated and drawn in on an unused portion of the Mollier diagram. (This procedure is facilitated by the fact that, under the saturation curve, the lines of constant pressure are straight lines.) The condition curve for the intermediate pressure group of stages terminates at its juncture with the saturation curve. The appropriate slope is selected from those drawn in as described above, transferred to this juncture, and the condition line extended a short distance into the low pressure region. The new pressure and moisture content are noted, and again the appropriate slope selected and transferred. In this manner the condition curve is extended to the selected exhaust pressure as a series of straight lines, each so short that, to the eye, the final condition line appears as a smooth curve. After a little practice, consistently accurate results can be obtained.

With the data from the condition curve, the internal turbine efficiency η_i can be calculated from the definition

$$\eta_i \equiv \frac{L_i}{\Delta i_s} \tag{5.1}$$

L_i is defined as the internal work produced per kilogram throttle steam; and Δi_s is the isentropic enthalpy drop from initial steam state to condenser pressure.

L_i consists of the actual enthalpy drop in the control stage, plus 98% of the actual enthalpy drops in the intermediate and low pressure groups, minus 98% of the exit loss. The last three values must be multiplied by 98% to account for the loss of gland seal steam (including dummy piston loss), which from experience data has been taken equal to a loss of 2% of total steam at the exit of the control stage.

Reduction of turbine work due to bleeding of steam for feed water heating (a factor normally encountered in a straight steam plant) is handled separately in paragraph V.4.

Overall internal turbine efficiencies thus calculated are reproduced in figure 18. These efficiencies are comparable with published experience data [5], [9], [34], [51].

V.2. Specific Turbine Work

For the combined cycle calculations, the specific steam turbine shaft work (L_n) is required. The mechanical efficiency of the turbine (η_M) has been assumed at 99%. For the purposes of this study, the power requirements of the auxiliaries (exclusive of feed pump) can be taken as a constant percentage of the total turbine power. Feed pump power, however, will vary with boiler pressure.

If we make the reasonable assumptions of an efficiency of 80% for the boiler feed pump and 90% for its drive motor, and assume that all other

auxiliaries combined absorb $1^1/_4\%$ of the total turbine power, we have all steam cycles on a comparable footing and we are in the neighborhood of operating experience [5], [19], [26].

Denoting the power consumption of all auxiliaries of the steam cycle as H% of the steam turbine shaft power:

$$L_n = L_i \eta_M (1 - H) \tag{5.2}$$

The values of H used are listed in the below table as a function of boiler pressure:

Table

Boiler Pressure (ata)	Auxiliary Load (%)
10	1.6
50	2.1
100	2.7
150	3.2
200	3.6
300	4.5

V.3. Interdependence of Inlet Pressure and Temperature

The overall steam-gas turbine cycle calculations can be simplified in some instances by eliminating certain of the standard series of turbines from consideration.

Let us consider a series of steam cycles of various turbine inlet pressures and temperatures. Let us also set aside for the moment the possibility of regenerative feed water heating (discussed later in paragraph V.4). Feed pump work adds little to the specific enthalpy of the feed water for the feed pressures normally encountered. Since the enthalpy of the feed water at the steam generator inlet is thus essentially independent of boiler pressure, the feed water enthalpy will be a constant for all cycles — namely, that corresponding to the temperature of the condensate leaving the condenser. Thus the heat input to the steam generator is a function only of the enthalpy of the steam at the steam generator outlet (i_o). Referring to the turbine state line on the *i-s* diagram (figure 17), for a fixed t_0 and constant condenser pressure we obtain an increasingly greater enthalpy drop in the turbine the further to the left we choose the initial steam state, point 0. Since heat input is relativeli constant, for highest steam cycle efficiency we want to operate as far to the left on the Mollier diagram as practical considerations will allow.

The limit in this case is the mechanical consideration of blade erosion caused by droplets of moisture impinging on the moving blades of the final turbine stages. This limit has been considerably pushed back in the last few years by the use of dewatering canals and special blading materials. The present

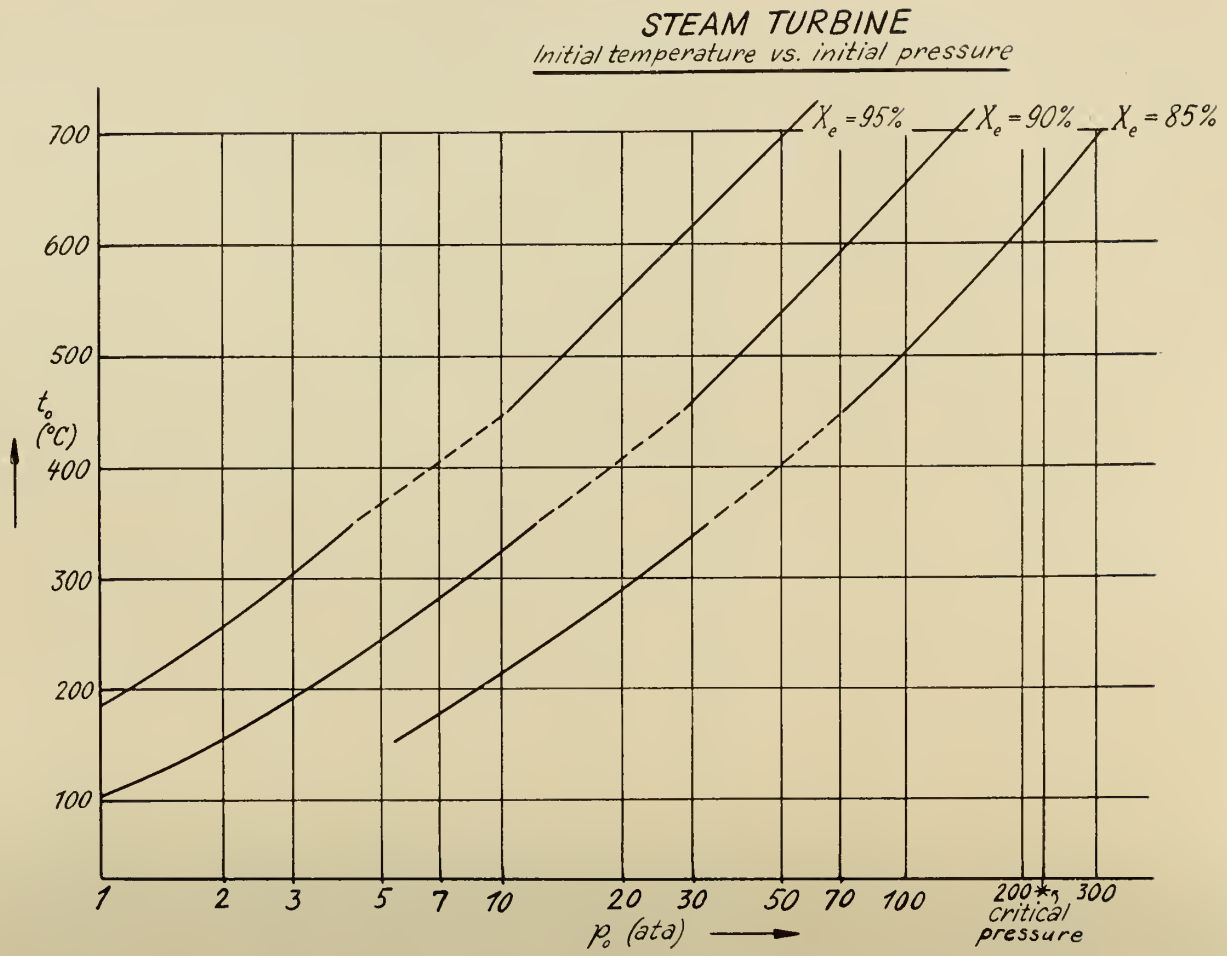

Fig. 19. Steam turbine inlet pressure-temperature relationships.

economic limit is in the vicinity of 15% moisture. Since it is often economically advantageous to work as closely to this limit as possible, from the calculated turbines we can interpolate to determine the initial states of all turbines whose steam quality at turbine exit is 85%. This yields a unique relationship between initial pressure and initial temperature.

The above has been based upon consideration of only the steam side of the power cycle. A complete thermodynamic analysis must also include consideration of the changes of state experienced by the combustion gases. In some cycles this consideration modifies the above to the extent that the maximum efficiency of the combined cycle occurs at a turbine exit steam quality greater than 85%.

In the cycle calculations it was usually found convenient to systematize the computations by relating steam turbine inlet pressure to the steam turbine inlet temperature by holding the turbine exit steam quality constant at 85%, 90% or 95%. This procedure automatically excluded from consideration any combinations of steam turbine inlet temperature and pressure which would result in the mechanically impractical situation of a turbine exit steam quality (X_e) of less than 85%. Since the maximum cycle efficiency rarely occurred at $X_e > 95\%$, this procedure also eliminated fruitless calculations at the other extreme.

The above pressure-temperature relationships at turbine inlet are illustrated in figure 19. The dashed sections between 350 C and 450 C result from slight discontinuities caused by the shift from an initial two-row Curtis stage for turbines with inlet temperatures of 450 C and above, to an initial single row impulse wheel for the control stage of turbines with inlet temperatures of 350 C or less (see paragraph V.1).

Since saturation temperature is a function of steam pressure, we may also express the relationships of figure 19 in terms of saturation temperature (t_{w_1}) and initial temperature (t_{w_2}). Interestingly, these are practically straight line relationships; and may be expressed mathematically for later use in the analytical treatment of the steam cycle.

For

$$X_e = 0.85: \quad t_{w_2} = 84.0 + 0.450\, t_{w_1} \tag{5.3}$$

$$X_e = 0.90: \quad t_{w_2} = 55.8 + 0.387\, t_{w_1} \tag{5.4}$$

$$X_e = 0.95: \quad t_{w_2} = 37.9 + 0.317\, t_{w_1} \tag{5.5}$$

V.4. Reduction of Specific Turbine Work Due to Bleeding Steam for Regenerative Feed Heating

In the normal steam plant an increase in overall efficiency is nearly always obtainable if the feedwater is partially pre-heated by steam extracted from

the lower pressure stages of the turbine. The mean temperature at which the steam cycle receives heat from the combustion gases is thereby raised. By the Second Law of Thermodynamics, this results in a gain in cycle efficiency. This regenerative feedwater pre-heating is accompanied by irreversibilities due to pressure drops and heat transfer across finite temperature differences in the pre-heaters, which tend to offset the above gain. For a fixed number of pre-heaters these irreversibilities increase with increasing final feedwater temperature. By a quantitive comparison of the gains due to the increased mean temperature at which the cycle receives heat with the losses due to irreversibilities in the feed heaters, we can eventually arrive at an optimum feedwater temperature.

As the feedwater temperature to the economiser is raised, less heat is extracted by the steam cycle from each kilogram of combustion gases unless an air preheater is used to cool the stack gases to the same final temperature. By heating the incoming air, the air preheater returns its recovered heat to the furnace and eventually to the steam cycle. Steam generator efficiency is thus little affected by regenerative feed heating, and a gain in steam cycle efficiency results in a gain in overall plant efficiency. The steam plant in which heat is furnished through a waste heat steam generator normally cannot utilize an air pre-heater, however. In the present application, for example, the combustion air is not at the temperature of the surroundings, as it is at the air pre-heater entrance of a fired steam generator; but has already been heated by the work of compression in the compressor of the gas turbine cycle.

The useful work output of the steam cycle is the product of cycle efficiency and heat received. For the waste heat application, even though the steam cycle efficiency may be increased by regenerative feed heating, the heat received is reduced; and the product of the two may or may not be greater than for the cycle without regenerative feed heating. The cycle conditions which will yield the maximum work must be determined by numerical calculations.

Another consideration is the economic restriction on steam generator size. Let us consider that the number of square meters of heat transfer surface for a given size plant is fixed by economic considerations. The heat transfer coefficient between condensing steam and the metal tubes of a regenerative feed heater is much greater than that between hot exhaust gases and the metal of an economizer surface. Any savings in economizer size can be used to increase boiler and superheater surfaces; thus decreasing the mean temperature difference between gas and steam (or water) in those units. Thus, for a fixed temperature of exhaust (from the gas turbine) at the steam generator entrance, we can generate more steam per kilogram exhaust gas, or generate it at a higher temperature and pressure, or both. The former effect would

increase the heat received by the steam cycle per kilogram of exhaust gas; the latter would increase steam cycle efficiency.

For the numerical calculations we need to know the reduction in specific steam turbine output caused by bled steam leaving the turbine before full expansion to condenser pressure. To estimate this reduction in output, the method used is essentially that developed by *J. K. Salisbury* [37]. The basic theory is somewhat involved, and only its application to the present study is herein outlined. A detailed development may be found in the quoted reference.

The Salisbury method considers only the steam cycle portion of a normal steam plant, and assumes that steam generator stack losses can be held constant by increasing the size of the air preheater as necessary to hold stack exit temperature constant. The terms "heat supplied" and "heat rejected" refer only to heat to and from the steam (or water). The method cannot, therefore, be extrapolated to a waste heat plant, including the entire steam generator, without taking account of possible additional stack losses.

The steam plant of the present study includes not only the steam cycle, but also the gas side of the steam generator; and the final results are considerably different from those given in the curves and tables of [37]. Nevertheless, with the true meanings of "heat supplied", "heat rejected", and "reduction in heat rate" in mind, the method can be used to estimate with more than adequate accuracy the reduction in turbine output occasioned by bleeding steam for use in a regenerative feed heating system; since the method is equally accurate for any steam cycle, regardless of the gas-side losses in the steam generator.

Salisbury has found that the enthalpy difference between steam extracted from an actual turbine and saturated water at the same temperature is approximately constant along the turbine state line. If this enthalpy difference is plotted against the fractional rise above hotwell enthalpy (denoted by χ, and defined as the actual rise of feedwater enthalpy in the regenerative feed heating system divided by maximum possible rise if heated to saturation at boiler pressure), the resulting curve can be accurately approximated by a quadratic equation. This enables analytical integration of the equations developed in [37] to represent the reduction in heat rate theoretically possible by regenerative feed heating in an infinite number of feed heaters (of zero terminal temperature difference and zero pressure loss) from hotwell temperatures to saturation temperature at boiler pressure.

This maximum reduction (denoted by G) has been calculated for various turbine inlet steam conditions, and the results given in curves and tables. The percentage of possible gain (denoted by P) obtainable for various χ with various finite numbers of heaters is also developed, calculated, and plotted. Finally, an equation for the reduction in specific turbine work is developed.

Denoting turbine initial steam enthalpy by i_0, enthalpy of feed water after regenerative heating by i_e, and enthalpy of the condensate by i_c:

$$\frac{\text{specific work with bleeding}}{\text{specific work without bleeding}} \equiv B = \frac{\frac{i_0 - i_e}{i_0 - i_c}}{(1 - P\,G)} \tag{5.6}$$

For the cycle presently under study, the reduction factor B was calculated for various χ, and multiplied by the non-extraction specific turbine work to obtain the specific work curves of figure 20. Here L_n is defined as the specific turbine work in kilojoules of shaft work per kilogram throttle steam. The numerical subscript denotes the "percentage preheating", or fractional rise above hotwell enthalpy (χ). Thus $L_{n_{100}}$ is the specific net turbine work for a cycle in which the feedwater is preheated by bled steam from condenser hotwell temperature (30 C) to the saturation temperature corresponding to boiler pressure (100% preheating).

To determine P, it was necessary not only to choose an appropriate χ, but also to select a practical number of feed heaters. Using existing steam plants as a guide, the number of heaters selected was the nearest integral number to that which would yield 85% of the gain possible using an infinite number of heaters to accomplish the "percent preheating" in question. Using this criterion, in no instance would an additional heater yield more than a $2^1/_2\%$ improvement in a gain which is in any case rather modest.

VI. Steam Generator

VI.1. Basic design considerations

The design of the steam generator depends on its location in the combined steam turbine-gas turbine cycle. If the steam cycle is to receive all of its initial heat from the exhaust of the gas turbine cycle, the steam generator is the familiar waste heat boiler in widespread industrial use. If the steam generator is utilized ahead of the gas turbine, as a method of cooling the very hot combustion gases down to the maximum permissible gas turbine inlet temperature (instead of the more common procedure of using great amounts of excess air), the steam generator would bear more resemblance to the combustion chamber of a Velox steam generator. The Velox steam generator is, in fact, a combined cycle in which the steam turbine produces almost all of the useful work.

More attractive still is a combination of the two, wherein the steam cycle condensate first receives heat from a "waste heat boiler" in the gas turbine exhaust; and then passes through tubes in the combustion chamber, where the heat required to bring the additional steam to its desired final state is received.

Let us consider first the problem of the steam generator whose heat is entirely supplied by the thermal energy of the gas turbine exhaust. This poses perhaps the most critical problem of the combined steam turbine-gas turbine cycle. Were we restricted only by the first law of thermodynamics, which provides that energy be mutually exchanged or converted from one form to another without creation or destruction of any portion thereof, we might expect that we could fully utilize the energy of the exhaust gases to generate steam at any desired temperature and pressure. The second law of thermodynamics, however, requires that the heat transfer of energy involve an increase of entropy at each point. If we isolate any infinitesimally small system, consisting of a particle of flue gas, a section of tube wall, and a particle of water (or steam), the heat transfer will take place only in that direction which involves an increase in the total entropy of this isolated system; i. e., from a region of higher temperature to one of lower temperature. This requires that we exclude from consideration any steam generator process wherein the temperature of the combustion gases at any point is equal to or less than the water (or steam) temperature.

This second law requirement is qualitative only — the above temperature difference must exist at all points. Far more stringent is the quantitative restriction imposed by practical economic considerations — namely, the temperature difference must be at all points sufficiently large that, when considered in conjunction with the heat flow required and the heat transmission coefficient practically obtainable, the resultant steam generator is of reasonable size. The quantitative evaluation of this restriction is the engineering problem now developed in greater detail.

VI.2. Temperature difference as related to heat transfer surface

Referring to the notation of figure 21, the heat transferred from the flue gases to the steam in the superheater is, viewed from the gas side:

$$\dot{Q}_S = \dot{m}_g \bar{c}_{p_S} (t_{g_1} - t_{g_2}) = k_S F_S \overline{\Delta t}_S \tag{6.1}$$

where $\bar{c}_p$ ≡ mean specific heat of flue gases, at constant pressure $\left(\frac{\text{kj}}{\text{kg C}}\right)$

F ≡ heat transfer surface (m^2)

k ≡ heat transmission coefficient $\left(\frac{\text{kj}}{\text{m}^2\,\text{C sec}}\right)$

$\dot{m}_g$ ≡ mass flow of gas (kg/sec)

$\dot{Q}$ ≡ heat flow (kj/sec)

t_{g_1}, t_{g_2} ≡ gas temperatures at superheater inlet and outlet, respectively (C)

$\overline{\Delta t}$ ≡ logarithmic mean temperature difference

$$\equiv \frac{\Delta t_2 - \Delta t_1}{\ln \frac{\Delta t_1}{\Delta t_2}}$$

Subscript S refers to superheater.

$$F_S = \frac{\dot{m}_g \bar{c}_{ps} (t_{g_1} - t_{g_2})}{k_S \overline{\Delta t}_S} = \frac{\dot{m}_g \bar{c}_{ps} \Theta_S}{k_S} \tag{6.2}$$

where $\Theta_S \equiv \frac{t_{g_1} - t_{g_2}}{\overline{\Delta t}_S}$, a dimensionless expression of temperature difference.

Similarly for the boiler section

$$F_B = \frac{\dot{m}_g \bar{c}_{pB} \Theta_B}{k_B} \tag{6.3}$$

And for the economiser

$$F_E = \frac{\dot{m}_g \bar{c}_{pE} \Theta_E}{k_E} \tag{6.4}$$

If we define $\bar{k}$ as the weighted mean of k_S, k_B, and k_E; and further determine a mean gas specific heat for the steam generator, $\bar{c}_p$, we can combine the above to obtain

$$F = F_S + F_B + F_E = \frac{\dot{m}_g \bar{c}_p}{\bar{k}} (\Theta_S + \Theta_B + \Theta_E)$$

or

$$F = \frac{\dot{m}_g \bar{c}_p}{\bar{k}} \Sigma \Theta \tag{6.5}$$

This gives us a measure of the steam generator size (and to a lesser extent, the cost) in terms of the temperature differences between flue gas and water (or steam).

VI.3. Determination of heat transmission and heat transfer coefficients

The resistance to convective heat transmission from flue gas to water (or steam) is the summation of the heat transfer resistances through the gas side and water side boundary layers, plus the resistances of tube wall, scale and soot. Assuming smooth tubes and negligible heat transfer by radiation at the temperatures involved:

$$\frac{1}{\bar{k}} = \frac{1}{h_g} + \frac{1}{\frac{D_i}{D} h_w} + \frac{\vartheta}{\bar{\lambda}} \tag{6.6}$$

h_g, h_w ≡ heat transfer coefficients, gas side and water side $\left(\frac{\text{kj}}{\text{m}^2\,\text{C}\,\text{sec}}\right)$

D ≡ Outer tube diameter (m)

D_i ≡ Inner tube diameter (m)

ϑ ≡ tube wall thickness, including deposits (m)

$\bar{\lambda}$ ≡ average wall thermal conductivity $\left(\frac{\text{kj}}{\text{m}\,\text{C}\,\text{sec}}\right)$

In well maintained steam generators the last two terms of equation (6.6) are generally small in comparison to the first. We therefore make no great

error in assuming [6] that the heat transmission coefficient k is a constant factor times the gas side transfer coefficient, or

$$k = \epsilon h_g \tag{6.7}$$

Experimental measurements of h_g have been correlated by several authorities. The arrangement usually encountered in steam generators is cross flow of gases, to obtain favorable heat transfer coefficients, in several passes so arranged as to approximate parallel flow of fluids in the steam generator as a whole.

The following heat transfer data for cross flow of hot gases over tube tanks have been reduced to a common form for comparison:

Traupel [46]:

$$\mathrm{Nu} = 0.315\,\sigma\,\frac{T_g}{T_B}\,\mathrm{Re}^{0.61}\,\mathrm{Pr}^{0.31} \tag{6.8}$$

McAdams [27]:

$$\mathrm{Nu} = 0.26\,\mathrm{Re}^{0.6}\,\mathrm{Pr}^{1/3} \tag{6.9}$$

for average σ, in-line tube banks.

Grimison [13], for air:

$$\mathrm{Nu} = 0.284\,\sigma\,\mathrm{Re}^{0.61} \tag{6.10}$$

In the above:

$\mathrm{Nu} \equiv \dfrac{h\,D}{\lambda} \equiv$ Nusselt number (dimensionless)

$\mathrm{Pr} \equiv \dfrac{c_p\,\mu}{\lambda} \equiv$ Prandtl number (dimensionless)

$\mathrm{Re} \equiv \dfrac{D\,w\,\gamma_B}{\mu} \equiv$ Reynolds number (dimensionless)

$T_B \equiv$ reference temperature (absolute scale) for heat transfer, defined as the mean of the tube wall and gas temperatures (i. e., the mean temperature of the boundary layer) (C)

$T_g \equiv$ absolute gas temperature (C)

$w \equiv$ gas velocity, at narrowest cross section of tube bank (m/sec)

$\gamma_B \equiv$ gas density, calculated at reference temperature T_B, (kg/m^3)

$\sigma \equiv$ tube arrangement factor (dimensionless)

$\mu \equiv$ viscosity $\left(\dfrac{\mathrm{kg}}{\mathrm{m/sec}}\right)$

It is widely agreed (e. g., [8], [16], [27], [41], [46], [49] that Nu is approximately proportional to $\mathrm{Pr}^{1/3}$. This allows adaption of the *Grimison* data for gases other than air. Throughout the steam generator calculations, the data for air is first used. Later a method is indicated for correcting the results for varying proportions of stoichiometric gas and excess air.

The expressions of *Traupel* and *McAdams* are based in part on the data originally correlated by *Grimison*. In addition, for the temperatures considered in this study, the following equation yields a good average of the expressions quoted above:

$$\mathrm{Nu} = 0.318\,\sigma\,\mathrm{Re}^{0.61}\,\mathrm{Pr}^{0.32} \tag{6.11}$$

Values of σ can be obtained from [13], (σ = *Grimison*'s F_a); or from [15] or [38] ($\sigma = f_a$ in the last two references).

Combining with the definition of the Nusselt number,

$$h_g = 0.318\,\frac{\lambda}{D}\,\sigma\,\mathrm{Re}^{0.61}\,\mathrm{Pr}^{0.32} \tag{6.12}$$

and with equation (6.7),

$$\bar{k} = \epsilon\, h_g = 0.318\,\epsilon\,\frac{\lambda}{D}\,\sigma\,\mathrm{Re}^{0.61}\,\mathrm{Pr}^{0.32} \tag{6.13}$$

Combining with (6.5), and introducing the continuity relationship

$$\dot{m}_g = w\,\gamma\,f \tag{6.14}$$

where $f \equiv$ minimum cross-sectional flow area (m^2), we obtain

$$\Sigma\Theta = 0.318\,\epsilon\,\sigma\,\frac{F}{f}\,\frac{\lambda}{D\,w\,\gamma\,\bar{c}_p}\,\mathrm{Re}^{0.61}\,\mathrm{Pr}^{0.32} \tag{6.15}$$

But $\frac{\lambda}{D\,w\,\gamma\,\bar{c}_p}$ is the reciprocal of a dimensionless grouping defined as the Pèclet number

$$\mathrm{Pè} = \mathrm{Re}\,\mathrm{Pr}. \tag{6.16}$$

Thus, in its simplest form, the heat transfer equation becomes the following relationship between solely dimensionless groupings:

$$\Sigma\Theta = \frac{0.318}{\mathrm{Re}^{0.39}\,\mathrm{Pr}^{0.68}}\,\epsilon\,\sigma\,\frac{F}{f} \tag{6.17}$$

This is recognized as a form similar to those sometimes appearing in analyses of optimal size of heat exchanger equipment.

For this study the analysis is clearer if the heat transfer equation is transformed to demonstrate directly the effect of manipulation of various physical design parameters (as opposed to dimensionless groupings). To this purpose, (6.13) is combined with (6.5) to obtain:

$$\Sigma\Theta = 0.318\,\epsilon\,\sigma\,F\left(\frac{\lambda}{\dot{m}_g\,\bar{c}_p\,D}\right)\mathrm{Re}^{0.61}\,\mathrm{Pr}^{0.32} \tag{6.18}$$

VI.4. Determination of Reynolds number

$\mathrm{Re} \equiv \frac{D\,w\,\gamma_B}{\mu}$, wherein γ_B and μ are determined by use of the reference temperature T_B.

The gas velocity w is dependent upon the pressure drop (Δp) across the tube banks. From [13] and [46]:

$$\Delta p = {}_l\zeta\, z\, \gamma_b \frac{w^2}{2}$$

or

$$z_l = \frac{2\,(\Delta p)}{\zeta\, \gamma_b\, w^2} \tag{6.19}$$

Herein: z_l ≡ number of tube rows longitudinal to gas flow
γ_b ≡ gas density, evaluated at the reference temperature T_b (kg/m³)
Δp ≡ pressure drop across tube banks (kg/m sec²)

ζ can be obtained from the articles of *Grimison* [13] or *Hofmann* [16]. (ζ is identical with *Hofmann's* ξ; or for *Grimison*'s friction factor f, $\zeta = 4f$). For calculating the pressure drop due to frictional resistance, a different reference temperature is used than that found best for correlation of heat transfer data. This empirical reference temperature is

$$T_b = T_g - 0.1\,(T_g - T_{wall}) \text{ for in-line banks} \tag{6.20}$$

or

$$T_b = T_g - 0.2\,(T_g - T_{wall}) \text{ for staggered banks} \tag{6.21}$$

Both staggered and in-line banks are commonly found in steam generators. *Grimison* [13] has found it convenient to standardize his heat transfer and flow friction data with reference to the characteristics of in-line banks with transverse tube spacing (s_t) equal to $1^3/_4$ tube diameters, and longitudinal tube spacing (s_l) equal to two tube diameters. The numerical calculations of this work are also based on this standard. Effects of deviation therefrom are evaluated in paragraph VII.7.

Denoting the number of tube rows in the direction transverse to gas flow by z_t, and the tube length by l, the cross sectional flow area f for flow across in-line banks of round tubes is

$$f = z_t\,(s_t - D)\,l \tag{6.22}$$

or

$$z_t\, l = \frac{f}{(s_t - D)} \tag{6.23}$$

The total gas side heat transfer area F is

$$F = z_l z_t \pi D\, l = \pi z_t D\,(z_l\, l) = \pi z_l \left(\frac{D}{s_t - D}\right) f \tag{6.24}$$

By continuity considerations

$$\dot{m}_g v = \frac{\dot{m}_g}{\gamma_b} = f w \tag{6.25}$$

or

$$f = \frac{\dot{m}_g}{w\, \gamma_b} \tag{6.26}$$

Substituting in (6.24): $F = \pi \cdot z_l \left(\frac{D}{s_t - D}\right) \frac{\dot{m}_g}{w\, \gamma_b}$ (6.27)

Utilizing:

$$z_l = \frac{2\,(\Delta\, p)}{\zeta\, \gamma_b\, w^2} \tag{6.19}$$

$$F = \frac{2\,\pi\,(\Delta\, p)\left(\frac{D}{s_t - D}\right)\dot{m}_g}{\zeta\, {\gamma_b}^2\, w^3} \tag{6.28}$$

or

$$w = \sqrt[3]{\frac{2\,\pi\,(\Delta\, p)\left(\frac{D}{s_t - D}\right)\dot{m}_g}{\zeta\, {\gamma_b}^2\, F}} \tag{6.29}$$

Therefore

$$\mathrm{Re} = \frac{D\, w\, \gamma_B}{\mu} = \frac{\gamma_B\, D}{\mu}\sqrt[3]{\frac{2\,\pi\,(\Delta\, p)\left(\frac{D}{s_t - D}\right)\dot{m}_g}{\zeta\, {\gamma_b}^2\, F}} \tag{6.30}$$

VI.5. Generalized Steam Generator Heat Transfer Relationship

Combining (6.30) with

$$\Sigma\Theta = 0.318\,\epsilon\,\sigma\, F\frac{\lambda}{\dot{m}_g\, c_p\, D}\,\mathrm{Re}^{0.61}\,\mathrm{Pr}^{0.32} \tag{6.18}$$

we obtain

$$\Sigma\Theta = 0.318\,\epsilon\,\sigma\, F\left(\frac{\lambda}{\dot{m}_g\, c_p\, D}\right)\frac{{\gamma_B}^{0.61}\, D^{0.61}}{\mu^{0.61}}\left[\frac{2\,\pi\,(\Delta\, p)\left(\frac{D}{s_t - D}\right)\dot{m}_g}{\zeta\, {\gamma_b}^2\, F}\right]^{0.203}\mathrm{Pr}^{0.32} \tag{6.31}$$

Substituting $\dfrac{\lambda}{c_p\,\mu} = \dfrac{1}{\mathrm{Pr}}$ and $2\,\pi = 6.283$

we obtain the generalized relationship:

$$\Sigma\Theta = 0.462\,\epsilon\,\sigma\left(\frac{F}{\dot{m}_g}\right)^{0.797}\left(\frac{\mu}{D}\right)^{0.39}{\gamma_B}^{0.61}\left[\frac{(\Delta\, p)\left(\frac{D}{s_t - D}\right)}{\zeta\, {\gamma_b}^2}\right]^{0.203}\mathrm{Pr}^{-0.68} \tag{6.32}$$

This equation relates explicitly the various steam generator parameters which are available for essentially independent variation by the design engineer.

The heat transfer relationships have been developed in some detail for the "waste heat" position since, as will be shown in the next chapter, economic considerations place a stringent limit on the proportion of the available thermal energy of the gas turbine exhaust which can be transferred to the steam cycle under these conditions.

Although illustrated for the case of the waste heat steam generator, the relationships are general; and would also hold — insofar as the empirical relationships of (6.9), (6.10) and (6.11) apply — to convective heat transfer for a steam generator placed between the combustion chamber and the gas turbine. Actually, such a steam generator would be integral with the combustion chamber, and a goodly portion of the heat transfer would be by radiation. This, combined with the observation that the gas side heat transfer coefficients would be somewhat better by higher pressures, and that the

temperature differences would be *much* higher, would mean that the heat transfer surface (F) for a steam generator in this position would be but a small fraction of that for the waste heat steam generator.

One easily sees that the economic limitations on size do not apply to a steam generator in this position. For the thermodynamic analysis, we know that we can economically and practically extract from the combustion gases whatever heat is required to bring the gas temperature to that desired at the gas turbine inlet.

VII. Steam Cycle

VII.1. Steam generator size as related to steam plant output

As mentioned in the last chapter, one of the most difficult problems in the analysis of the combined steam turbine-gas turbine cycle is the quantitive evaluation of the economic restriction on the amount of gas turbine exhaust heat that may be transferred to the steam cycle. Since the temperatures involved are relatively low, the problem is primarily one of size — of the number of square meters of heat transfer surface required. The heat transfer surface economically feasible is of course related closely to the power output of the plant; and may perhaps best be expressed by the quantity $\frac{F}{N}$, the number of square meters of heat transfer surface per kilowatt output of the plant under consideration.

Defining:

$L_n \equiv$ specific net steam turbine shaft work per kilogram of steam (kj/kg)
$L_N \equiv$ specific net steam turbine shaft work per kilogram of combustion gases (kj/kg)
$\dot{m}_g \equiv$ mass rate of flow of combustion gases (kg/sec)
$\dot{m}_w \equiv$ mass rate of flow of steam (kg/sec)
$M \equiv$ flow ratio $\dot{m}_g/\dot{m}_w$ (dimensionless)

$$N \equiv \dot{m}_w L_n \tag{7.1}$$

where L_n can be obtained from the curves of figure 20, chapter V. Further,

$$N = \dot{m}_g L_N \tag{7.2}$$

and

$$L_N = L_n(\dot{m}_w/\dot{m}_g) = L_n/M \tag{7.3}$$

Substituting equation (7.2) in equation (6.32):

$$\Sigma\Theta = 0.462\,\epsilon\,\sigma\,{L_n}^{0.797}\left(\frac{F}{N}\right)^{0.797}\left(\frac{\mu}{D}\right)^{0.39}{\gamma_B}^{0.61}\left[\frac{(\Delta p)\left(\frac{D}{s_t - D}\right)}{\zeta\,{\gamma_b}^2}\right]^{0.203}\mathrm{Pr}^{-0.68} \tag{7.4}$$

With the aid of equation (7.4), figures 20 and 21, and experience data that will enable us to intelligently fix the remaining parameters, we can now determine the steam generator size which will result under various selections of gas turbine exhaust temperature (t_{g_1}), initial steam conditions (t_{w_1} and p_0), and feed water temperature at economiser inlet (t_{w_4}).

VII.2. Numerical evaluation of cycle parameters with steam generator in "waste heat" position

To evaluate equation (7.4), the various design parameters are assigned numerical values which are consistent with current good design practice. In paragraph VII.7 means are outlined for adjusting the finally obtained results to correspond with any desired variation in any of these arbitrarily assigned values.

Grimison's correlations [13] are based on a standard of in-line banks, $s_t = 1^3/_4 D$, $s_l = 2D$, for which case $\sigma = 1$.

Hence $$\left(\frac{D}{s_l - D}\right) = {}^4/_3 = 1.333.$$

Tube diameter D is assumed at 38 mm (0.038 m). From [6], $\epsilon \approx 0.9$.

From [13], for the above conditions and

$$2000 < \mathrm{Re} < 30{,}000: \ \zeta = 4 \times 0.071 = 0.284.$$

From operating data, the pressure drop in a steam generator is generally less than 0.015 ata. It may be expected that the waste heat steam generator may be larger than one that is fired; on the other hand the pressure lost to assure good mixing in the combustion process is charged to the combustion chamber of the gas turbine and not to the steam generator. Therefore $\Delta p = 0.015$ ata ($\approx 1500\,\mathrm{kg/m\,sec^2}$) is chosen. (For the cycle calculations, an additional 0.005 ata pressure drop in the ducting between the gas turbine and the steam generator is assumed.)

$$\gamma = \frac{p}{RT} = \frac{356}{T} \tag{7.5}$$

γ_B is to be evaluated at temperature T_B; and γ_b at T_b.

Grouping all properties that are dependent functions of T_B alone, and defining

$$\Lambda \equiv \left(\frac{\mu^{0.39}}{\mathrm{Pr}^{0.68}\, T_B{}^{0.61}}\right) = \left(\frac{\lambda^{0.68}}{c_p{}^{0.68}\, \mu^{0.29}\, T_B{}^{0.61}}\right) \tag{7.6}$$

equation (7.4) becomes

$$\Sigma\Theta = 29.8 \left(\frac{F}{N}\right)^{0.797} L_N{}^{0.797}\, T_b{}^{0.407}\, \Lambda \tag{7.7}$$

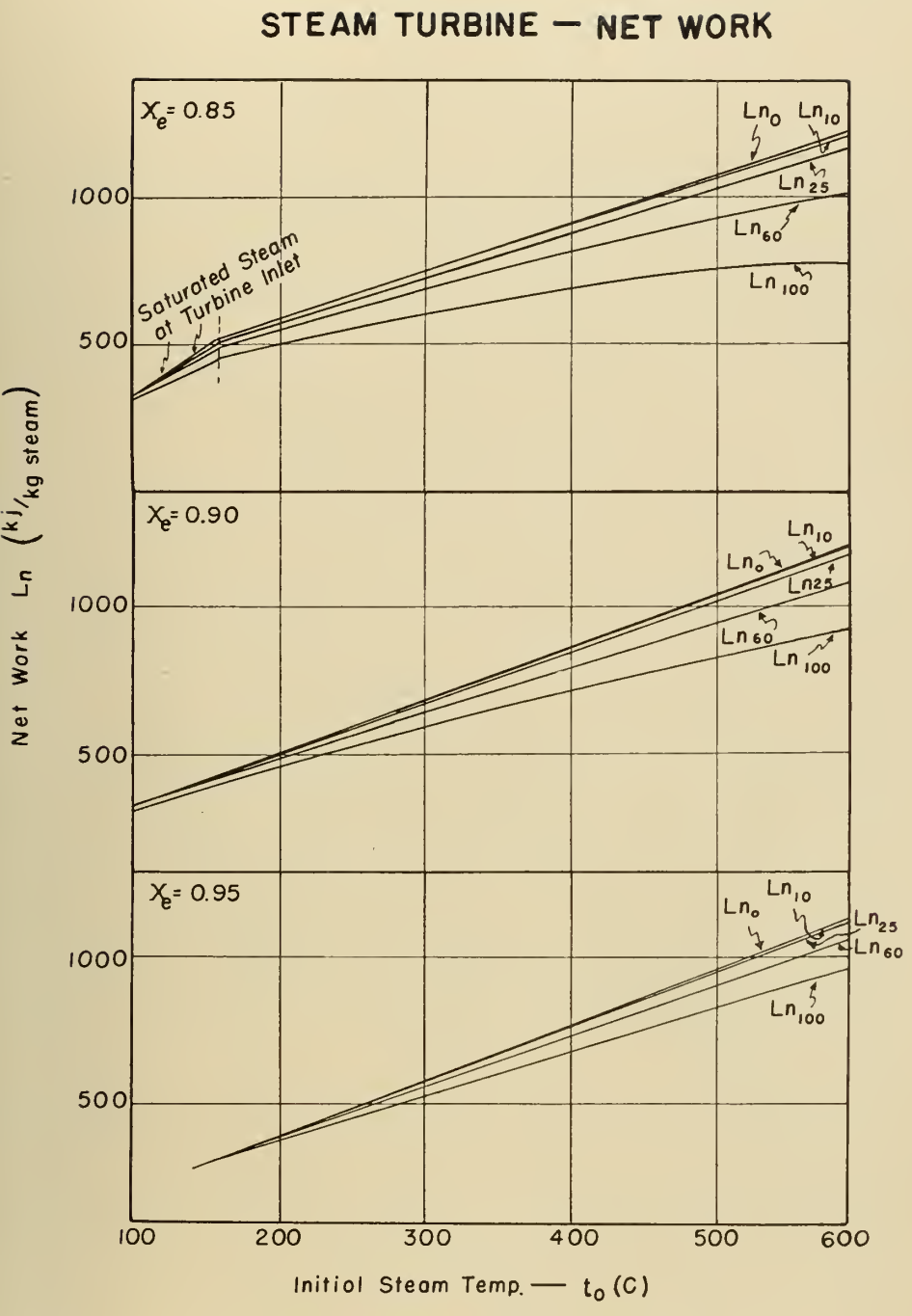

Fig. 20. Net steam turbine work.

As developed in chapter VI, $\Sigma\Theta$ is defined by

$$\Sigma\Theta \equiv \Theta_S + \Theta_B + \Theta_E$$

$$\Sigma\Theta = \frac{t_{g_1} - t_{g_2}}{\Delta t_S} + \frac{t_{g_2} - t_{g_3}}{\Delta t_B} + \frac{t_{g_3} - t_{g_4}}{\Delta t_E} \tag{7.8}$$

Although these equations express the steam generator relationships quite simply, the presentation of results will be much clearer if we select our independent and dependent variables in the form of normal steam cycle design parameters. The question of primary interest is: With exhaust gas of a given temperature at our disposal, what is the maximum specific work we can extract therefrom for a given capital investment (i. e., for a given value of F/N)?

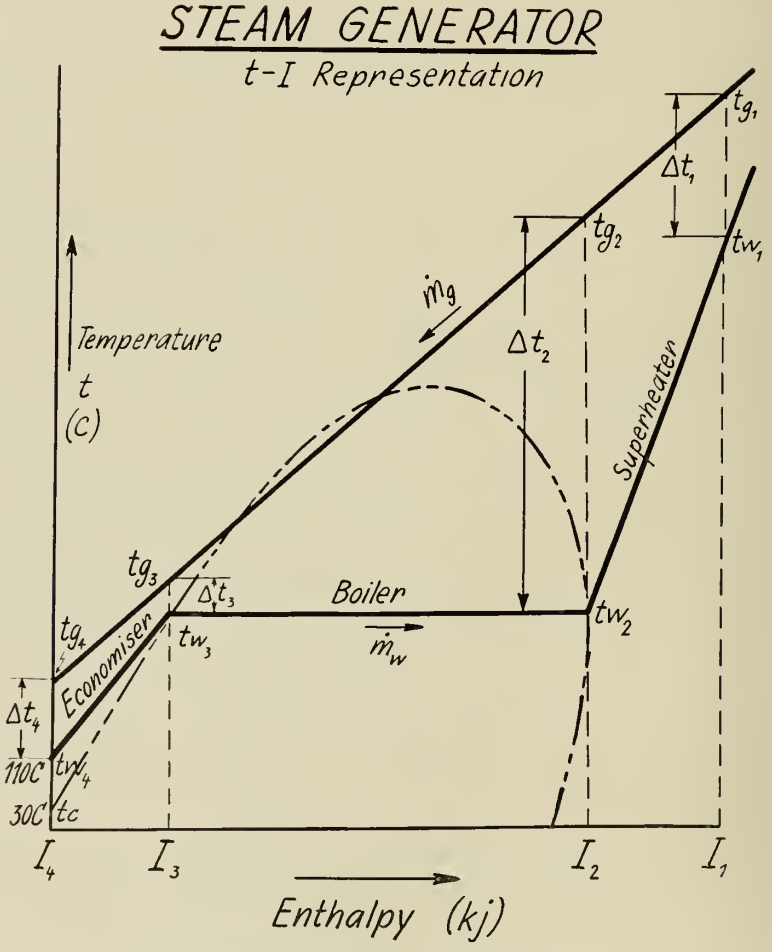

Fig. 21. Steam generator heat transfer diagram.

We can conveniently present the answer to this question in the form of curves if we select t_{g_1}, F/N and L_N as three of our design variables.

L_N is calculable from

$$L_N = L_{n/M} \tag{7.3}$$

L_N is in turn a function of t_{w_1} and p_0; or as developed in paragraph V.3, of t_{w_1} and X_e. If regenerative feed heating is used (paragraph V.4), L_N is also a function of χ. These relationships are graphed in figure 20.

t_{w_2} and t_{w_3} are dependent on p_0; or alternatively on X_e and t_{w_1}. Thus selecting t_{w_1}, X_e, and t_{w_4} as independent variables will fix all waterside temperatures and enthalpies; and by adding χ as an independent variable we can readily determine L_N.

If we also select t_{g_1} and M as independent variables we can calculate t_{g_2} from the following relationships:

$$\dot{m}_g \bar{c}_{p_s} (t_{g_1} - t_{g_2}) = \dot{m}_w (i_{w_1} - i_{w_2}) \tag{7.9}$$

or

$$M \bar{c}_{p_s} (t_{g_1} - t_{g_2}) = (i_{w_1} - i_{w_2}) \tag{7.10}$$

Similar expressions enable calculation of t_{g_3} and t_{g_4}.

Δ is a function of T_B alone, and T_B and T_b can be calculated from the gas and waterside temperatures. Δt_S, Δt_B, and Δt_E are also functions of these temperatures.

The design parameters in which we are interested are therefore:

$$L_N,\ \chi,\ F/N,\ t_{g_1},\ X_e,\ M,\ t_{w_1}, \text{ and } t_{w_4}.$$

Let us now consider the feedwater temperature t_{w_4}. As discussed in paragraph V.4, we do not expect regenerative feed heating to yield the same results in this application that we are accustomed to obtain in a normal steam cycle. To investigate what *may* be obtained, we can sometimes systemize the calculations by making t_{w_4} dependent upon the fractional rise above hotwell enthalpy, χ, which can be more systematically varied than can t_{w_4} independently. This would eliminate t_{w_4} as an independent variable for these instances. Any other means of feedwater preheating (such as by the heat of cooling in the compressor intercooler of the gas turbine cycle) can then be related to this variable.

VII.3. Considerations of flue gas corrosion, as affected by feedwater temperature

We have, however, another important restriction on the variation of feedwater temperature. This is the occurrence of severe economiser corrosion if t_{w_4} is allowed to fall too low. It is therefore necessary to consider briefly how this limit can be properly reflected in the steam cycle calculations.

The occurrence of corrosion at the cold end of economisers and air preheaters has been the subject of long investigation. It has been ably and widely

discussed in the literature (e. g. [14], [17], [20], [21], [36]); but, unfortunately, the theory is somewhat complex, and complete agreement among investigators is lacking. For this study, therefore, it will suffice to outline the problem only in sufficient detail to justify the selected numerical evaluation of this limit for the particular case in hand.

The corrosion in question appears to be due primarily to the formation of sulfur trioxide (SO_3) during the combustion process. If the temperature of the flue gases falls below the dew point upon contact with a metal surface, the water vapor in the flue gas will condense on the cool surface. The moisture and the SO_3 will combine to form a dilute solution of sulfuric acid (H_2SO_4), which will rapidly corrode the metal surface.

The pre-determination of the flue gas dewpoint temperature is not a simple matter, however. It is strongly affected by the presence of SO_3, and to some extent by SO_2 and other gases. For example [17], if only 0.002% of SO_3 is added to moist air with a 50 C dewpoint, the dewpoint is raised to 150 C. The presence of hygroscopic materials, such as flue dust and certain corrosion products, will also markedly raise the dewpoint [18].

The formation of SO_3 in the combustion process (or the later oxidation of SO_2 to SO_3) is affected by the temperature at which the reaction takes place, and by the time the gases remain at that temperature. It is also affected by the amount of oxygen available (the amount of excess air in the combustion process). The maximum reaction takes place [14] at about 40% excess air (if air is presumed saturated with moisture), and becomes progressively higher with decreasing temperature. However, since the reaction time is greatly increased at lower temperatures, probably most of the uncatalysed reaction takes place only at combustion chamber temperatures.

Even if the above factors were calculable, the question of SO_3 formation is rendered much more complex by the action of various catalytic agents. *Gumz* [14] credits V_2O_5 and Fe_2O_3 as accelerating agents, and discusses the inconsistent effect of various inhibiting agents. *Karlsson* and *Hammond* [21] mention activated carbon (at temperatures in excess of 1000 C) as an accelerating catalyst; *Johnstone* [20] blamed ferric sulfate. In any case, there does not seem to be much doubt but that the amount and the nature of the unburned particles in the combustion process influence the formation of SO_3. Combined with the hygroscopic effects of flue dust and of any deposits on the economiser tube banks, these greatly influence the flue gas dewpoint and the ensuing corrosion. Good combustion and maintenance of clean equipment are essential to avoiding difficulty with today's fuels.

In the final analysis most agree that, in the light of present knowledge, only an empirical approach to the problem has much promise of success. The dewpoint is dependent primarily on economiser (or air-heater) metal temperature, and is little affected by flue gas temperature. From empirical data, a

correlation can be made between safe minimum metal temperature and fuel sulfur content, for various types of fuel, e. g. [21]. From this data it can be deduced that, for practically all fuels likely to be encountered, a safe temperature for the entering feedwater is about 110 C. Consequently, the steam cycle calculations have been carried out with this minimum value for t_{w_4}.

In the practical installation this could be obtained by preheating the condensate from hotwell temperature (assumed at 30 C) to 110 C by bled steam from the final turbine stages. This would cause a minor loss of turbine work. An alternate scheme would be to recirculate a portion of the feedwater from the economiser outlet to the economiser inlet. In this case the stack gases would be cooled to the same temperature as though the condensate entered the economiser at hotwell temperature; but since the mean gas-to-water temperature difference would be less, a larger economiser would be required.

In the following calculations, to allow χ to be a completely independent variable, recirculation as outlined above is presumed for all cases in which the entering feedwater temperature would otherwise be less than 110 C. t_{w_4} is therefore either fixed at 110 C, or is a dependent function of χ; and we can eliminate it from further discussion of variables in the numerical calculations.

The remaining variables are now t_{g_1}. M, t_{w_1}, X_e, χ, F/N and L_N. Only five of these are independent. For example, if we independently select values for t_{g_1}, M, t_{w_1}, X_e, and χ, we have fixed all gas and waterside temperatures, can calculate L_N from figure 20 and equation (7.3), can calculate $\Sigma\Theta$ from equation (7.8) and can determine F/N from equation (7.7). F/N and L_N would then be dependent variables.

What we are primarily interested in, however, is to determine the maximum L_N for a *fixed* F/N and a given t_{g_1}. We would thus like to retain F/N as an independent variable. This is somewhat difficult to carry out, since all of the five variables t_{g_1}, M, t_{w_1}, X_e, and χ are required to fix all gas and waterside temperatures, all of which are initially needed to avoid complications in the calculation of the logarithmic mean temperature differences $\overline{\Delta t}_S$, $\overline{\Delta t}_B$, and $\overline{\Delta t}_E$.

One method of attaining the desired result is to select six independent variables, and separately solve equations (7.7) and (7.8) for $\Sigma\Theta$. The results will in general not agree; but if we adjust one of the independent variables and repeat the calculations, we can attain agreement in a series of successive approximations.

Several approaches have been tried, as the calculations are in any case quite laborious. The one found most effective is first to hold χ, t_{g_1}, F/N, X_e, and M fixed, and vary t_{w_1} until the two $\Sigma\Theta s$ calculated from equations (7.7) and (7.8) are in agreement. This is repeated for various values of M and X_e. Plotting the resulting values of L_N against the two independent variables X_e and M gives a curved three dimensional surface. The highest point of this

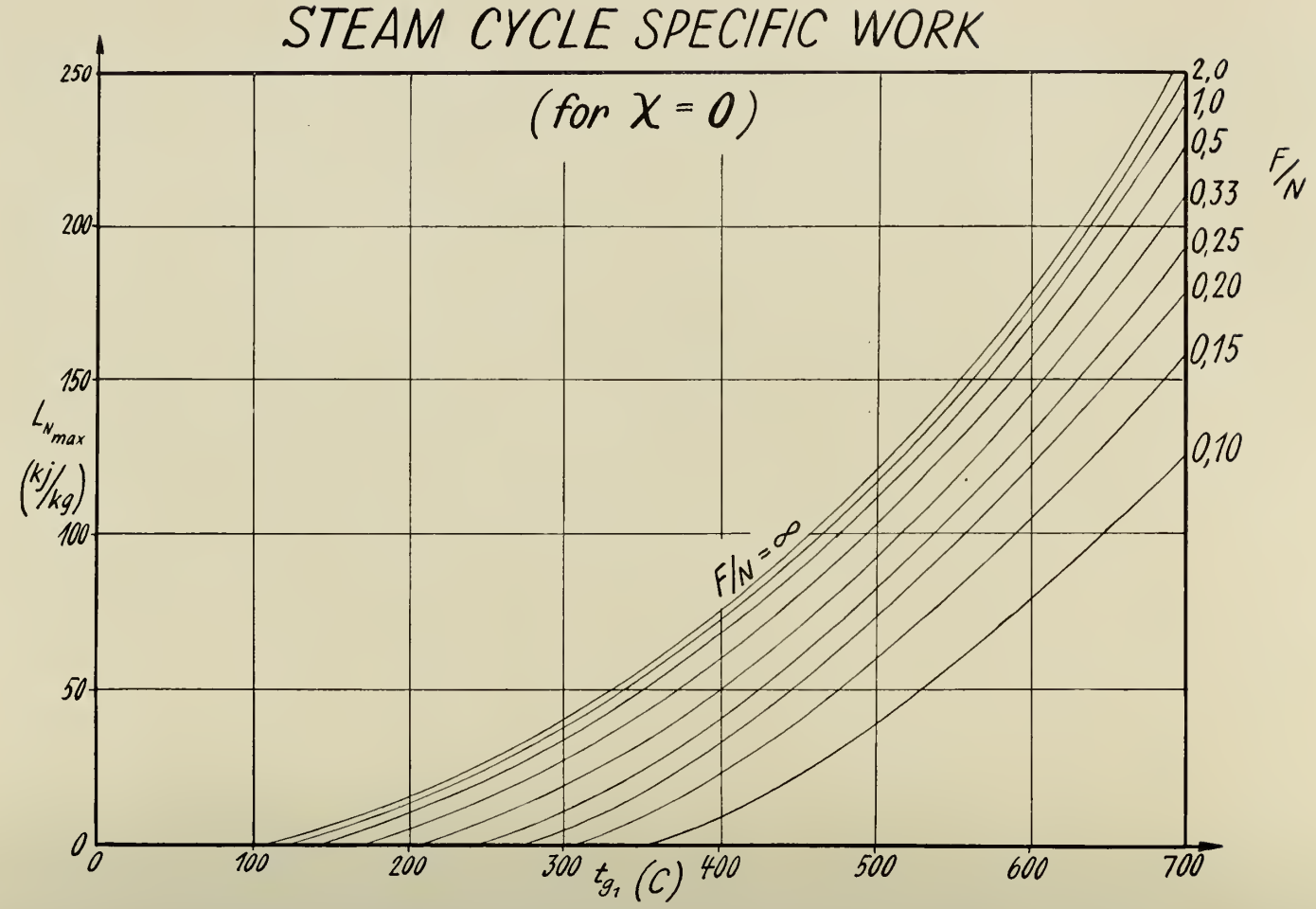

Fig. 22. Steam cycle specific work (as function of steam generator inlet temperature and size).

surface represents the maximum L_N for the arbitrarily chosen values of χ, t_{g_1}, and F/N. This value is labeled $L_{N_{max}}$.

The above is repeated for new values of t_{g_1}, and we finally obtain a curve of $L_{N_{max}}$ versus t_{g_1}; F/N and χ held constant. Repeating the entire procedure for various F/N gives a family of curves. Figure 22 is such a family for $\chi = 0$.

VII.4. Graphical solution of steam cycle with steam generator in "waste heat" location

Equation (7.8) may be solved analytically, as described in paragraph VII.5. However, for the great number of calculations required, a graphical solution was found to be quicker. First a $t - I$ diagram is constructed for water, with the aid of the steam tables [25] (as extended by [10]). This consists of the steam dome (– – – – on figure 21), with the lines $t_c \rightarrow t_{w_3} \rightarrow t_{w_2} \rightarrow t_{w_1}$ for various pressures from 1 ata to 300 ata. (Use of a $t - I$ diagram is more convenient for heat transfer work, since the process lines are usually nearly straight.) Using the same temperature and enthalpy scales, a $t - I$ diagram for combustion gases is constructed on transparent paper, utilizing the properties of air listed in the gas tables [23]. Lines for various M are drawn, by multiplying the tabulated i_g for each temperature by the various selected values of M. For example, in figure 21, $I_1 = M\, i_{g_1}$ at every temperature t_{g_1}.

An average stack temperature of 200 C is assumed; and the diagram is drawn with the various M lines radiating from a zero point of $i_4 = 0$, $t_{g_4} = 200$ C. No I or t values are marked on the transparent paper. Thus by sliding this paper vertically, if we could assume no changes in c_p, the diagram would hold equally well for a stack temperature other than 200 C. In actual fact, the error is negligible for the stack temperatures encountered in these calculations. On each pressure line on the steam diagram may also be marked the t_{w_1} which corresponds to an X_e of 0.85, and a line drawn to represent the locus of all such points. This is repeated for $X_e = 0.90$ and $X_e = 0.95$.

The calculation then proceeds as previously outlined (refer figure 21). Denoting fixed values by an asterisk (*), from the selected X_e* and t_{w_1}*, the point (t_{w_1}, I_1) is located on the steam diagram at the intersection of the lines $t = t_{w_1}$* and $X_e = X_e$*. The point (t_{g_1}, I_1) is vertically above (t_{w_1}, I_1) on the line $t = t_{g_1}$*. The transparent combustion gas diagram is moved vertically until the selected line $M = M$* crosses the point (t_{g_1}, I_1), and the combustion gas diagram is then secured in place.

If the point (t_{w_1}, I_1) does not coincide with one of the pressure lines drawn on the diagram, t_{w_2} ($= t_{w_3}$) may be found from equations (5.3), (5.4) or (5.5), or from the more exact curves for this relationship prepared during the turbine calculations. The point (t_{w_2}, I_2) is then the right hand intersection of the $t = t_{w_2}$ line and the steam dome; (t_{w_3}, I_3) is at the left hand intersection;

and the points (t_{g_2}, I_2) and (t_{g_3}, I_3) are on the selected M^* line directly above these two points.

For $\chi = 0$, we know that $t_{w_4} = 110\,\mathrm{C}$, since the hotwell temperature $t_c = 30\,\mathrm{C}$ is below this permissible feedwater temperature. Yet, although the feedwater temperature has been raised from 30 C to 110 C by recirculation, all of the energy required to raise the feedwater temperature from 30 C to t_{w_3} will have to be transferred to the feedwater in the economiser — since this is the only place where transfer of heat to the feed water takes place. Thus I_4 is the enthalpy corresponding to the temperature of the feedwater leaving the preheater (or, for $\chi = 0$, the condenser). $I_4 \neq i_{w_4}$ unless $t_{w_4} > 110\,\mathrm{C}$, in which case no recirculation is required. The heat balance relationships are clearer if the recirculation line is considered a part of the economiser.

The combustion gases must furnish the energy $(I_3 - I_4)$ to the feedwater in the economiser; and the point (t_{g_4}, I_4) is thus located. In actual fact, we have thus altered $\dot{m}_w$ through the economiser, and $M_E \neq M^*$. The feedwater in the economiser will nevertheless be warmed from (t_{w_4}, I_4) to (t_{w_3}, I_3); and the combustion gases must be correspondingly cooled from (t_{g_3}, I_3) to (t_{g_4}, I_4). Therefore, the solid lines $t_{g_3} \rightarrow t_{g_4}$ and $t_{w_3} \rightarrow t_{w_3}$ on figure 21 accurately represent the process on the $t - I$ diagram, as far as the temperature differences in the heat transfer process are concerned.

VII.5. Analytical solution of steam cycle with steam generator in "waste heat" location

Reference is made to figure 21. The selected independent variables are χ^*, $t_{g_1}{}^*$, $(F/N)^*$, $X_e{}^*$, M^* and $t_{w_1}{}^*$. The solution of equation (7.8) is first considered.

Superheater

t_{w_2} can be found from formulæ (5.3) to (5.5). For example, for $X_e{}^* = 0.85$:

$$t_{w_2} = 84.0 + 0.450\, t_{w_1} \tag{5.3}$$

The corresponding saturation pressure is also p_0, which may be found from the steam tables.

$$\dot{m}_g \bar{c}_{p_s} (t_{g_1} - t_{g_2}) = \dot{m}_w (i_{w_1} - i_{w_2}) \tag{7.9}$$

or

$$t_{g_2} = t_{g_1} - \frac{(I_1 - I_2)}{M \bar{c}_{ps}} \tag{7.11}$$

where $\bar{c}_{p_s} \equiv$ mean specific heat at constant pressure of flue gases in the superheater $\left(\frac{kj}{kg\,C}\right)$

$i_{w_1} = I_1 \equiv$ enthalpy of steam at t_{w_1} and p_0

$i_{w_2} = I_2 \equiv$ enthalpy of saturated steam at t_{w_2}

$$\Delta t_1 \equiv t_{g_1}{}^* - t_{w_1}{}^* \tag{7.12}$$

$$\Delta t_2 \equiv t_{g_2} - t_{w_2} \tag{7.13}$$

$$\overline{\Delta t}_S \equiv \frac{\Delta t_2 - \Delta t_1}{\ln \frac{\Delta t_2}{\Delta t_1}} \tag{7.14}$$

$$\Theta_S \equiv \frac{t_{g_1} - t_{g_2}}{\overline{\Delta t}_S} \tag{7.15}$$

Boiler

Similar to the derivation of (7.11):

$$t_{g_3} = t_{g_2} - \frac{(I_2 - I_3)}{M \bar{c}_{p_B}} \tag{7.16}$$

where $I_3 = i_{w_3}$, the enthalpy of saturated water at $t_{w_3} = t_{w_2}$.

Δt_3 and $\overline{\Delta t}_B$ are also derived in a manner similar to the above, and

$$\Theta_B = \frac{t_{g_2} - t_{g_3}}{\overline{\Delta t}_B} \tag{7.17}$$

Economiser

As long as the feedwater leaving the preheaters is at a temperature less than 110 C, we must recirculate sufficient water from economiser exit to entrance so that the resulting temperature of the feedwater is 110 C at this point. From the definition of the percent preheating (χ), paragraph V.4, we derive the following equation for the temperature (t_f) of the feedwater leaving the preheaters:

$$t_f = \chi t_{w_3} + (1 - \chi) t_c \tag{7.18}$$

If $t_f > 110$ C, $t_{w_4} = t_f$. If $t_f > 110$ C, $t_{w_4} = 110$ C.

As outlined in paragraph VII.4, I_4 is the steam table enthalpy corresponding to saturated water at t_f in all instances, and not to t_{w_4} when these two temperatures differ.

Following reasoning similar to that of the superheater and boiler:

$$t_{g_4} = t_{g_3} - \frac{I_3 - I_4}{M \bar{c}_{p_E}} \tag{7.19}$$

and

$$\Theta_E = \frac{t_{g_3} - t_{g_4}}{\overline{\Delta t}_E} \tag{7.20}$$

Finally,

$$\Sigma\Theta = \Theta_S + \Theta_B + \Theta_E \tag{7.8}$$

The calculations then proceed as outlined previously.

VII.6. Results

The primary results desired are:

For a given temperature (t_{g_1}) of exhaust from the gas turbine, how much useful work per kilogram of gas ($L_{N_{max}}$) may be obtained with various sizes (F/N) of steam generators? These basic results are presented in figure 22.

The babsolute maximum spccific work obtainable is that for a steam generator of infinite heat transfer surface. By relating $L_{N_{max}}$ for the various F/N to this absolute maximum specific work, we obtain the curves of figure 23.

From this plot, the economic limits on steam generator size are immediately evident; and we thus have (for this application) a graphic answer to the last of the three basic questions posed in chapter I. We see, for example, that extremely little is to be gained by increasing the size of a "waste heat" steam generator beyond $F/N = 1.5$. For the higher temperatures, increasing F/N beyond about 0.6 could hardly be considered practicable. On the other hand, whereas some modern large steam generators have an F/N as low as 0.2, this value could hardly be considered suitable for the present application.

A study of figure 23 leads one to the conclusion that, for a plant where overall efficiency is of prime importance, increasing steam generator size up to a value of $(L_{N_{max}}/L_{N_{max_\infty}}) \approx 0.85$ will yield appreciable gains. Any attempt to extract a much greater proportion of the available energy of the exhaust gases will involve an increasingly prohibitive investment in heat transfer surface.

Large modern steam generators, designed for relatively high pressures and temperatures, have (F/N)s of from 0.2 to 0.4 [6], [11], [32]. Regenerators for industrial gas turbine may have (F/N)s of as high as 1.15 [3]. These are designed for lower pressures and generally lower maximum temperatures.

A glance at figure 23 reveals that the selected value of 85% for $(L_{N_{max}}/L_{N_{max_\infty}})$ gives us steam generators of roughly the same size and overall cost for the corresponding pressures and temperatures. At the higher t_{g_1}s calculated, the steam pressures and temperatures approach those of a large modern fired steam generator. The waste heat steam generator is an unfired vessel, however. It requires no space for the combustion chamber and none of the blowers, fuel pumps, and other combustion apparatus. These are all furnished by the gas turbine cycle. In addition, the metallurgical requirements of an unfired pressure vessel are lower. Thus the size and cost per installed kilowatt of the waste heat steam generator will not differ greatly from that of its high pressure fired counterpart.

At the low temperature end of the scale, the size of the waste heat steam generator for $(L_{N_{max}}/L_{N_{max_\infty}}) = 0.85$ is in the vicinity of that of a gas turbine regenerator. The pressures are also of the same order; therefore the relative costs should not differ greatly.

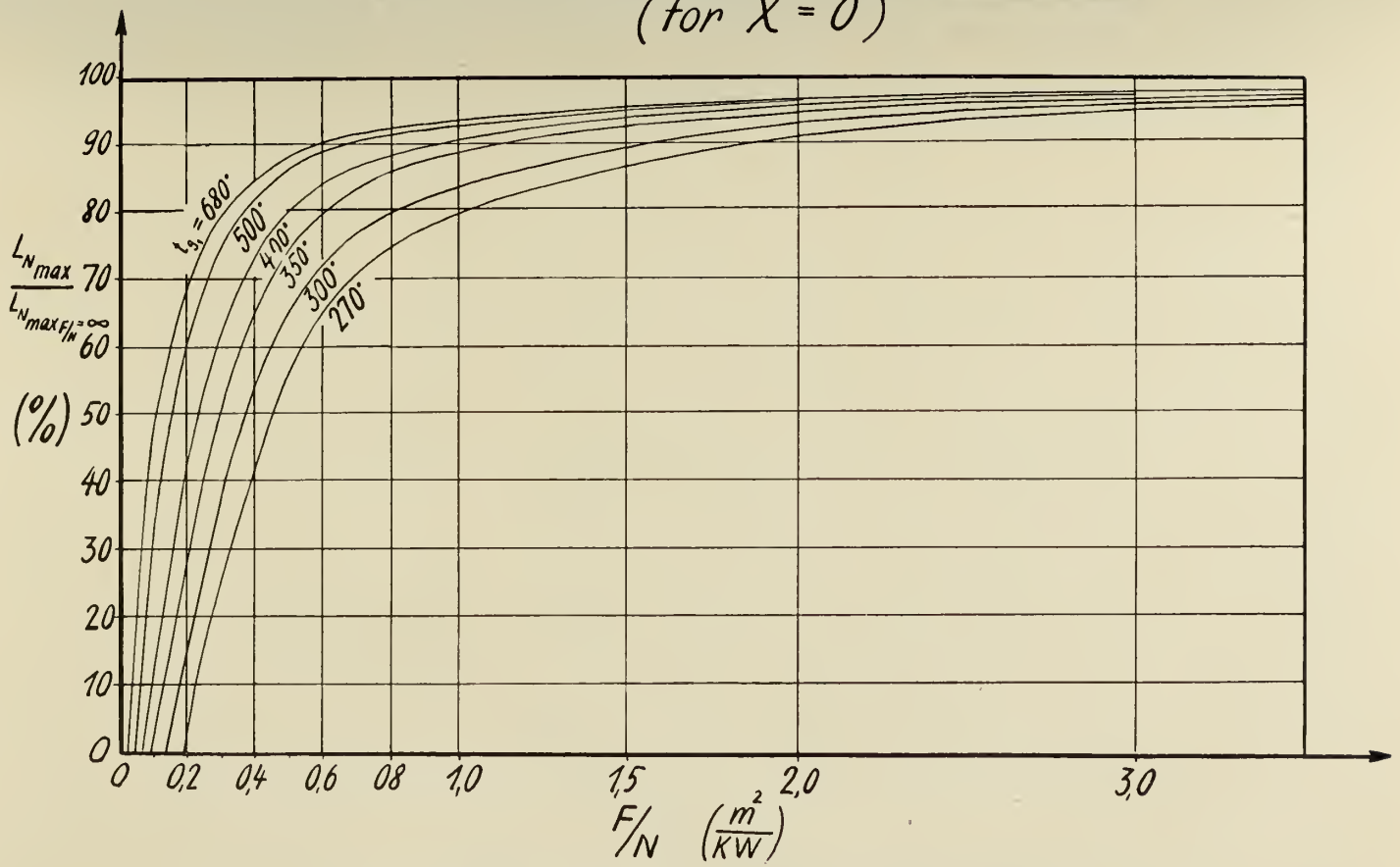

Fig. 23. Steam cycle specific work (as percent of maximum possible).

This dimensionless ratio ($L_{N_{max}}/L_{N_{max_\infty}}$) thus serves somewhat the same purpose as the regenerator effectiveness (η_R) of the gas turbine cycle. One important difference is to be noted. Selecting a value of say 85% for this ratio does not in general mean that 85% of the energy of the exhaust gases (based upon zero enthalpy at a gas temperature equal to that of the entering feedwater) is recovered by the steam generator, as is the case with the gas turbine regenerator. $L_{N_{max_\infty}}$ is the maximum specific work obtainable when the combustion gas isobar (figure 21) rests upon the water-steam isobar at any point of the heat transfer process; i. e., when the temperature difference between gas and water becomes zero at any point in the steam gencrator. This would occur to Δt_1 and Δt_3 as long as the mass flow ratio (M) is greater than about 5. This is almost invariably the case when the sole source of heat for the steam cycle is the energy of the gas turbine exhaust. The energy transferred to the steam cycle is thus somewhat less than 85% of the maximum possible under these circumstances. Only when Δt_4 is the minimum temperature difference in the steam generator ($M < 5$) is approximately 85% of the maximum possible energy transferred from the combustion gases to the steam cycle.

To recapitulate, figure 23 is an aid to the designer in weighing the economic factors involved in the selection of an appropriate size of waste heat steam generator for the combined cycle. Figure 24 plots the same values as figures 22 and 23, so arranged as to facilitate direct reading of the specific work obtainable at various t_{g_1}, once a value of ($L_{N_{max}}/L_{N_{max_\infty}}$) has been selected.

For the cycle calculations of this study (chapter VIII), a value of ($L_{N_{max}}/L_{N_{max_\infty}}$) of 85% has been selected. Where space, weight, or first cost are restricted — as in marine or peak load plants — a smaller value may be appropriate. Under conditions of very high fuel costs, use of a still higher value may be desirable.

VII.7. Influence of variations in arbitrarily selected steam generator design parameters

In substituting fixed numerical values for certain of the variables in equation (7.4), care was taken to insert only values which were near the mean of good design practice. These are not the only practical values for these design parameters, however. It is now proposed to investigate the influence of reasonable changes in these parameters. We can do this by successively varying each design parameter in equation (7.4) as an independent variable, noting the effect on any chosen dependent variable. The dependent variables of most interest are F/N and L_N.

In paragraph VII.6 it was demonstrated that the most reasonable procedure in the cycle evaluations was to hold L_N as a fixed percentage of its maximum value, in which case the resulting F/N would strike a balance

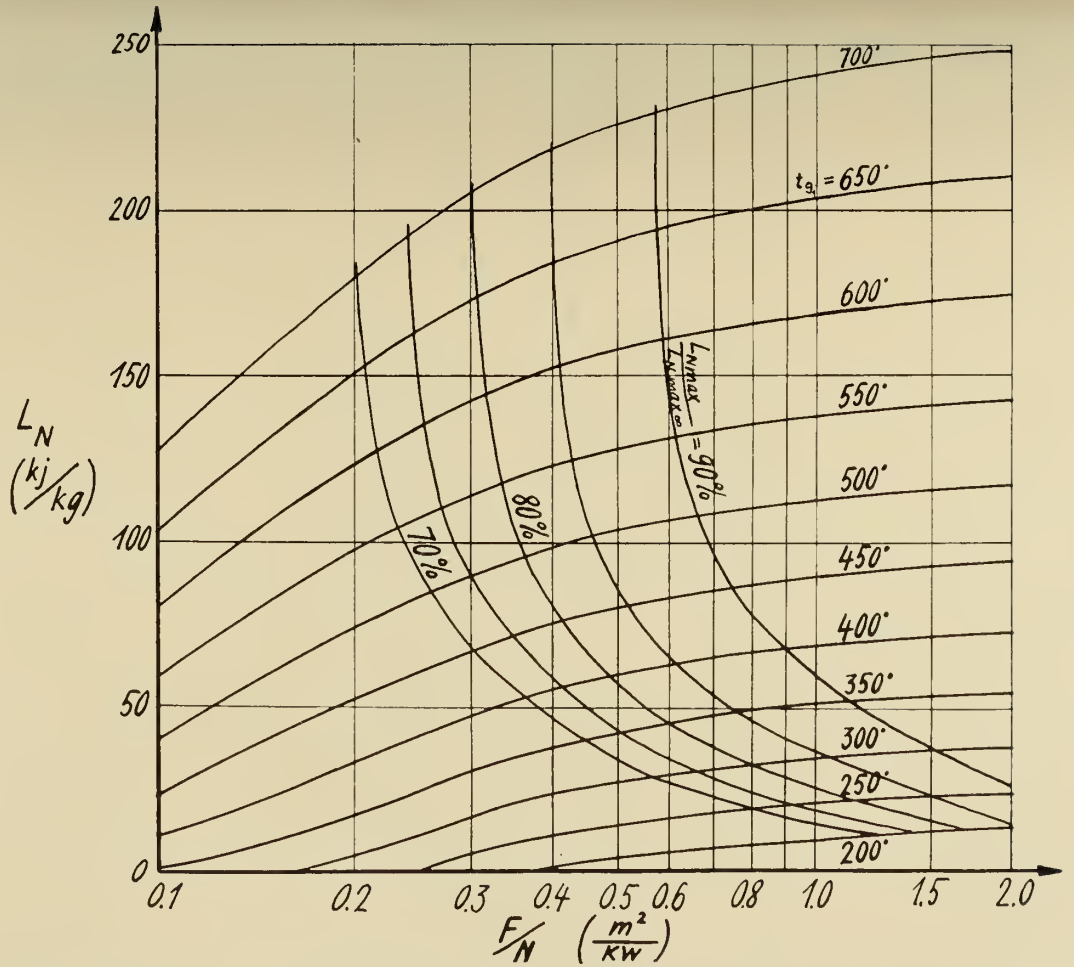

Fig. 24. Steam cycle specific work (as function of steam generator size and inlet temperature).

between operating costs and fixed charges which experience has proved to be reasonable. Consequently, L_N is now held constant while other design parameters are varied, and the results expressed as savings or increases in the heat transfer surface F/N.

Certain of the variables in equation (7.4) are not design parameters; that is, they are not physically subject to independent variation by the design engineer. The quantities $\Sigma\Theta$, μ, γ_B, γ_b, Pr and L_N are all functions of the gas and waterside temperatures, and are thus dependent variables of the quantities t_{g_1}, M, t_{w_1}, X_e, and χ, whose effects as independent variables have previously been calculated. Holding these constant, equation (7.4) may be rearranged to

$$\frac{F}{N} = (\text{constant}) \frac{D^{0.489}\, \zeta^{0.255}}{(\epsilon\, \sigma)^{1.254}\, (\Delta\, p)^{0.255} \left(\frac{D}{s_t - D}\right)^{0.255}} \tag{7.21}$$

a) *Tube diameter*

Holding other parameters constant,

$$\frac{F}{N} \sim D^{0.489} \tag{7.22}$$

For example, halving the tube diameter to 19 mm (and accepting the attendant increase in cleaning cost and the possible increase in ϵ due to dirtier tubes), would make it possible to decrease the heat transfer surface to $(0.5)^{0.489} = 71.3\%$ of its previous area.

Change in D also affects the Reynolds number. Its primary effect, for average σ and ζ, is as in equation (7.22). By its effect on the Reynolds number, however, it has irregular secondary effects through its influence on σ and ζ. For more exact results these should be evaluated for the particular Reynolds numbers concerned by the empirical data of [13], [15], [16], and/or [38].

b) *Heat transmission factor*

From (7.21), the direct influence of ϵ is

$$\frac{F}{N} \sim \frac{1}{\epsilon^{1.254}} \tag{7.23}$$

A secondary influence is that, for a first approximation, the tube temperature has been assumed equal to the waterside temperature. In the determination of L_N, the error from this assumption, for $\epsilon = 0.9$, has been calculated to average less than 1%. A substantial decrease in ϵ will increase the error to the point it may no longer negligible. This may be roughly accounted for as follows:

$$\begin{aligned} Q &= F\, h_g\, (t_g - t_{wall}) = F\, \epsilon\, h_g\, (t_g - t_w) \\ (t_g - t_{wall}) &= \epsilon\, [(t_g - t_{wall}) + (t_{wall} - t_w)] \end{aligned} \tag{7.24}$$

or $$(t_{wall} - t_w) = \frac{1-\epsilon}{\epsilon}(t_g - t_{wall}) \tag{7.25}$$

For $(L_{N_{max}}/L_{N_{max_\infty}}) = 85\%$, Δt_1 is reasonably constant at about 40 C. With t_{g_1} as the independent variable, we can utilize this value to obtain a rough uncorrected value of t_{w_1}. Substituting this same value of Δt_1 for $(t_g - t_{wall})$ in equation (7.25) enables estimating a corrected t_{w_1}. Assuming that the other temperatures vary proportionately, the L_n versus t_{w_1} curves of figure 20 may be entered with the corrected and uncorrected values of t_{w_1} to determine an approximate variation in L_n (and hence L_N, since $L_N \sim L_n$ for constant M). The curves of figures 22, 23 and 24 may then be consulted to determine the effect on F/N.

c) *Variation in* σ, ζ, *and* $\dfrac{D}{s_t - D}$

The true design parameters here are the longitudinal and transverse spacings, s_1 and s_t. Their influence on σ and ζ must be taken from the empirical data of the references quoted previously. Then from equation (7.21):

$$\frac{F}{N} \sim \zeta^{0.255} \tag{7.26}$$

$$\frac{F}{N} \sim (\sigma)^{-1.254} \tag{7.28}$$

$$\frac{F}{N} \sim \left(\frac{D}{s_t - D}\right)^{-0.255} \tag{7.29}$$

d) *Variation in pressure drop,* Δp

$$\frac{F}{N} \sim (\Delta p)^{-0.255}$$

Care must also be taken to examine the secondary influences on σ and ζ. Δp influences the Reynolds number, through its effect on the velocity w; and σ and ζ are functions of Re.

e) *Variation in* c_p

The steam generator calculations were made on the basis of pure air as the exhaust gas from the gas turbine, since the most reliable data available is based on this substance. For varying amounts of fuel burned in the combustion chamber (varying x), we will vary the properties of our combustion gases. This will not have appreciable effect on the heat transfer coefficient (h_g); but through the influence on c_p, it will make a difference in the total enthalpy available in cooling the combustion gases from t_{g_1} to t_{g_4}. With a higher x we have a higher c_p; and for a given gas turbine exhaust temperature, we can thereby obtain more work from the steam cycle.

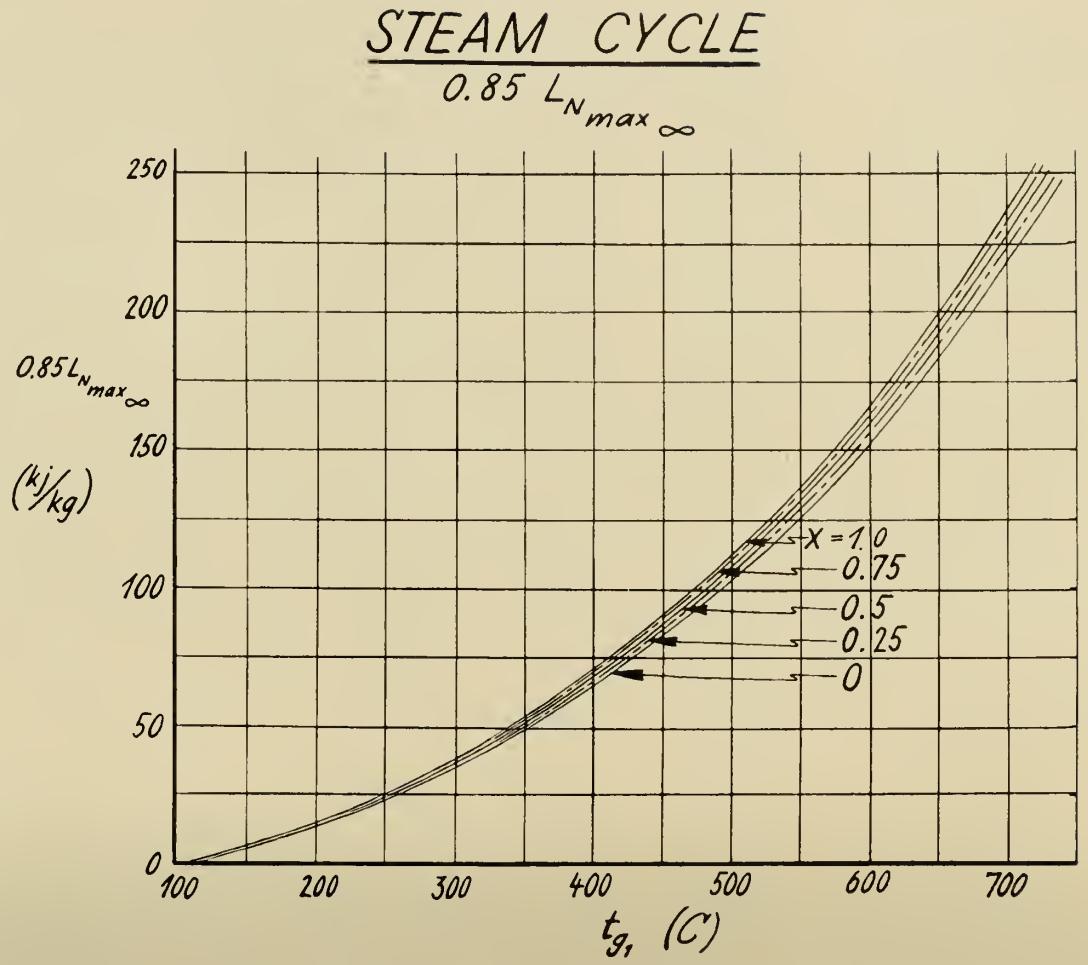

Fig. 25. Steam cycle specific work (85% of maximum).

This effect is reflected in figure 25, wherein the values of 0.85 $L_{N_{max_\infty}}$ are plotted versus t_{g_1}, for various x.

VII.8. Effect of regenerative feed heating

The curves of figures 22, 23 and 24 were prepared for cycles without regenerative feed heating; that is, for $\chi = 0$. Adding this new variable greatly increases the number of numerical and graphical calculations required. No general pattern was found, but the following points were established.

First, a complete calculation for various χ and X_e were made for $t_{g_1} = 350\,\mathrm{C}$, $F/N = 0.25$. This established that the X_e for maximum L_N was essentially independent of χ. Thus, once the optimum X_e was established for $\chi = 0$, other values of X_e could be ignored in calculating the benefits to be gained by regenerative feed heating.

The percentage gain in L_N was found to be considerably greater at smaller values of F/N, amounting to 10% gain in L_N for $t_{g_1} = 350\,\mathrm{C}$, $F/N = 0.25$. For values of F/N in the usable range for industrial installations ($L_{N_{max}}/L_{N_{max_\infty}} \approx 0.85$), the optimum gain amounted to only 4% for the cycles calculated. The maximum gains always occurred in the general vicinity of $\chi = 25\%$ to 30%.

From these calculations it can be concluded that a small amount of regenerative feed heating for the waste heat steam generator would result in modest gains. The actual gain would have to be calculated for each individual case. In any event, the gain would not approach that of a normal steam cycle; and a regenerative feed heating system of the size encountered in a normal plant would generally result in loss rather than gain in specific work. Some of the reasons for this relatively small gain are discussed in paragraph V.4.

VIII. Combined Cycle

VIII.1. Combinations selected

With the steam cycle and gas turbine characteristics determined, these components may now be arranged to form a variety of combined cycles. The simpler arrangements have been selected for detailed calculation; since experience with the development of the gas turbine has indicated that, although the more complex cycles may have attractive characteristics from a thermodynamic viewpoint, their development tends to be retarded by troublesome mechanical difficulties. The basic components and flow paths of the working fluids for the cycles selected are diagrammed in figures 26 to 31. In addition to the features diagrammed, the effects of intercooling in the compressor and,

where applicable, of regenerative feedwater heating in the steam cycle are also investigated.

Symbols used in figures 26 to 31 are:

C ≡ Compressor
Cond ≡ Condenser
CC ≡ Combustion Chamber
GT ≡ Gas Turbine
P ≡ Pump
SG ≡ Steam Generator
ST ≡ Steam Turbine

As can be seen from the diagrams, cycles II and IIa are equivalent to cycles I and Ia with relatively low pressure steam plants added to each to utilize part of the otherwise wasted heat of the gas turbine exhaust. In cycles III and IIIa the steam generator has been made integral with the combustion chamber. It there serves to cool the gases in the chamber from the combustion temperature to the maximum allowable turbine entrance temperature, thus obviating the necessity of great amounts of excess air for this purpose. In cycle IV the steam generator is divided. The high temperature portion receives heat from the high temperature gases in the combustion chamber; the low temperature portion, from the "waste" heat of the gas turbine exhaust. Cycle IVa is the same cycle with a regenerator added between the gas turbine exhaust and the low temperature portion of the steam generator. This arrangement results in a lower stack temperature and a better cycle efficiency than for a corresponding cycle with the positions of the last two elements reversed.

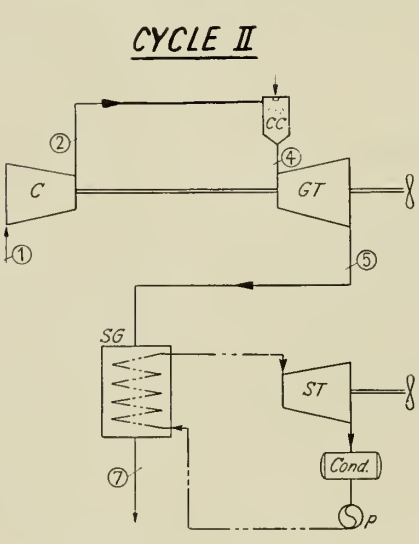

Fig. 26. Cycle II diagram.

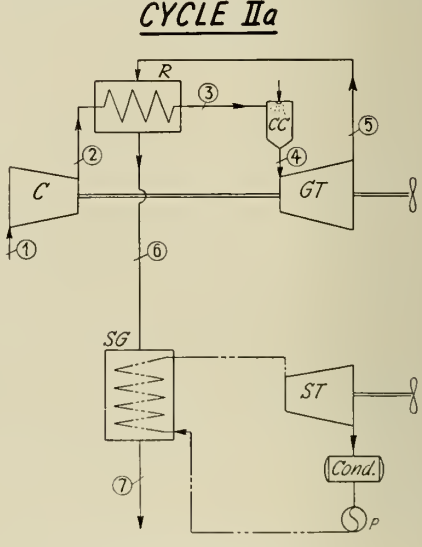

Fig. 27. Cycle IIa diagram.

The bulky items in any cycle are usually the heat transfer apparatus. To be practical, this apparatus must not be excessively large in comparison to the power output of the cycle. The regenerator in each of the above cycles has been properly proportioned to the gas turbine output; and the steam generator has not been allowed to exceed a size carefully related to the steam turbine output (chapter VII).

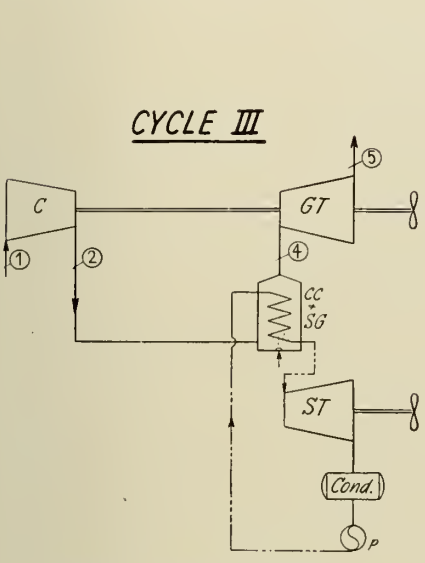

Fig. 28. Cycle III diagram.

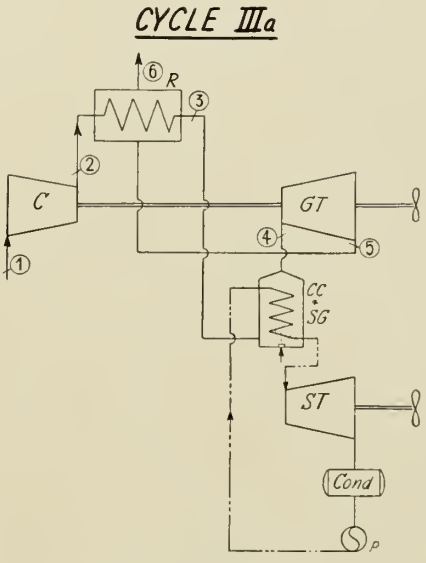

Fig. 29. Cycle IIIa diagram.

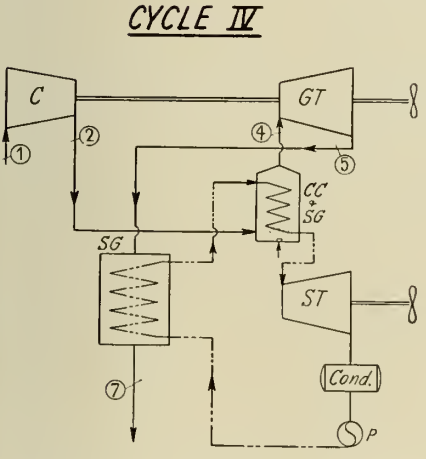

Fig. 30. Cycle IV diagram.

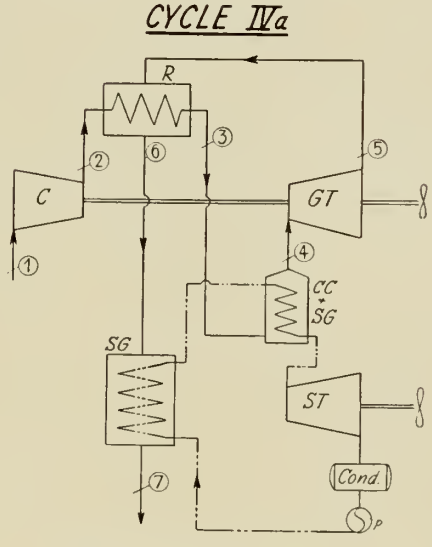

Fig. 31. Cycle IVa diagram.

The analyses have been made for open cycle gas turbine arrangements. There are, of course, certain advantages in closed-cycle gas turbine plants. Lighter gases or higher mean gas pressures can be used to improve regenerator effectiveness without increase in size of this component, for example. This would tend to improve the overall efficiency. The closed-cycle plant has certain additional losses, however, in the air heater and in the after-cooler. In the final analysis the full load efficiencies of the two types are not far different; and any advantages claimed for one type over the other generally lie in part-load economy, initial cost, weight and space requirements, or in relative maintenance costs. For a thermodynamic analysis based on full load conditions, the plants with closed cycle gas turbines show similar overall efficiencies to those of the open plants. It is to be noted that since all the heat supplied to the working fluid of a closed cycle gas turbine must be transferred through metal tube walls, the closed cycle will be much more severely limited as to maximum cycle temperature than will be the open cycle.

In cycles II and IIa large amounts of excess air are used in the combustion chamber to hold the exit gas temperature to that required at the gas turbine inlet. Thus the gases at the steam generator entrance still contain considerable oxygen, giving rise to the possibility of burning additional fuel in the steam generator. Thermodynamically, this is practically equivalent to cycles IV and IVa. A considerable increase in heat transfer surface will be necessary to hold the same stack temperature, however, since the benefits of pressurized combustion are lost; and, as will be seen later, the mean temperature difference between combustion gas and steam is less. Additional burners and furnace refractory will also be required in the steam generator.

To demonstrate that cycle IV is equivalent to cycle II with this additional combustion in the steam generator, let us assume equal pressure ratios for the compressors and gas turbines of the two cycles. If we divide the remaining processes of each cycle into a series of infinitely small steps, we will find differences in the loss of available energy in corresponding steps of the two cycles, since the temperatures throughout the two cycles are not identical. However, by properly selecting the point at which we begin and end each of a series of corresponding finite steps, we can prove that the transfer of available energy to the working fluid and the loss of available energy for each step is the same for both cycles, and that the cycles are therefore thermodynamically similar.

Let us consider that the combustion chamber process of cycle IV is arbitrarily divided into three steps. First, sufficient fuel is burned to raise the gas temperature to the gas turbine inlet temperature (t_4). Second, additional fuel is burned until the maximum practicable amount of oxygen in the combustion air is consumed, thereby raising the temperature an amount Δt. Third, heat is transferred to the steam cycle to cool the combustion gases by

the amount Δt, back to the temperature of the gases at the beginning of step two. The gases then pass through the gas turbine, and drop in temperature to the gas turbine exit temperature t_5.

For the modified cycle II the first step of the combustion process is identical: sufficient fuel is burned to raise the gas temperature to t_4. Thus the loss in available energy in step one of the combustion process is the same for each cycle. Further, the available energy and the enthalpy at gas turbine entrance are also essentially the same for the two cycles. The only differences are those due to the slightly different combustion gas properties; since the gases of the modified cycle II contain more excess air at this point.

Step two of the combustion chamber process for cycle IV corresponds to the combustion process in the steam generator of the modified cycle II. Equal amounts of fuel are burned in the two cycles during this step, since equal amounts were burned in step one; and the total fuel burned in each cycle is equal (i. e., that amount necessary to consume the maximum practicable amount of the available oxygen). Therefore, neglecting small differences in c_p, the temperature rise Δt will be the same in each case.

In step three of the combustion chamber process of cycle IV the combustion gases are cooled by the amount Δt until the gas turbine inlet temperature t_4 is again reached. The heat transferred to the steam is equal to that supplied by the combustion of fuel in step two. A corresponding cooling for step three of modified cycle II will result in the same amount of heat transferred to the steam cycle and in the same temperature drop in the combustion gases. Since steam can be generated at the optimum (same) temperature and pressure in each cycle, the energy transferred to the steam cycle in this step will have not only the same absolute value but also the same availability after the transfer process.

Now, considering the net effect of what has taken place in steps two and three, we find that equal amounts of fuel have been burned in each cycle, and that equal amounts of available energy have been transferred to the steam in each cycle. Further (neglecting small differences in gas properties due to changed composition after the additional combustion) the state of the combustion gas in each cycle is the same at the conclusion of step three as it was at the beginning of step two.

The next step considered in each cycle is the identical cooling of the combustion gases from t_5 to equal stack temperatures. The waterside temperatures and pressures are again identical for the two cycles; hence both the absolute quantities and the availability of the energy transferred to the steam cycles will be equal.

Since the gas turbine and the compressor of cycle IV operate at the same initial temperatures and through the same pressure ratios as the like components of the modified cycle II, the losses of available energy will be the same

in each case for these components. This is also true of all steam cycle components.

Thus each process in cycle IV results in the same transfer and in the same loss of available energy as in the corresponding process in the modified cycle II, even though the processes do not take place in the same order. The two cycles are thus thermodynamically similar; and a separate numerical evaluation of the modified cycle II is not necessary.

By similar reasoning, cycle IVa results are the same as would be obtained by burning additional fuel in the waste heat steam generator of cycle IIa.

Even though the purely thermodynamic calculations for cycles IV and IVa are respectively the same as for cycles II and IIa with additional combustion in the "waste heat" steam generator, there are certain practical differences. Until such time as burning coal in a combustion chamber whose exhaust gases pass through the gas turbine is fully practical, only oil or gaseous fuels could be used in cycles IV and IVa. In the modified cycles II and IIa coal can be burned without difficulty in the steam generator. Thus in some areas of the world part of the fuel requirements could be satisfied with a cheaper fuel.

To gain this advantage, however, the waste heat steam generator of cycle II (or IIa) must be converted to a fired steam generator, with fire-box, coal handling equipment, combustion-control apparatus, and more expensive metal in part of the unit. In addition more heat transfer surface will be required than for the steam generator of cycle IV. First of all the, higher heat transfer rates that accompany pressurized combustion have been lost. Secondly, the mean temperature difference between gas and steam is less for the modified cycle II (or IIa).

It will be noted that the temperature rise Δt in step two of the combustion chamber process of cycle IV began at the gas turbine *inlet* temperature. Step two of cycle II involved the same temperature rise, but starting at the gas turbine *exhaust* temperature. In step three for both cycles the gases were cooled through the identical temperature range Δt by transfer of heat to the steam cycle. Thus the mean gas temperature of step three is lower for the modified cycle II than for cycle IV. Since the steam-side temperatures in both cycles are the same, the temperature difference across the heat transfer surface of the modified cycle II is less. (The same holds for a comparison between cycles IIa and IVa).

If it is desired to use only coal as a fuel, part of it could be gasified to produce a gaseous fuel for the initial combustion chamber of a modified cycle II or IIa, and the remainder burned in the steam generator.

Alternatively, the initial combustion chamber could be replaced by an air heater coil in the steam generator. The absolute value of the total energy released in the combustion process will of course be the same as in the foregoing

cycles. If the heat transfer surface is of sufficient size, the enthalpy and the available energy of the air throughout the gas turbine cycle will also be as before (neglecting the small differences between the characteristic properties of air and combustion gases). The same holds for the steam cycle. Thus, even though available energy may be lost in differing amounts at various points in the three types of cycles considered (cycle IV, cycle II with combustion in gas turbine combustion chamber and in steam generator, and cycle II with combustion in a combined steam generator and air heater) the total losses are the same, and the cycles are thermodynamically similar. The reasoning also holds for these same three cycles with regenerators in the gas turbine circuit.

In the order last mentioned, however, each cycle requires successively greater amounts of heat transfer surface. In an actual installation it might well be necessary to compromise the efficiency of the coal burning cycle to avoid excessive cost and size of plant. Finally, use of an air heater severely limits the maximum working fluid temperature of the gas turbine cycle.

VIII.2. Calculation procedure

a) *Cycles II and IIa*

The calculation method is quite similar to that for the gas turbine cycles alone. An additional pressure drop must be added: $\left(\frac{\Delta p}{p}\right) = 0.02$ for the steam generator. The calculation proceeds in a straight forward manner until the enthalpy of the exhaust gases from the gas turbine cycle is determined (point 5 for cycle II; point 6 for cycle II a). The gas tables are entered with this enthalpy and with the appropriate x (see paragraph II.1), to determine the temperature of the gases entering the steam generator. The steam cycle net work can then be read directly from figure 25. The total cycle work is the sum of the net outputs of the steam and gas turbines. The efficiency is this total cycle work divided by the heat supplied in the combustion chamber.

b) *Cycle III*

In the following cycles the amount of heat supplied the cycle is limited only by the amount of fuel which can be burned per kilogram of entering air. The combustion chamber is under pressure; it is therefore desirable to make it small. Consequently, the rather conservative figure of 35% excess air ($x = 0.75$) is chosen. This results in a heat release of 2190 kj/kg, regardless of compressor pressure ratio. Of this only 2102.4 kj/kg (deducting 2% each for combustion chamber and stray losses) is usable in the cycle.

The total enthalpy available immediately after combustion is thus $i_2 + 2102.4$ (refer figure 28 for state notation). i_4 is obtained from the gas

tables for $t_4 = 700\,\mathrm{C}$, $x = 0.75$; and is subtracted from the above total enthalpy to determine the heat transferred to the steam cycle. The rest of the gas turbine cycle proceeds as before.

How can the heat supplied to the steam cycle most efficiently be used? It is noted that the combustion gases are always at a temperature in excess of 700 C — usually far in excess of this temperature. The limits on steam cycle maximum temperature are therefore only those imposed by the present state of development of the steam cycle itself. This maximum temperature has been arbitrarily set at 600 C. With steam turbines calculated as outlined in chapter V, and without regenerative feed heating, the maximum utilization of heat supplied ($\eta_{st} = 36.55\%$) is obtained by initial steam condition $t_0 = 600\,\mathrm{C}$; $p_0 = 180$ ata.

The gain due to regenerative feed heating may be directly calculated by the methods of [37], since no limitations of steam generator temperature differences or utilization of exhaust heat here apply. With regenerative feed heating, 42.9% of the heat supplied the cycle can be converted to shaft work. (The detailed assumptions are as in paragraph V.4.)

The steam turbine work is then added to the gas turbine net work to obtain the net work of the cycle. This is divided by the heat supplied the cycle (2190 kj/kg) to obtain the cycle efficiency.

c) *Cycle IIIa*

The calculations for cycle IIIa are similar to the above except for the addition of the regenerator and its appropriate pressure drops. The total enthalpy of the gases immediately after combustion is now $(2102.4 + i_3)$. i_3 is determined by $(i_3 - i_2) = \eta_R (i_5 - i_2)$.

It is found by trial that the gas turbine calculations are negligibly affected by a change in x. This latter variation does, however, have an appreciable effect on i_4 and i_5. i_4 may be read from the gas tables for the appropriate t_4 and x. Assuming that L_i for the turbine remains unaffected by varying x, and denoting the properties for two different x by primed and double primed quantities:

$$i_5' = i_4' - L_i \tag{8.1}$$

$$i_5'' = i_4'' - L_i \tag{8.2}$$

or

$$i_5'' = i_5' + (i_4'' - i_4') \tag{8.3}$$

This procedure enables accurate cycle calculations without the necessity of repeating the turbine calculations for varying x.

d) *Cycles IV and IVa*

For the steam portion of these cycles, the steam generator heat transfer diagram will be similar to figure 21. Let us consider first the case for a gas

turbine pressure ratio $\Pi = 0$; i. e., no gas turbine at all in the cycle. The temperature corresponding to t_{g_1} of figure 21 will be the theoretical combustion temperature; and the combustion gas cooling line (labeled $\dot{m}_g$ on figure 21) will have a very steep slope. It is thus evident that the critical temperature difference will be Δt_4. For a steam generator of infinite heat transfer surface, $\Delta t_4 = 0$. This gives a base point for calculating the maximum possible work from the steam cycle ($L_{N_{max_\infty}}$), as outlined in the preceding chapter.

Examining cycle IV for the case $\Pi > 0$, we will have a transfer of heat from the combustion gases to the steam cycle as the gases cool from combustion temperature to the maximum permissible gas turbine inlet temperature. For this section of the steam generator, as in cycle III, the heat transferred will be equal to 100% of the enthalpy drop of the combustion gases, namely $(i_2 + 2102.4) - i_4$.

The combustion gases next drop in temperature (and enthalpy) in the gas turbine, without heat transfer to the steam cycle. The gases then enter a waste heat steam generator at the temperature of the gas turbine exhaust (t_5). Following the reasoning outlined near the end of paragraph VII.6, a practical waste heat steam generator will transfer approximately 85% of the maximum possible heat to the steam cycle. As long as the combustion gas cooling line is steeper than the water heating line in the economiser (which condition does exist for all Π encountered in these calculations), this heat transferred will amount to 85% of the combustion gas enthalpy difference between t_5 and t_f.

Here $t_f \equiv$ temperature of feed water entering the steam generator (C). Thus

$$q_{st}^{\swarrow} = (i_2 + 2102.4 - i_4) + 0.85\,(i_5 - i_f) \tag{8.4}$$

and

$$L_{N_{st}} = \eta_{st} q_{st}^{\swarrow} \tag{8.5}$$

where $q_{st}^{\swarrow} \equiv$ total heat transferred to the steam cycle.

(Following through the above procedure for the limiting case of $\Pi = 0$, and adding an air preheater, results in an average steam generator efficiency of slightly over 90% for a straight steam cycle.)

The advantages of regenerative feed heating cannot be determined without numerical computations, for reasons discussed in paragraph V.4. Therefore, for each gas turbine pressure ratio the steam cycle output is calculated for various values of χ, and the maximum cycle output used for the final overall efficiency curves. The methods of [37] are used to determine η_{st}.

For the higher values of χ and the lower values of t_4, in some cases the gas temperature at regenerator outlet (t_6) is lower than that of the feedwater at economiser inlet (t_f). There is no "waste heat" portion of the steam generator under such circumstances, and the cycle becomes identical with cycle IIIa.

The gas turbine work is computed as before, added to the steam turbine

CYCLE II

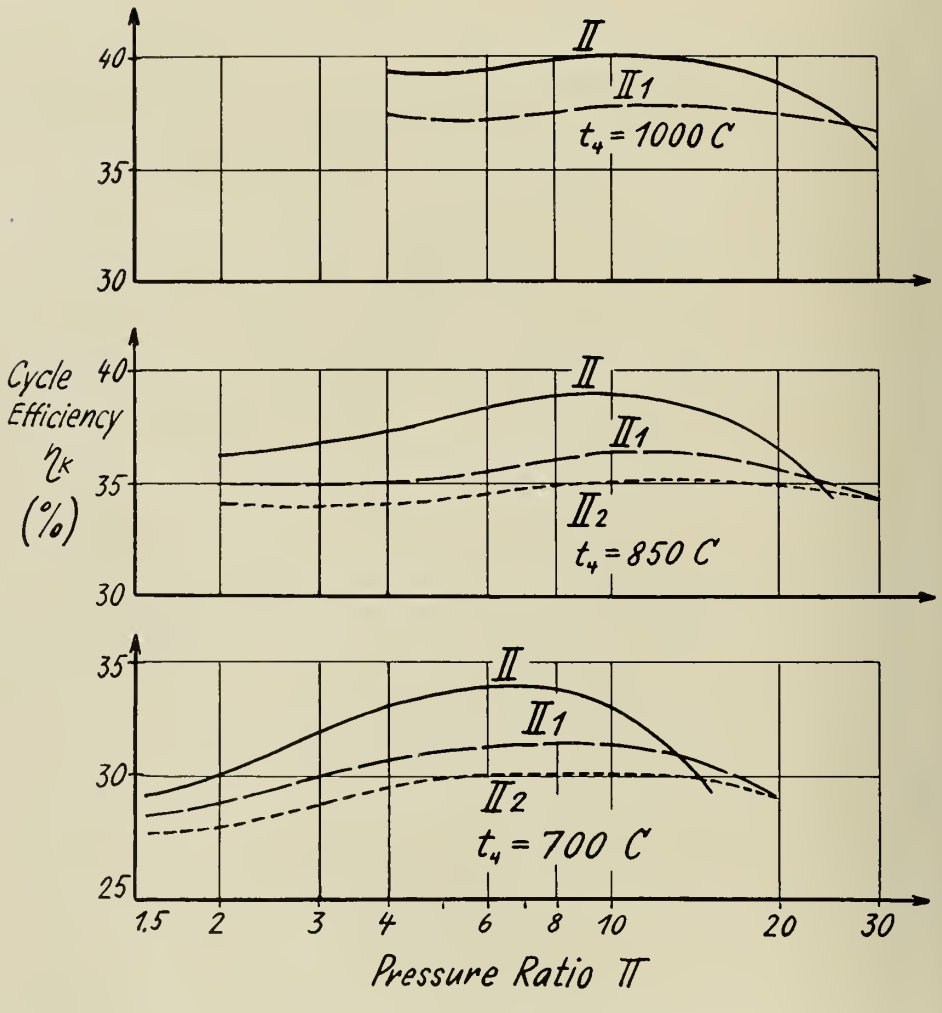

Fig. 32. Cycle II efficiency curves.

CYCLE IIa

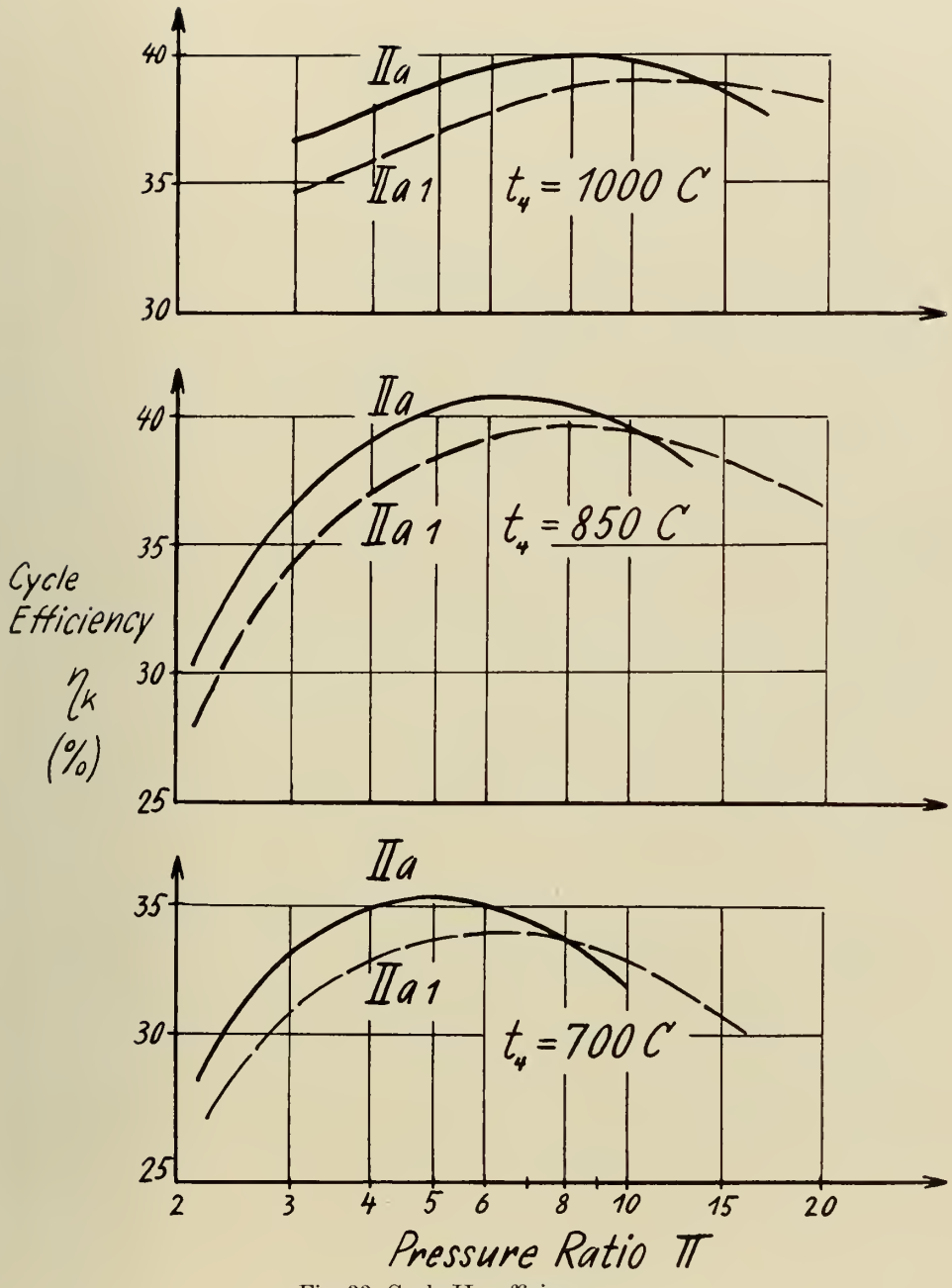

Fig. 33. Cycle IIa efficiency curves.

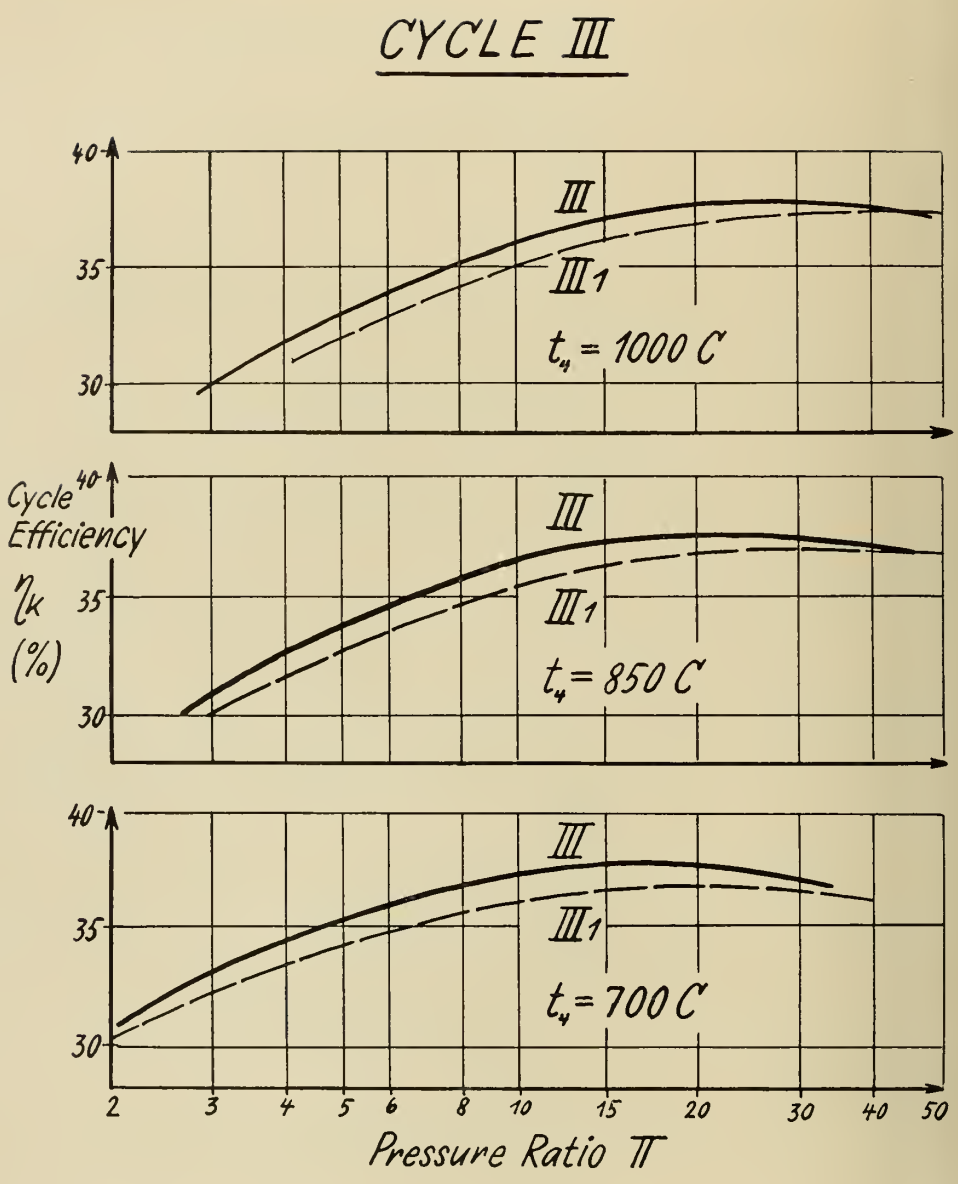

Fig. 34. Cycle III efficiency curves.

CYCLE IIIa

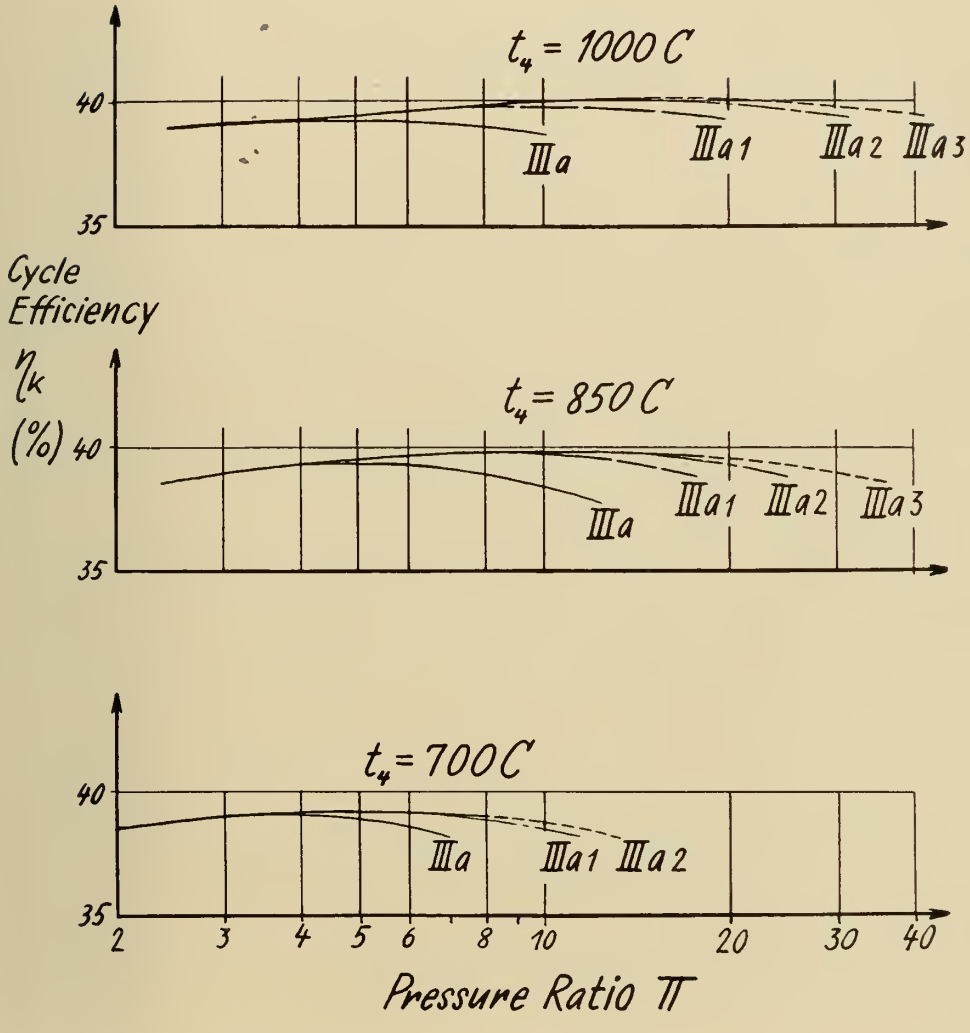

Fig. 35. Cycle IIIa efficiency curves.

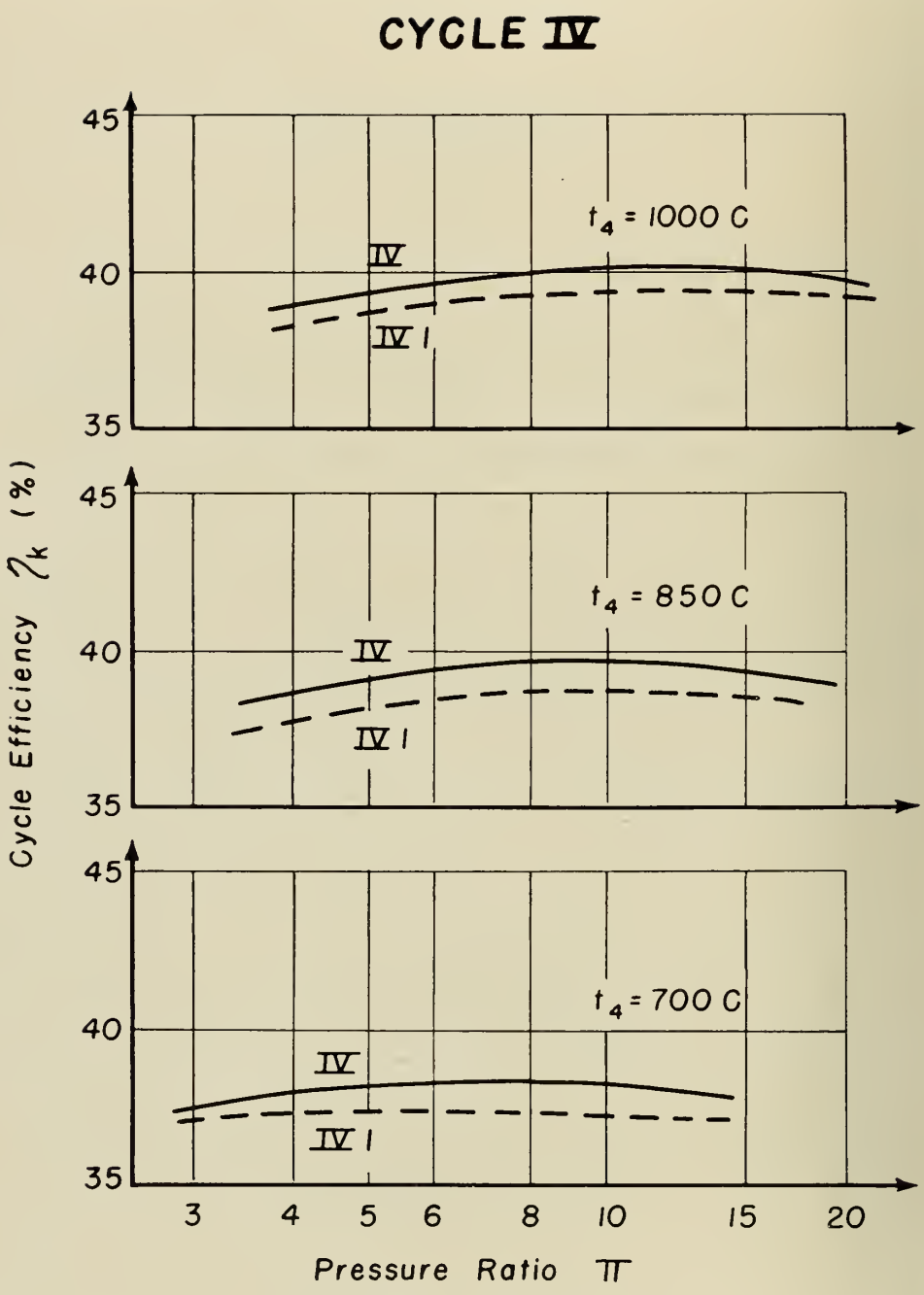

Fig. 36. Cycle IV efficiency curves.

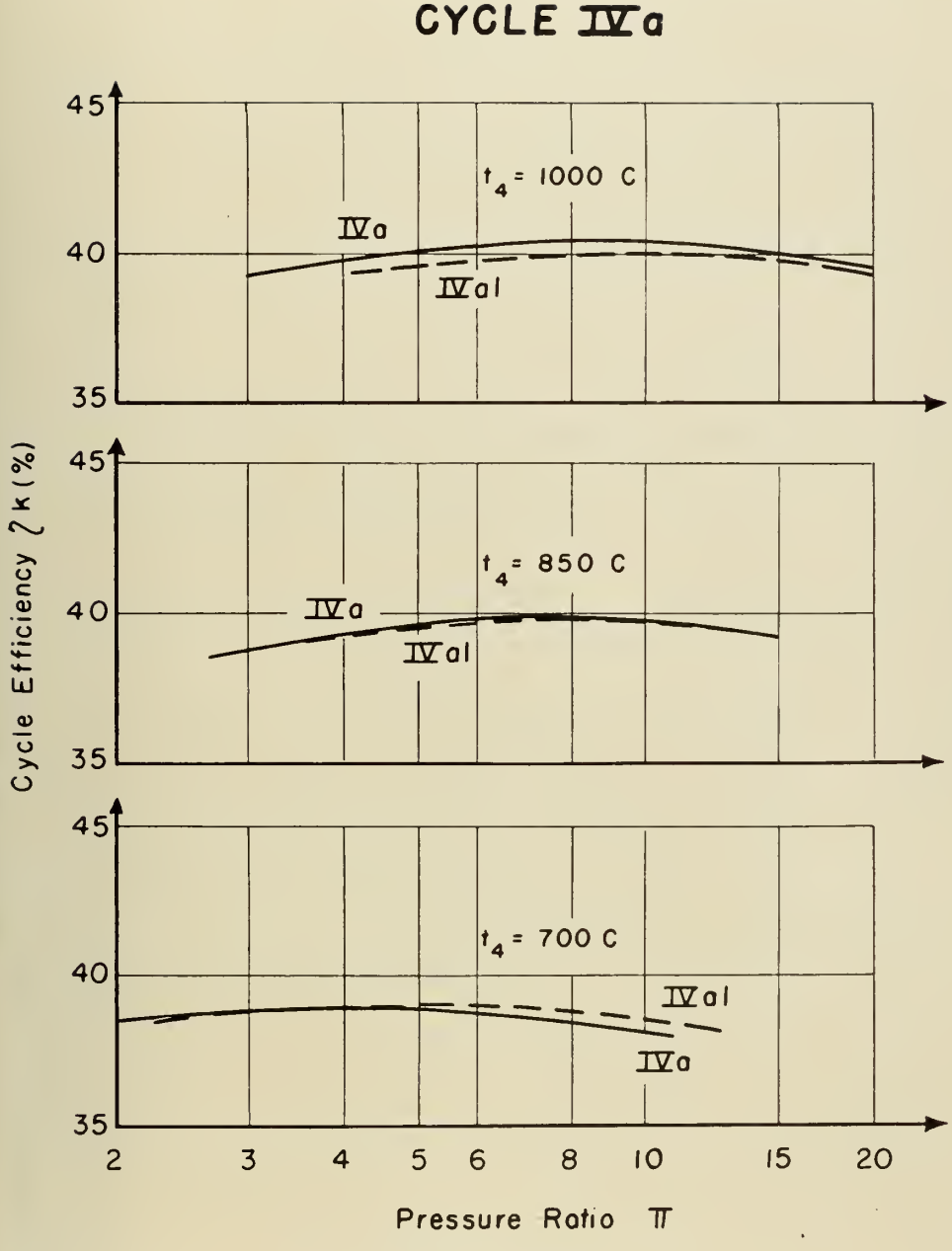

Fig. 37. Cycle IVa efficiency curves.

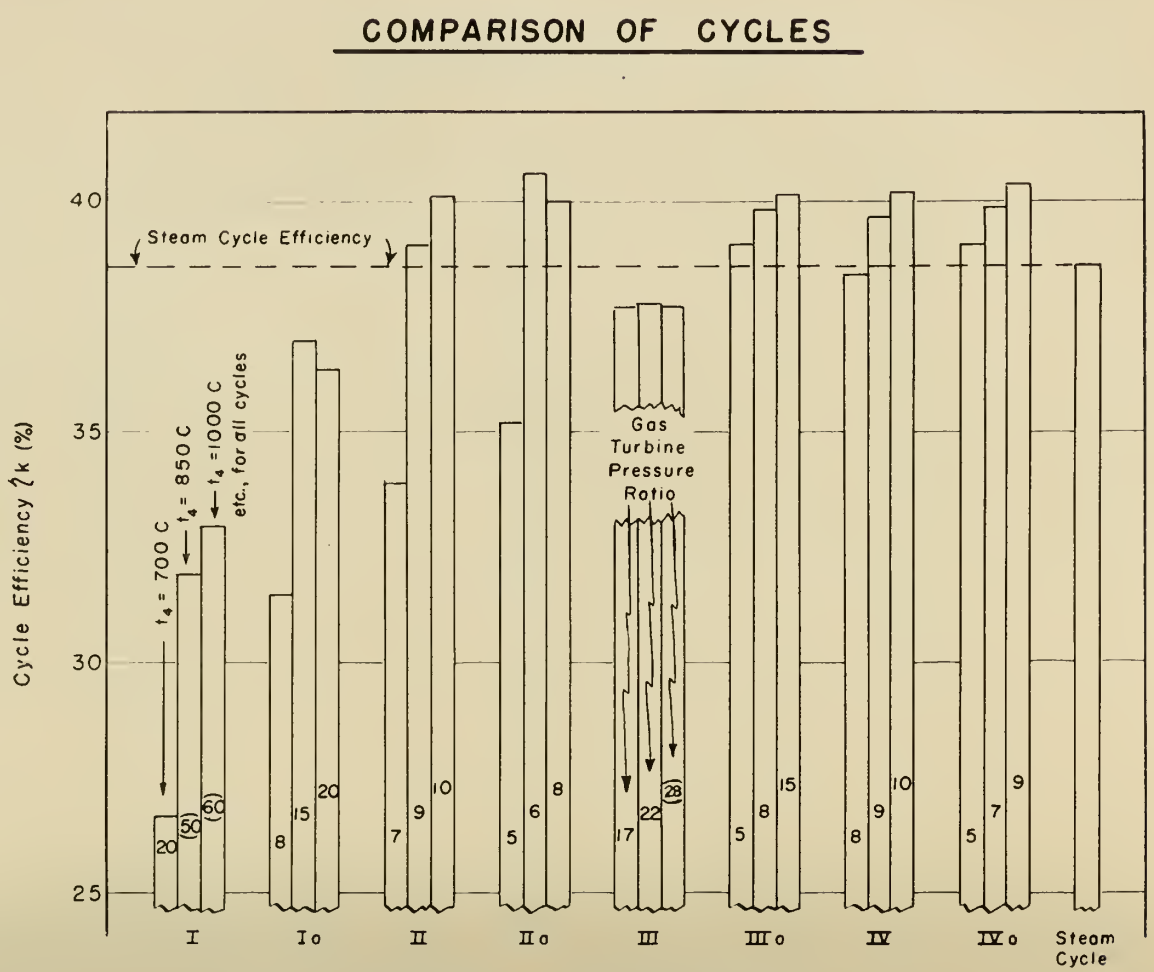

Fig. 38. Comparison of cycles (efficiency).

work to obtain the cycle work, and the total divided by the heat supplied to the cycle (2190 kj/kg) to obtain the overall cycle efficiency.

The individual cycle efficiencies are plotted in figures 32 to 37. For graphical comparison the maximum efficiency of each cycle (including the straight gas turbine cycles) is plotted as a bar graph in figure 38. The straight steam cycle is also included for purposes of comparison. This is the $t_0 = 600\,\mathrm{C}$, $p_0 = 180\,\mathrm{ata}$ cycle used above, with an assumed steam generator efficiency of 90%.

The pressure ratio for the gas turbine portion of each cycle is indicated on its corresponding bar. As outlined in paragraph III.1, practical design considerations impose an upper limit on this pressure ratio. Those pressure ratios which lie above this limit are enclosed in parentheses on the bar graph; and the corresponding efficiencies would be very difficult to obtain in practice. The practically obtainable efficiency for any desired lower pressure ratio may be obtained from the cycle efficiency curves.

e) *Cycle specific work*

The term specific work up to this point has always been based upon unit mass of either steam or gas. The overall cycle specific work should take into account that both fluids are flowing in parallel through the combined cycle. The cycle specific work is therefore defined as

$$L_{sp} \equiv \frac{N}{\dot{m}_g + \dot{m}_w} \tag{8.6}$$

To relate this quantity to the work per kilogram of combustion gas (L_N) we use

$$N = \dot{m}_g L_N \tag{3.7}$$

whence

$$L_{sp} = \frac{\dot{m}_g L_N}{\dot{m}_g + \dot{m}_w} = \frac{M}{M+1} L_N \tag{8.7}$$

This reasoning also applies to a normal steam plant; since this cycle also has, in reality, the same two working fluids.

Since the state of each working fluid is determinable at any point from the cycle calculations, the mass flow ratio (M), if not already determined previously, may be calculated from a first law heat balance on the steam generator.

$$\dot{m}_g \Delta i_g = \dot{m}_w \Delta i_w \tag{8.8}$$

where $\Delta i_g \equiv$ drop in specific enthalpy of the combustion gases in the steam generator (kj/kg),

and $\Delta i_w \equiv$ rise in specific enthalpy of the water (steam), in the steam generator (kj/kg).

Whence

$$M \equiv \frac{\dot{m}_g}{\dot{m}_w} = \frac{\Delta i_w}{\Delta i_g} \tag{8.9}$$

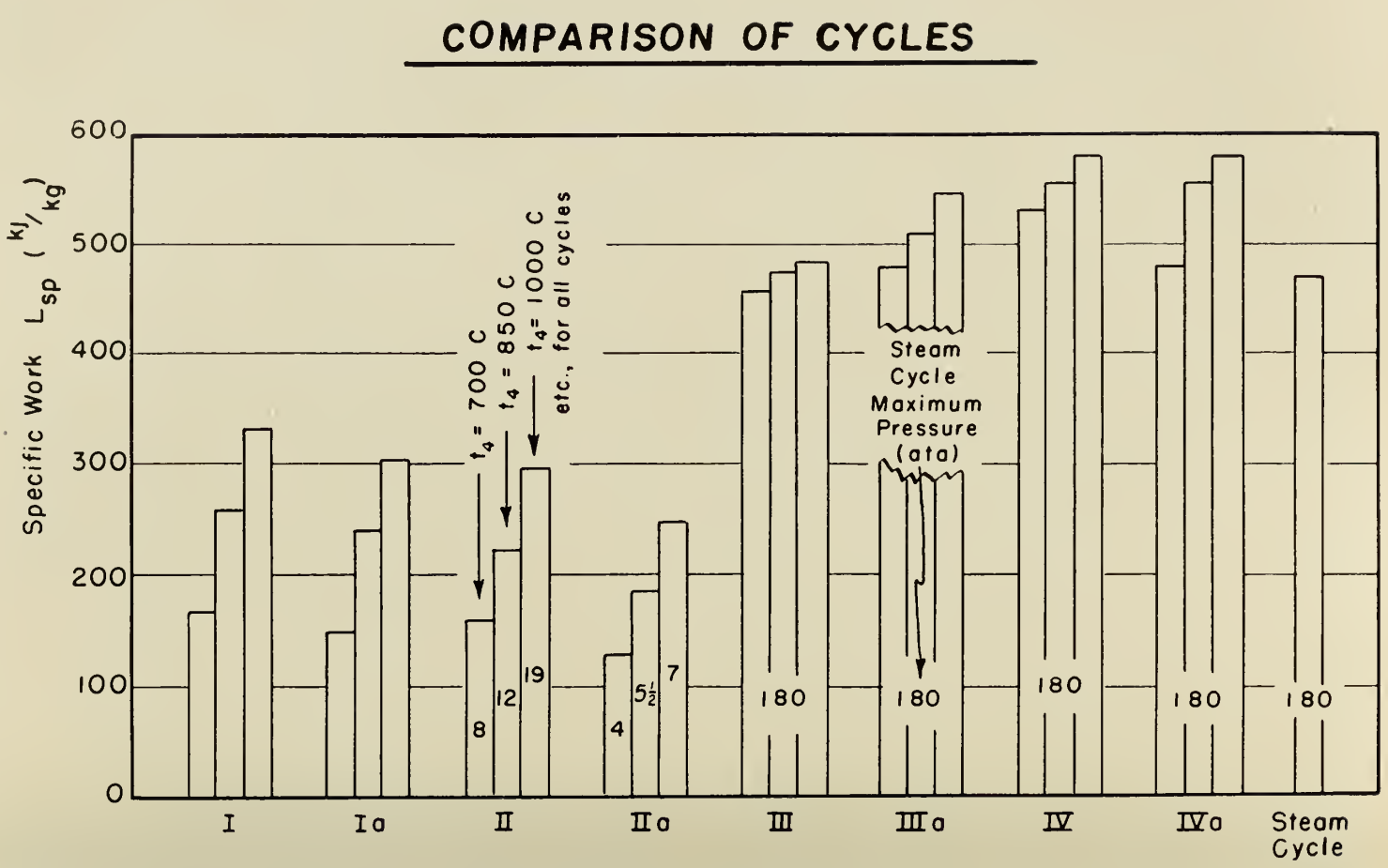

Fig. 39. Comparison of cycles (specific work).

The cycle specific work has been calculated for the maximum efficiency point of each cycle; and the results plotted as a bar graph in figure 39. As a matter of interest, the maximum steam pressure in ata of the steam portion of each cycle is indicated on its corresponding bar.

f) *Power output limitations*

Each type of prime mover has certain inherent upper and lower power limits beyond which it cannot operate at competitive efficiencies. These limits are not sharply defined; and the special circumstances surrounding the choice of a prime mover for a given application cause countless deviations from the generally established pattern. But where efficiency and long life are of major importance, the pattern at present is as follows:

For very low powers, under 100 horsepower, the normal choice is a gasoline engine. From 100 horsepower to about 10,000 horsepower the diesel engine is the most efficient power plant available. Above about 50,000 KW the steam turbine plant is unchallenged. Its efficiency begins to fall rather rapidly at lower powers; but because of its ability to burn a variety of fuels, its low maintenance costs and the flexibility of layout afforded by this type of plant, it is in widespread use down to powers of 5000 KW and less. The position of the gas turbine is not firm, although it has rapidly established itself for applications wherein efficiency and long life are secondary to plant size, weight, or first cost. Where efficiency is of first importance, the hope of the gas turbine is the field between the large diesel and the large steam plant, say 7500 KW to 30,000 KW.

The detailed calculations of this study have been based on design parameters of long life high efficiency plants. It is of interest to establish approximately the power limits within which the calculated efficiencies may be expected to apply.

As previously indicated, cycles III, IIIa, IV and IVa utilize a steam plant of the maximum efficiency practically obtainable today with a nonreheat cycle. Steam is generated at a pressure of 180 ata and a temperature of 600 C. For normal steam plants with this maximum temperature and pressure, overall efficiency is relatively constant for power outputs of about 60,000 KW or greater. Efficiency falls if such a plant is designed for lower full load power.

This is due to a deterioration of turbine stage efficiency as the volume rate of steam flow decreases below a certain value. As volume flow decreases, blades necessarily become shorter; and tip and clearance losses become proportionately larger. Empirically [39], this decrease in stage efficiency is very gradual until a volume rate of flow of about 2 m^3/sec is reached. Below this flow rate the decrease in stage efficiency is quite rapid.

For the turbines of the standard series (chapter V) a 60,000 KW turbine

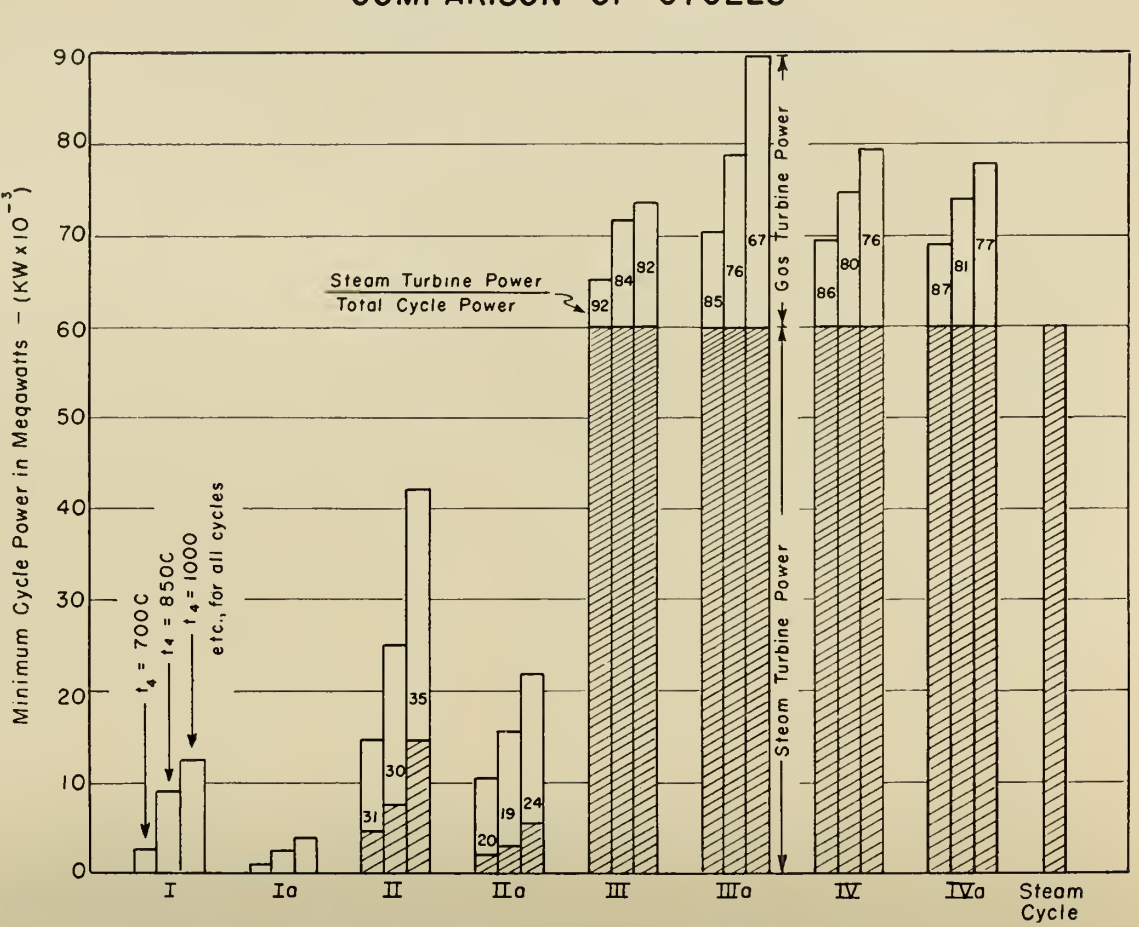

Fig. 40. Comparison of cycles (minimum practical power output).

with inlet steam at 600 C and 180 ata will have a volume rate of steam flow of 2.3 m^3/sec at the exit of the Curtis stage. Utilizing the data of [39], this volume flow rate will give an average stage efficiency (excluding the Curtis stage) of about 88%, as assumed in paragraph V. 1. (This value is prior to the correction for moisture, where applicable.)

This gives us a criterion for calculating the minimum size of plant to which the efficiencies calculated for each cycle will apply; namely, the volume flow rate at the entrance of the steam turbine (or at the exit of the Curtis stage, if present) must be 2.3 m^3/sec or greater. A similar check must be made for the gas turbine.

With data from the previously completed cycle calculations, the steam turbine power that results from this minimum steam flow rate may be determined. The mass flow ratio M is already known; therefore the gas turbine useful output may also be calculated. The sum is the minimum power output at design load at which the calculated efficiencies may be expected to be attained. Lower power outputs can be obtained, of course, by using smaller volume flow (thereby reducing turbine efficiency) or lower pressure at turbine inlet (thereby decreasing basic cycle efficiency).

The results are plotted as a bar graph in figure 40. The shaded portion of each bar represents steam turbine power; the unshaded portion represents gas turbine net output. The percent of total power that is furnished by the steam turbine is indicated by the figures atop the shaded areas.

g) *Availability diagrams*

It is perhaps of interest to analyze a few of the cycles from the point of view of the second law of thermodynamics, to indicate wherein the greatest losses of availability — and hence the greatest possibilities for improvement of cycle efficiency — lie.

The concept of availability was first introduced in 1889 by *Gouy* [12] who used the term "energie utilisable". *Stodola* [45] used the term "technisch freie Energie"; and utilized the concept in cycle analyses. In the English literature the subject of availability and second law analysis is thoroughly covered by *Keenan* [22].

The availability of a substance can be defined as the maximum work which it can theoretically produce under a given set of boundary conditions, unaided by other than cyclic changes in the surrounding medium. The availability of the chemical (or nuclear) energy of a fuel is defined as 100%; since it is conceivable that a reversible heat engine, operating between an infinitely high upper temperature and a sink temperature of absolute zero, could convert all of this energy to useful work. For a steady flow process such as those involved in the cycles of this study, it can be shown [22] that the availability

of a quantity of working fluid is equal to its available enthalpy (A). This is defined by

$$A = (I - T_0 S) - (I_0 - T_0 S_0) \tag{8.10}$$

Here I and S are, respectively, the enthalpy and entropy of the quantity of working fluid at its present state; and I_0 and S_0 are the enthalpy and entropy of the working fluid at sink temperature (T_0) and sink pressure (p_0).

A working fluid may gain or lose availability in a given process. If heat is transferred to a working fluid, for example, its increase in availability is the excess of its availability as it leaves the process over its availability as it enters the process. It may lose availability through cooling, through the production of useful work, or through irreversible actions — such as throttling, heat transfer across a finite temperature difference, of the production of friction work. The degree of irreversibility of a process may thus be measured by the loss of available energy occasioned by these irreversible actions.

The states of the working fluids entering and leaving each component of the cycles under consideration can be determined from the cycle calculations. The difference between the availability entering and the availability leaving is the loss due to irreversibilities. The results of availability analyses of representative cycles are presented as Sankey flow diagrams, figures 41 to 45.

VIII.3. Analysis of results

a) *Effect of intercooling*

From figures 32 to 37 it is evident that intercooling does not give the same advantages that it does for the gas turbine cycle alone. In essence, intercooling consists of the removal of useful energy from the cycle, and generally results in a reduction in the mean temperature at which heat is supplied to the working fluid. This in turn results in a greater loss of available energy. Only when overbalancing considerations are present is this advantageous.

For example, when a regenerator is used as the final element in the combustion gas flow path, intercooling the compressor results in cooler air at the regenerator inlet. This allows a greater heat transfer from exhaust gas to incoming air than is possible with a regenerator of the same effectiveness in a non-intercooled cycle. Thus the air temperature at combustion chamber inlet, and the mean temperature at which heat is transferred to the working fluid, are lowered relatively little in comparison with the non-intercooled cycle. On the other hand the exhaust gas temperature is considerably lower. Thus the available energy discarded in the stack gases, and the mean temperature of heat rejection from the cycle, are markedly lower. These last effects overbalance the losses due to intercooling, and the net result is a gain

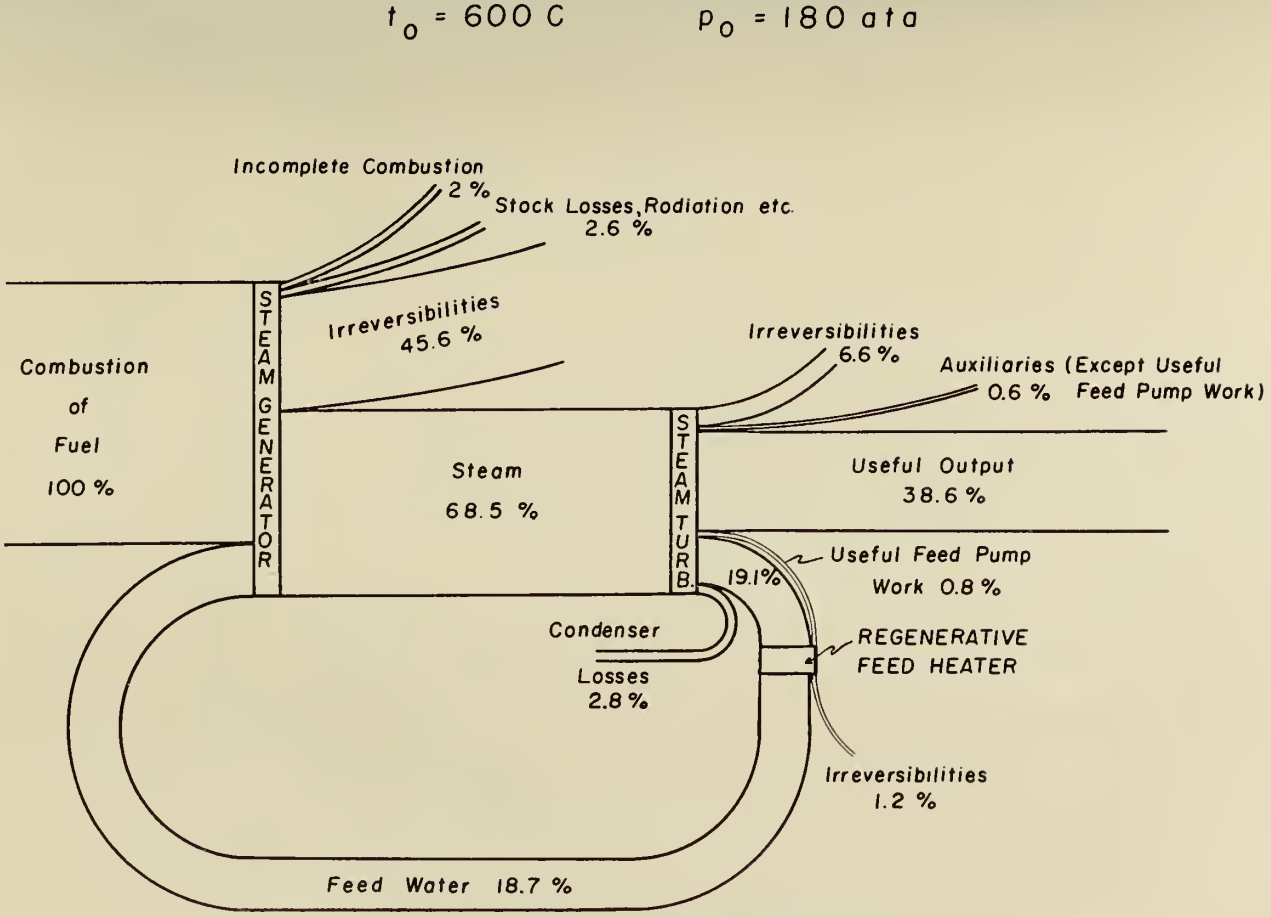

Fig. 41. Steam cycle availability diagram.

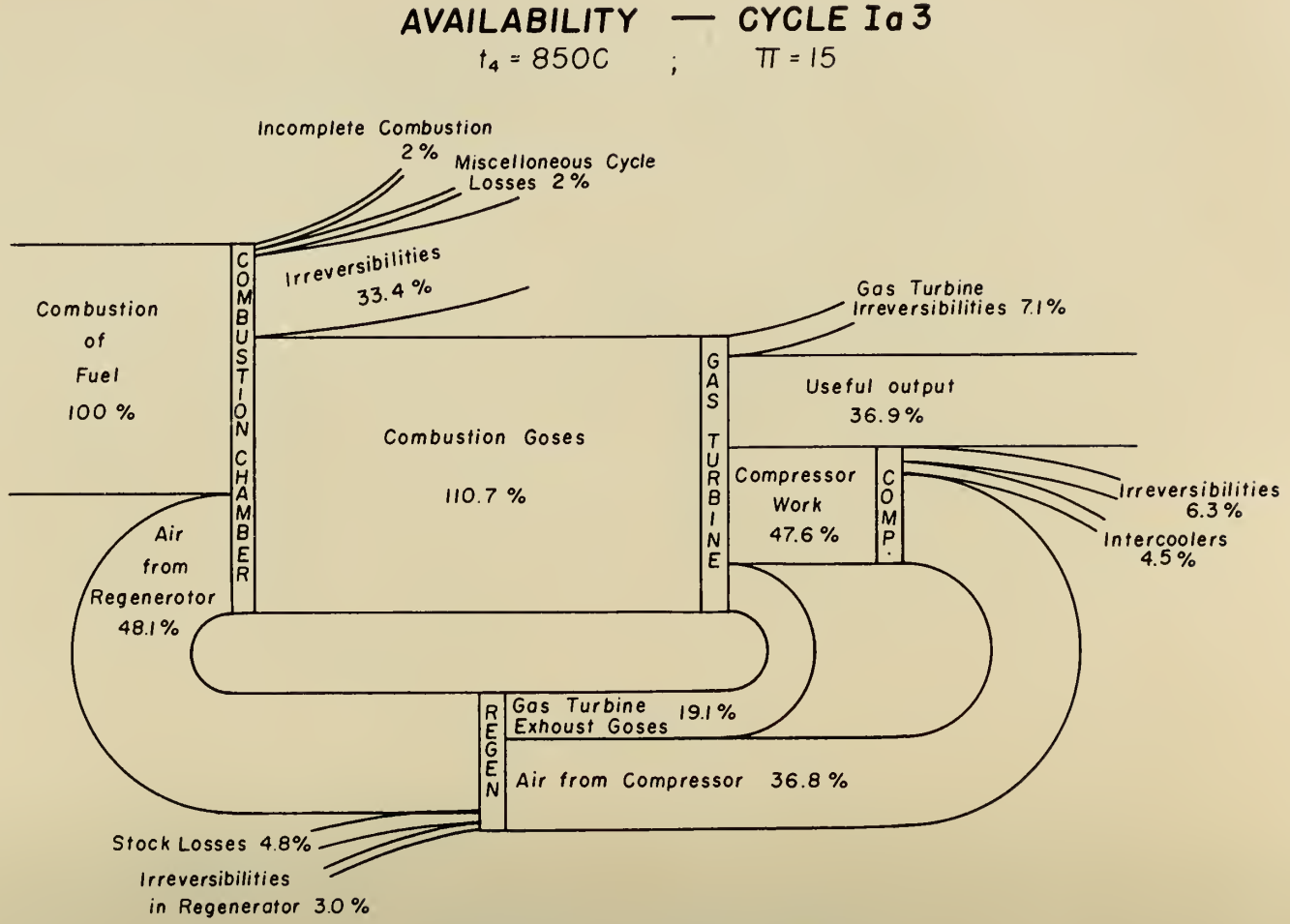

Fig. 42. Cycle Ia 3 availability diagram.

AVAILABILITY — CYCLE II

$t_4 = 1000$ $\pi = 10$

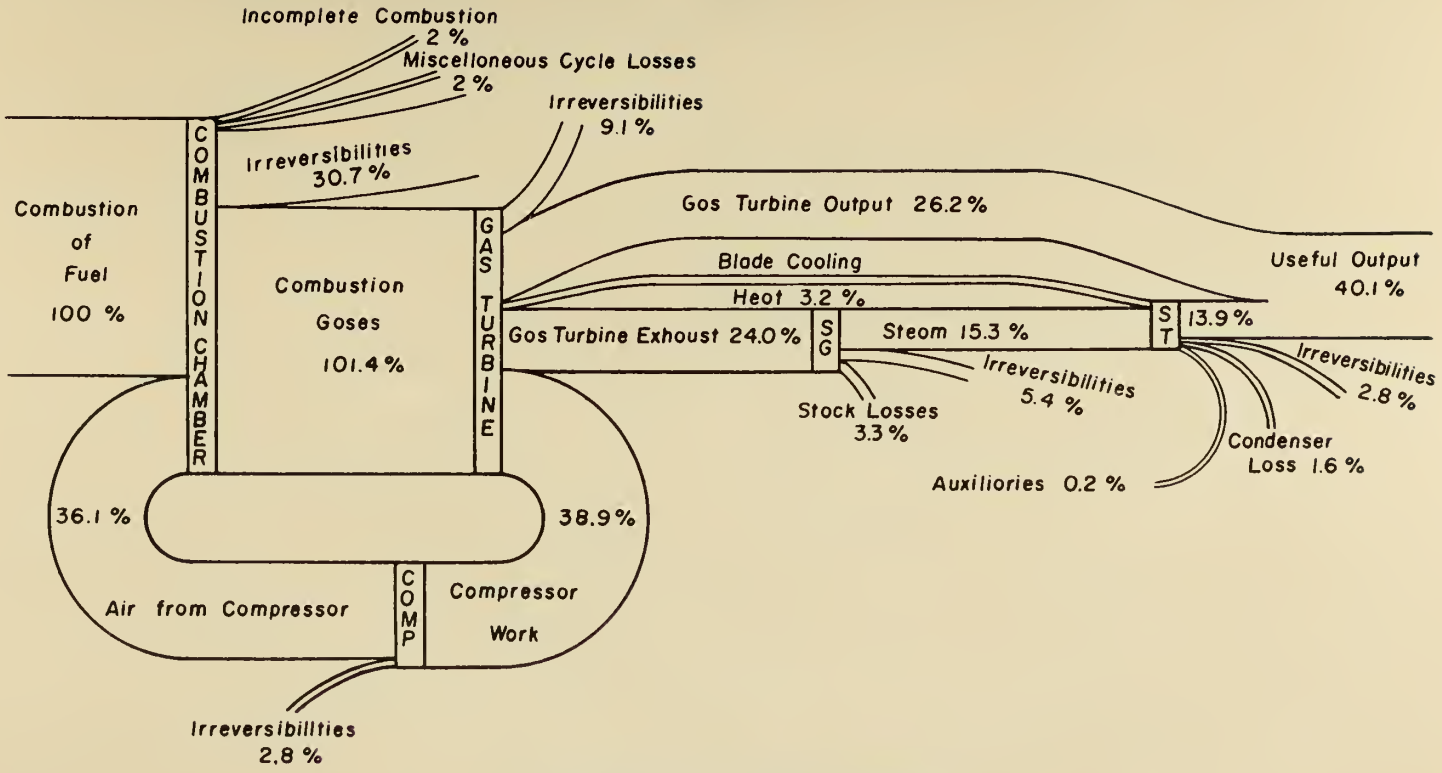

Fig. 43. Cycle II availability diagram.

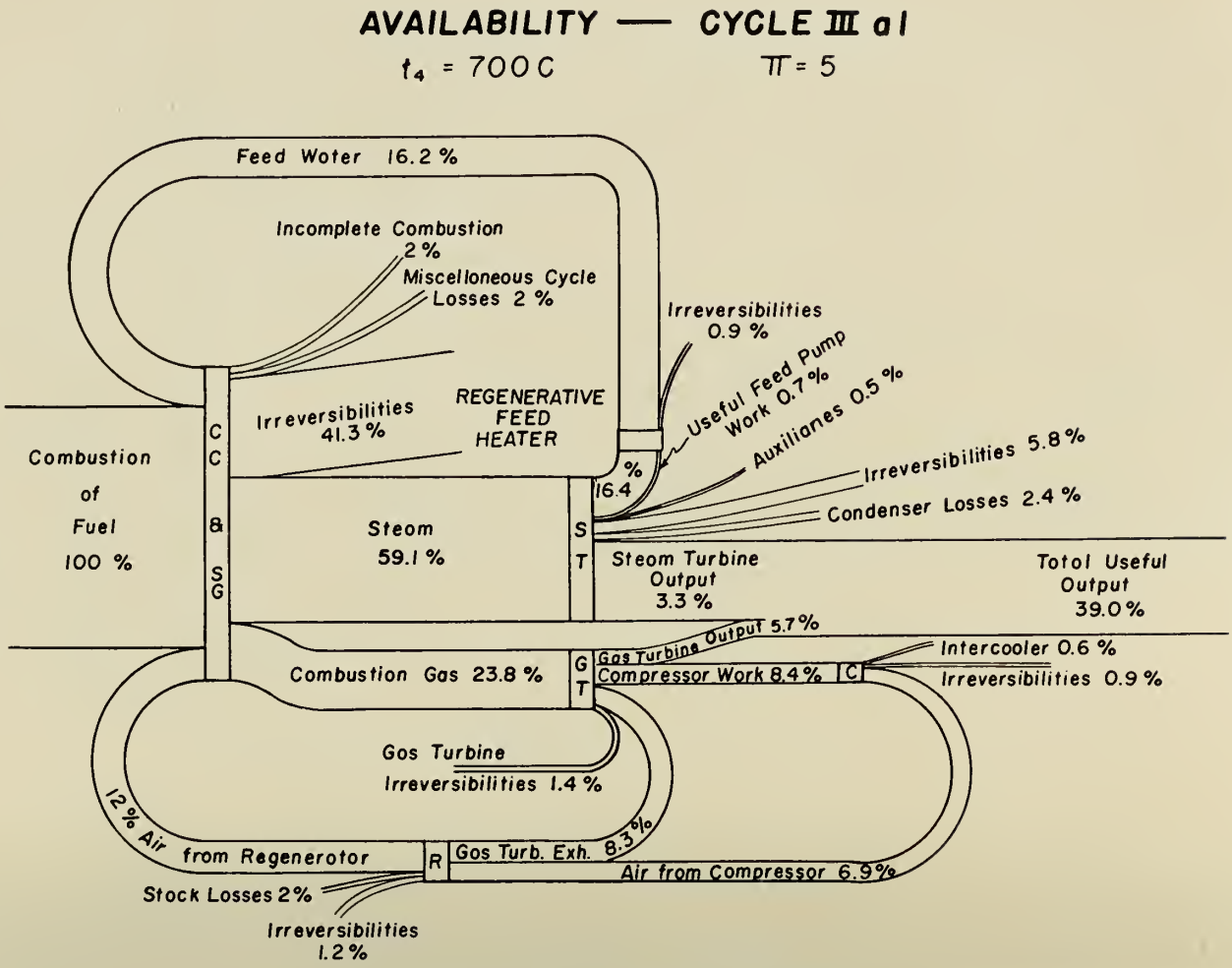

Fig. 44. Cycle IIIa1 availability diagram.

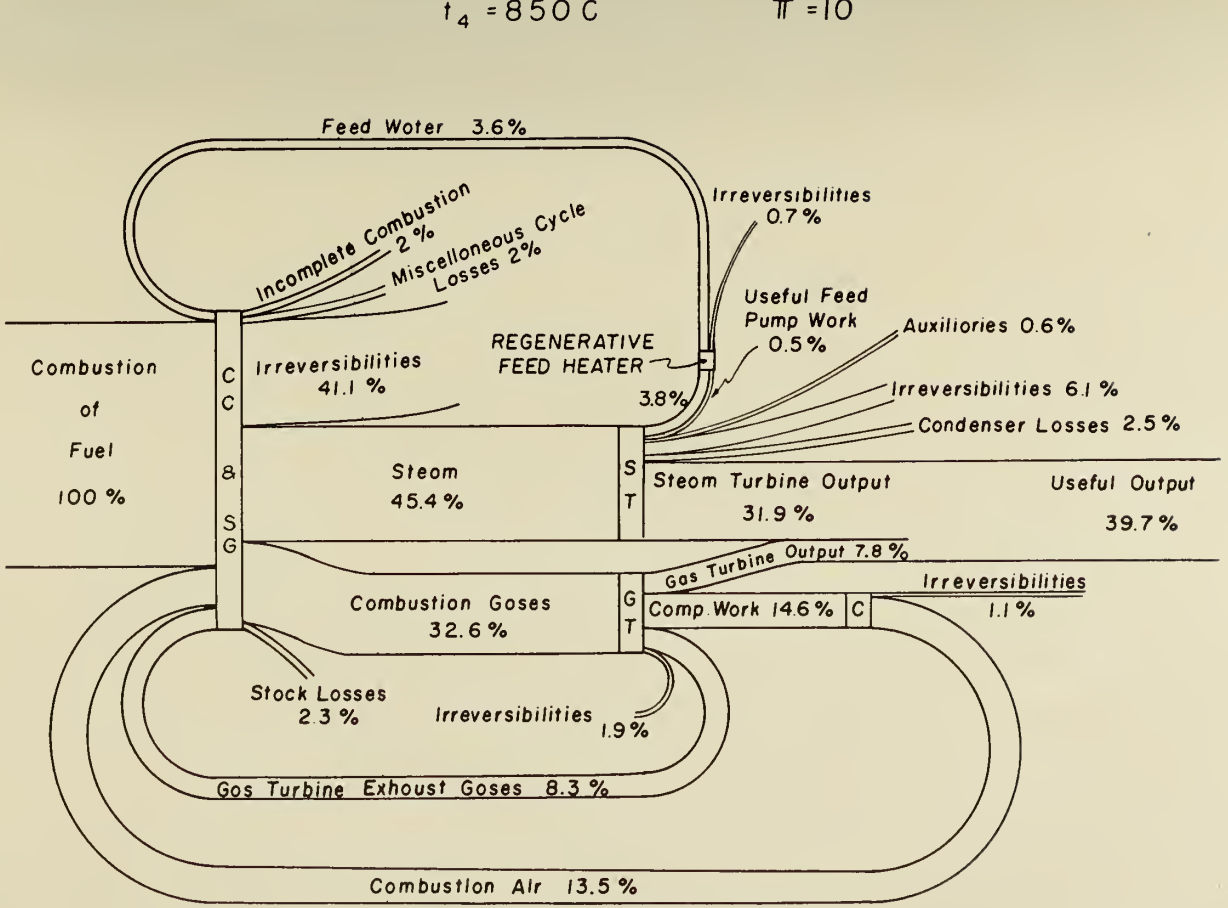

Fig. 45. Cycle IV availability diagram.

in overall cycle efficiency. This is illustrated by the numerically calculated efficiency curves for cycle IIIa, figure 35.

Cycles II, IIa, IV and IVa each have a waste heat steam generator as the final element; and the stack temperature is little affected by intercooling in the compressor. Intercooling has little effect on the exhaust gas temperature of cycle III as well, which has no heat recovery apparatus following the gas turbine. It does, however, reduce the mean temperature at which heat is supplied to each of these cycles. For these cycles the losses due to intercooling are therefore greater than the gains, as evidenced by the curves of figures 32, 33, 34, 36 and 37. (The one exception is cycle IVa for $t_4 = 700$ C, wherein $t_6 < t_f$ under most conditions — thereby obviating the waste heat portion of the steam generator and making the cycle identical to cycle IIIa for these conditions.)

The question sometimes arises as to the possible advantage to be gained in preheating the steam cycle feedwater by circulating it as a coolant in the compressor intercoolers, in lieu of all or part of the normal feedwater preheating by the use of bled steam from the steam turbine. This would result in increasing the heat supplied to the steam cycle, and also in increasing the specific work output. The gain can be estimated by calculating the maximum possible rise in feedwater temperature if circulated as cooling water in the intercoolers, and by calculating the additional work produced in the steam turbine by the steam that would otherwise have been bled for regenerative feed heating to produce this same rise in feedwater temperature.

From the previous cycle calculations, the mass flow ratio M and the state of each working fluid throughout a given cycle have already been determined. Assuming that the temperature difference between air and coolant in the intercooler must nowhere be less than 15 C, the maximum practicable temperature rise of the feedwater in the intercooler is calculated. This corresponds to a certain fractional rise above hotwell enthalpy (χ). From the curves of figure 20 the saving in steam turbine work can be estimated.

No other steam cycle characteristics are affected, since the total feedwater preheating remains unchanged. The only change has been to substitute the compressor intercoolers for one or more of the feedwater heaters nearest the condenser.

It is in no case possible to recover the entire heat of intercooling. The condensate leaves the condenser at a temperature higher than that of the outside cooling water, which is at sink temperature. If we maintain a minimum temperature difference of 15 C between air and coolant in the intercooler, only part of the cooling can be accomplished by the condensate, and it will always be necessary to accomplish the final heat removal by a separate cooling coil supplied with outside cooling water.

Since the specific heat of water is about four times that of air, the mass

flow ratio M must be greater than 4 to obtain a terminal feedwater temperature exactly 15 C lower than that of the hot air entering the intercooler. For $M < 4$, and a single intercooler, this terminal feedwater temperature will be correspondingly lower. For multiple intercoolers the feedwater will enter each succeeding intercooler at a higher temperature, and will extract proportionately less heat from the compressed air. All these factors must be considered in the calculations.

Figures 32 and 33 illustrate that cycles II and IIa operate more efficiently without intercoolers, if the heat removed from the compressed air in the intercoolers is discarded. To determine possible gains by preheating feedwater in the intercoolers, the procedure is therefore to calculate the possible improvements from this source in cycles II 1 and IIa 1, and compare the efficiencies of the thereby improved intercooled cycles with the previously calculated results for the non-intercooled cycles.

The numerical calculations reveal that utilization of the heat of intercooling results in very little improvement in efficiency for cycles II 1 and IIa 1. The steam turbine work is only a fraction of the total useful work of the combined cycle in these cases (on the order of 20% to 30% — see figure 40); and any improvement in steam cycle efficiency has but small effect on overall efficiency. As a result, the non-intercooled cycles are considerably more efficient. Intercooling does improve the gas turbine specific work, however.

Specifically, the intercooled cycles with heat recovery in the intercoolers show about a 20% gain in specific work at the cost of about $2^1/_2$ efficiency points ($2^1/_2$%), in comparison with the non-intercooled cycles.

In cycle III the gain due to heat recovery from a single intercooler just about equals the loss in overall cycle efficiency due to intercooling. Discounting the effects of the additional pressure drop occasioned by a larger than normal intercooler, there would be an overall efficiency gain of about one-third of one efficiency point (0.33%) at negligible change in specific work. For the high compressor pressure ratios involved, the main advantage in intercooling would lie in the simplification of the compressor design problems.

Use of two intercoolers results in an appreciable loss in efficiency.

In cycle IIIa use of a single intercooler with heat recovery yields a gain of about four-tenths of an efficiency point (0.44%) at a negligible loss in specific work compared with optimum efficiency condition without this feature. Results with two and three intercoolers yield negligible changes in both quantities.

Introduction of this feature in cycles IV and IVa results in slight losses in efficiency and negligible gains in specific work, compared with the non-intercooled cycles, except for cycle IVa at the lower gas turbine inlet temperatures. Under these conditions the exhaust gases from the regenerator are at such a low temperature that no waste heat portion of the steam generator is practicable; and the cycle becomes identical with cycle IIIa.

b) *Effect of regenerative feed heating*

Cycles II and IIa utilize only the waste heat steam generator as a source of heat supply to the steam cycle. The beneficial effect of regenerative feed heating for such a steam cycle is rather small, as discussed in paragraph VII.8. Further, the steam turbine furnishes only a fraction of the total cycle output. As a result, regenerative feed heating produces only a slight gain in overall cycle efficiency — less than half of one efficiency point (0.5%) at best. The effect on other cycle characteristics is negligible.

For cycles III and IIIa the available temperature differences are quite large, and the advantages of regenerative feed heating are unquestioned. The gain is about five efficiency points (5%) at maximum cycle efficiency. The efficiency curves of figures 34 and 35 are calculated with optimum practical regenerative feed heating (refer paragraph V.4).

For cycles IV and IVa the advantages of regenerative feed heating cannot be established without numerical investigation. Use of regenerative feed heating will result in higher stack temperatures; since, unlike the normal steam cycle's steam generator, these plants have no air preheater following the economiser. Thus it is possible that any improvement in steam cycle efficiency may be offset by a reduction in the amount of heat transferred to the steam cycle.

The cycles were cylculated with various amounts of regenerative feed heating, and the optimum values were chosen for the curves of figures 36 and 37. The gain averages two to two and a half efficiency points at maximum cycle efficiency. Maximum gain was usually with χ between 30% and 40%.

c) *Comparison of cycles*

Figures 38 and 39 illustrate that, even with high temperatures, the simpler gas turbine cycles do not approach the normal steam cycle in either efficiency or specific work. Adding the steam cycle to the gas turbine exhausts (cycles II and IIa) gives a superior efficiency only if the gas turbine can be designed for high initial temperatures. The specific work is higher than that of the gas turbine alone, but still not as high as that of the steam plant. Use of a regenerator in this cycle gives some improvement.

The remarkable feature of these cycles is the practicability of building very high efficiency plants for low power outputs. For example, use of cycle IIa with 850 C inlet temperature gas turbines makes it possible to build a 15,000 KW plant with an efficiency equal to that of the largest and most modern reheat steam plants — plants which must have output powers in excess of 100,000 KW to attain such an efficiency. Interpolating the data to estimate the possibilities with longer life 800 C inlet temperature gas turbines (many of which are in operation today), we find that a combined

cycle small power output plant, using inexpensive low pressure and low temperature steam generating equipment and steam turbine, will attain the same overall efficiency as an expensive high pressure, high temperature straight steam plant of necessarily much larger power output. This characteristic makes these cycles particularly attractive for such applications as small industrial plants, stationary power plants in remote areas, or commercial marine power plants.

Interestingly, if the steam generator is placed before the gas turbine, with no provision for utilizing the gas turbine exhaust heat (cycle III), the plant efficiency is practically unaffected by gas turbine inlet temperature. As pointed out in chapter VI, the steam generator for this cycle would be quite small in comparison with that of a normal steam plant, yet the efficiency and specific work are nearly as great. This should make this arrangement particularly attractive where a heavy premium is placed on space and weight considerations — as, for example, in a large naval power plant.

Only with cycles IIIa and IVa will a plant with a gas turbine inlet temperature of 700 C produce an efficiency greater than that of the normal steam plant. Since the steam generator operates with high gas side pressures and high temperature differences between gas and steam (or water), the combined plant would be less bulky than that of cycles II and IIa. Since the specific work is also quite high, this saving in bulk is further enhanced.

Cycle IV gives the same efficiencies at the higher gas turbine temperatures, with about the same size plant, as cycle IIIa. Cycle IVa gives slightly better efficiencies, at the cost of additional plant equipment.

The efficiency gains of cycles IIIa, IV and IVa over that of the normal steam cycle do not appear to be particularly great — no more than could be obtained, for example, by the simple addition of a stage of reheat to the straight steam cycle. It should be noted, however, that these are gains over the basic steam cycle used for comparison; and similar gains could be made above the reheat cycle efficiency, if that were used as the basic steam cycle. Further, a gain of even one or two efficiency points is an item of major importance in a very large power plant.

d) *Conclusions*

(1) The combined steam turbine-gas turbine power cycle has very attractive theoretical possibilities for high thermal efficiencies. When designed to practical equipment sizes, however, the efficiency advantages over normal cycles are, in general, rather modest.

(2) The outstanding advantage of the combined cycle is that efficiencies normally obtainable only in turbine plants of very high power outputs can also be realized in relatively low power output plants.

(3) One of the combined cycles can be used to produce plants of very

large power outputs and reasonably high efficiencies with low space and weight requirements — considerably lower than those of normal steam plants.

(4) Certain of the combined cycles, suitable for large central station generating plants, demonstrate small but important efficiency gains over straight steam plants for the same purpose.

(5) The combined cycle realizes its greatest advantages only when the maximum permissible gas turbine inlet temperature is considerably in excess of the maximum permissible steam temperature.

APPENDIX A

Derivation of Reheat Factor for a Cooled Turbine

A.1. "Perfect Vapor" Relationships

Within limits, the perfect gas relationships can be applied to certain processes involving real gases or vapors without undue loss of accuracy. These limits can be greatly extended by use of the similar "perfect vapor" relationships [48].

For a perfect vapor

$$p v = \omega R T \tag{a.1}$$

where ω is a function of p and T.

By definition, for an isentropic process,

$$p v^{\kappa} = \text{constant}. \tag{a.2}$$

Care must be taken to note that for a perfect vapor, $\kappa \neq c_p/c_v$; but rather, in accordance with the *Eichelberg* Law [7],

$$\kappa = \kappa_T \frac{c_p}{c_v} \tag{a.3}$$

where κ_T is the empirically determined exponent in the equation

$$p v^{\kappa_T} = \text{constant} \tag{a.4}$$

for an isothermal process.

For a perfect gas: $\omega = \kappa_T = 1$.

Differentiating (a.2) and dividing by $(\kappa - 1) v^{\kappa - 1}$

$$\frac{\kappa}{\kappa - 1} p\, d v + \frac{1}{\kappa - 1} v\, d p = 0$$

$$\frac{\kappa}{\kappa - 1} p\, d v + \frac{1}{\kappa - 1} v\, d p + v\, d p = v\, d p$$

$$\frac{\kappa}{\kappa - 1} (p\, d v + v\, d p) = \frac{\kappa}{\kappa - 1} d (p v) = v\, d p \tag{a.5}$$

By the first law of thermodynamics:

$$d q = d u + d L \tag{a.6}$$

For most processes involving a system of constant composition, we can represent total work by $dL = p\,dv$.

Therefore
$$dq = du + p\,dv = di - v\,dp. \tag{a.7}$$

For an adiabatic process, $dq = 0$, and
$$v\,dp = di_s \tag{a.8}$$

Substituting in (a.5)
$$\frac{\kappa}{\kappa - 1} d(pv) = di_s \tag{a.9}$$

or
$$i = \frac{\kappa}{\kappa - 1} pv + i^* \tag{a.10}$$

Selecting the zero reference such that $i^* \equiv 0$,
$$i = \frac{\kappa}{\kappa - 1} pv. \tag{a.11}$$

Combining with (a.1):
$$i = \frac{\kappa}{\kappa - 1} \omega RT \tag{a.12}$$

Therefore
$$T = \frac{\kappa - 1}{\kappa} \frac{i}{\omega R} \tag{a.13}$$

and
$$v = \frac{\kappa - 1}{\kappa} \frac{i}{p} \tag{a.14}$$

Applying the second law of thermodynamics to equation (a.7)
$$dq_{rev} = T\,ds = di - v\,dp \tag{a.15}$$

The foregoing were derived, in large part, by the use of isentropic processes between state points. T, i, p and v, however, are vapor (or gas) properties and are independent of the process used. With the restriction that κ and R be sufficiently constant for the region considered, these equations will thus be applicable in the general case for those real gases and vapors wherein ω is constant for constant s (i. e., ω is a function of the property s).

Experience data shows [48] that these conditions are quite well satisfied for air, for superheated steam, and also in narrow regions for carbon dioxide. Combustion gases, comprising principally nitrogen, excess air, superheated steam, and relatively small amounts of CO and CO_2, can be expected to show only slight variations from the perfect vaport laws. Therefore the below derivations are applicable to both steam and gas turbines.

A.2. The Cooled Turbine Stage

The following is principally an extension of [44] and [47].

Considering first a turbine with infinitesimally small stages, we can assume a polytropic process within each stage, and

$$\eta_{st} \approx \eta_p \tag{a.16}$$

The definition for the polytropic exponent n is

$$p v^n = \text{constant} \tag{a.17}$$

Operating as earlier with equation (a.2) we obtain

$$\frac{n}{n-1} d(pv) = v\,dp \tag{a.18}$$

Rearranging equation (a.9)

$$d(pv) = \frac{\kappa - 1}{\kappa} di \tag{a.9}$$

Whence

$$v\,dp = \frac{\kappa - 1}{\kappa} \frac{n}{n-1} di \tag{a.19}$$

$$v\,dp = di - dq_{rev} \tag{a.15}$$

$$1 - \frac{dq_{rev}}{di} = \frac{\kappa - 1}{\kappa} \frac{n}{n-1} \tag{a.20}$$

We can represent the polytropic process in our infinitesimal stage as a series of three reversible processes (referring to figure 46):

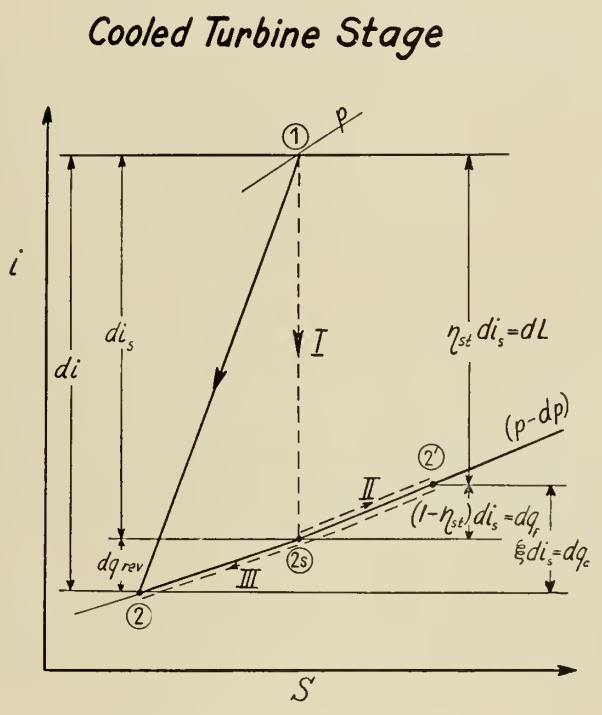

Fig. 46. Cooled turbine stage.

I — isentropic expansion from p to $(p - dp)$
II — reversible heat transfer to the working fluid of the friction energy, dq_f
III — reversible heat transfer from the working fluid of the heat of cooling, dq_c (for cooled turbine blading)

By the definition of the stage efficiency η_{st}, the internal work of the stage is (for infinitesimal stages)

$$dL_i = (\eta_{st})\, di_s = (\eta_p)\, di_s \tag{a.21}$$

and

$$dq_f = (1 - \eta_{st})\, di_s = (1 - \eta_p)\, di_s \tag{a.22}$$

Expressing the heat transferred in cooling the turbine (dq_c) in relation to the isentropic enthalpy drop, we define the cooling factor

$$\xi \equiv \frac{dq_c}{di_s} = \xi_p \tag{a.23}$$

or

$$dq_c = \xi_p\, di_s \tag{a.24}$$

Thus

$$dq_{rev} = dq_c - dq_f = (\eta_p + \xi_p - 1)\, di_s \tag{a.25}$$

From figure 46:

$$di = di_s + dq_{rev} = (\eta_p + \xi_p)\, di_s \tag{a.26}$$

Substituting in (a.20):

$$1 = \frac{dq_{rev}}{di} = 1 - \frac{(\eta_p + \xi_p - 1)\, di_s}{(\eta_p + \xi_p)\, di_s} = \frac{1}{\eta_p + \xi_p} = \frac{\kappa - 1}{\kappa}\,\frac{n}{n-1} \tag{a.27}$$

whence

$$\frac{n}{n-1} = \frac{\kappa}{\kappa - 1}\left(\frac{1}{\eta_p + \xi_p}\right) \tag{a.28}$$

or

$$n = \frac{\kappa}{\kappa - (\eta_p + \xi_p)(\kappa - 1)} \tag{a.29}$$

A.3. "Reheat" Factor for a Multistage Cooled Turbine

If the blade temperature is kept relatively constant throughout a cooled turbine, the heat transferred per stage will be largely controlled by the varying temperature difference between the working fluid and the blades. Such was the situation for the water-cooled turbine in chapter II. The calculations were thus carried through stage by stage, which automatically accounts for the "reheat" factor.

If, however, we have a turbine or section of turbine for which we can assume an average cooling loss factor ξ, which can be considered as remaining relatively constant from state to stage, we can develop a general formulation of the "reheat" factor. This will also hold for the uncooled turbine by merely setting $\xi = 0$.

Referring to figure 47, Δi_s is defined as the stage isentropic enthalpy drop, and Δi is defined as the actual enthalpy drop per stage. The overall turbine efficiency η_T is defined by the equation

$$\eta_T \equiv \frac{L}{(i_0 - i_{es})} = \frac{\Sigma(\eta_{st} \Delta i_s)}{(i_0 - i_{es})} \tag{a.30}$$

or, for constant η_{st},

$$\eta_T = \frac{\eta_{st} \Sigma \Delta i_s}{(i_0 - i_{es})} \tag{a.31}$$

whence the reheat factor

$$(1+\rho) \equiv \frac{\eta_T}{\eta_{st}} = \frac{\Sigma \Delta i_s}{(i_0 - i_{es})} \tag{a.32}$$

Following the same reasoning that led to equation (a.26) we have

$$\Delta i_s = \frac{\Delta i}{\eta_{st} + \xi} \tag{a.33}$$

From figure 47: $$\Sigma \Delta i = (i_0 - i_e) \tag{a.34}$$

Therefore $$\Sigma \Delta i_s = \frac{\Sigma \Delta i}{\eta_{st} + \xi} = \frac{i_0 - i_e}{\eta_{st} + \xi} \tag{a.35}$$

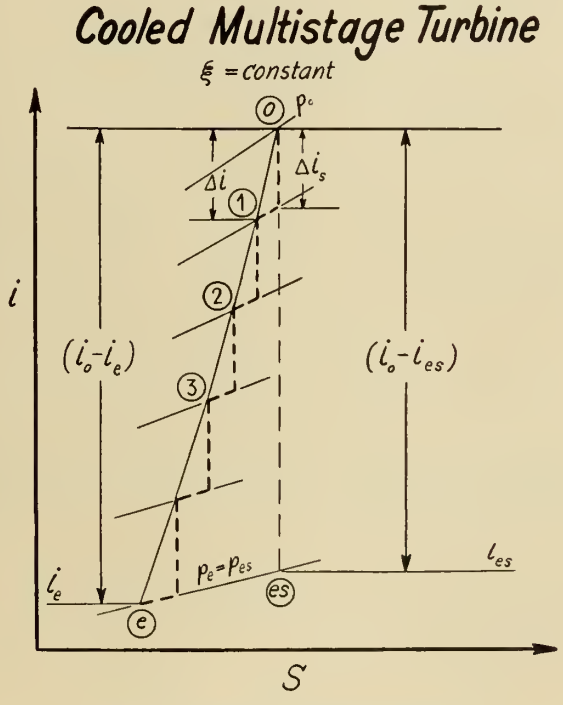

Fig. 47. Cooled multistage turbine.

From (a.11):

$$i_0 = \frac{\kappa}{\kappa - 1} p_0 v_0 \tag{a.36}$$

and

$$i_{es} = \frac{\kappa}{\kappa - 1} p_e v_{es} \tag{a.37}$$

For an isentropic process:

$$p v^{\kappa} = \text{constant} = p_0 v_0{}^{\kappa} = p_e v_{es}{}^{\kappa} \tag{a.38}$$

whence

$$v_{es} = \left(\frac{p_0}{p_e}\right)^{1/\kappa} v_0 \tag{a.39}$$

and

$$(i_0 - i_{es}) = \frac{\kappa}{\kappa - 1}\left[p_0 v_0 - p_e v_0 \left(\frac{p_0}{p_e}\right)^{1/\kappa}\right] \tag{a.40}$$

or

$$(i_0 - i_{es}) = \frac{\kappa}{\kappa - 1} p_0 v_0 \left[1 - \left(\frac{p_e}{p_0}\right)^{\frac{\kappa-1}{\kappa}}\right] \tag{a.41}$$

or setting $\frac{p_0}{p_e} \equiv \Pi$ (pressure ratio)

$$(i_0 - i_{es}) = \frac{\kappa}{\kappa - 1} p_0 v_0 \left[1 - \left(\frac{1}{\Pi}\right)^{\frac{\kappa-1}{\kappa}}\right] \tag{a.42}$$

For a polytropic process (i. e., number of stages $= \infty$ and $\eta_{st} = \eta_p$) by similar reasoning we obtain

$$(i_0 - i_e) = \frac{\kappa}{\kappa - 1} p_0 v_0 \left[1 - \left(\frac{1}{\Pi}\right)^{\frac{n-1}{n}}\right] \tag{a.43}$$

Substituting (a.43) in (a.35):

$$\Sigma \Delta i_s = \frac{1}{\eta_{st} + \xi} \frac{\kappa}{\kappa - 1} p_0 v_0 \left[1 - \left(\frac{1}{\Pi}\right)^{\frac{n-1}{n}}\right] \tag{a.44}$$

and finally combining with (a.32) and (a.42)

$$(1 + \rho)_{\infty, \Pi} = \frac{\Sigma \Delta i_s}{i_0 - i_{es}} = \frac{1}{\eta_{st} + \xi} \frac{\left[1 - \left(\frac{1}{\Pi}\right)^{\frac{n-1}{n}}\right]}{\left[1 - \left(\frac{1}{\Pi}\right)^{\frac{\kappa-1}{\kappa}}\right]} \tag{a.45}$$

Now let us consider a turbine with a finite number (z) of stages, all of equal pressure ratio (Π_{st}). Then

$$\Pi = (\Pi_{st})^z \tag{a.46}$$

For the first stage, by reasoning similar to that used in the derivation of equation (a.42):

$$(\Delta i_s)_1 = \frac{\kappa}{\kappa - 1} p_0 v_0 \left[1 - \left(\frac{1}{\Pi_{st}}\right)^{\frac{\kappa-1}{\kappa}}\right] \tag{a.47}$$

For the second stage:

$$(\Delta i_s)_2 = \frac{\kappa}{\kappa - 1} p_1 v_1 \left[1 - \left(\frac{1}{\Pi_{st}}\right)^{\frac{\kappa-1}{\kappa}}\right] \tag{a.48}$$

For the zth stage:

$$(\Delta i_s)_z = \frac{\kappa}{\kappa - 1} p_{z-1} v_{z-1} \left[1 - \left(\frac{1}{\Pi_{st}}\right)^{\frac{\kappa-1}{\kappa}}\right] \tag{a.49}$$

whence

$$\sum_1^z \Delta i_s = \frac{\kappa}{\kappa - 1} [p_0 v_0 + p_1 v_1 + p_2 v_2 + \cdots + p_{z-1} v_{z-1}] \left[1 - \left(\frac{1}{\Pi_{st}}\right)^{\frac{\kappa-1}{\kappa}}\right] \tag{a.50}$$

For the polytropic process within the stage:

$$p_0 {v_0}^n = p_1 {v_1}^n \tag{a.51}$$

or

$$p_1 v_1 = p_0 v_0 \left(\frac{p_1}{p_0}\right)^{\frac{n-1}{n}} = p_0 v_0 \left(\frac{1}{\Pi_{st}}\right)^{\frac{n-1}{n}} \tag{a.52}$$

similarly

$$p_2 v_2 = p_1 v_1 \left(\frac{1}{\Pi_{st}}\right)^{\frac{n-1}{n}} = p_0 v_0 \left(\frac{1}{\Pi_{st}}\right)^{2\frac{n-1}{n}} \tag{a.53}$$

and

$$p_{z-1} v_{z-1} = p_0 v_0 \left(\frac{1}{\Pi_{st}}\right)^{(z-1)\frac{n-1}{n}} \tag{a.54}$$

The formula for the sum of a geometric series [18]:

$$1 + x + x^2 + x^3 + \cdots + x^{z-1} = \frac{1 - x^z}{1 - x} \tag{a.55}$$

Thus $p_0 v_0 + p_1 v_1 + p_2 v_2 + \ldots p_{z-1} v_{z-1} =$

$$p_0 v_0 \left[1 + \left(\frac{1}{\Pi_{st}}\right)^{\frac{n-1}{n}} + \left(\frac{1}{\Pi_{st}}\right)^{2\frac{n-1}{n}} + \cdots + \left(\frac{1}{\Pi_{st}}\right)^{(z-1)\frac{n-1}{n}}\right] = p_0 v_0 \frac{\left[1 - \left(\frac{1}{\Pi_{st}}\right)^{z\frac{n-1}{n}}\right]}{\left[1 - \left(\frac{1}{\Pi_{st}}\right)^{\frac{n-1}{n}}\right]} \tag{a.56}$$

Substituting in (a.50) and remembering (a.46) that $\Pi = (\Pi_{st})^z$

$$\Sigma \Delta i_s = \frac{\kappa}{\kappa - 1} p_0 v_0 \frac{\left[1 - \left(\frac{1}{\Pi}\right)^{\frac{n-1}{n}}\right]}{\left[\frac{1 - \left(\frac{1}{\Pi_{st}}\right)^{\frac{n-1}{n}}}{1 - \left(\frac{1}{\Pi_{st}}\right)^{\frac{\kappa-1}{\kappa}}}\right]} \tag{a.57}$$

Combining with the definition of the reheat factor (a.32) and with equation (a.42):

$$(1+\rho)_{z,\Pi} = \frac{\left[\dfrac{1-\left(\dfrac{1}{\Pi}\right)^{\frac{n-1}{n}}}{1-\left(\dfrac{1}{\Pi}\right)^{\frac{\kappa-1}{\kappa}}}\right]}{\left[\dfrac{1-\left(\dfrac{1}{\Pi_{st}}\right)^{\frac{n-1}{n}}}{1-\left(\dfrac{1}{\Pi_{st}}\right)^{\frac{\kappa-1}{\kappa}}}\right]} \tag{a.58}$$

Finally comparing with (a.45) we find that

$$(1+\rho)_{z,\Pi} = \frac{(1+\rho)_{\infty,\Pi}}{(1+\rho)_{\infty,\Pi_{st}}} \tag{a.59}$$

APPENDIX B

Symbols

(The dimensions of each quantity are in parentheses following its definition. For dimensional system used, and symbols therefor, see paragraph I.3.)

A	Available enthalpy (kj)
B	Ratio of steam turbine work with bleeding to turbine work without bleeding (dimensionless)
C	Specific working fluid velocity, absolute, in turbine blading (dimensionless) Also degrees Centigrade (C)
D	Tube diameter (m)
F	Heat transfer area (m^2)
G	Maximum gain obtainable by regenerative preheating of feedwater in steam cycle (dimensionless)
H	Steam cycle auxiliary power (dimensionless)
I	Enthalpy (kj)
K	Degrees Kelvin (K)
L	Specific work (kj/kg)
L_i	Internal work (kj/kg)
L_n or L_N	Net useful work (kj/kg)

M	Ratio of gas flow to water flow in steam generator (dimensionless)
N	Power (KW = kj/sec)
Nu	Nusselt number $\equiv h D/\lambda$ (dimensionless)
P	Percent of G obtainable by partial feedwater preheating in a finite number of heaters (dimensionless)
$Pè$	Pèclet number $\equiv Re\ Pr$ (dimensionless)
Pr	Prandtl number $\equiv c_p \mu/\lambda$ (dimensionless)
Q	Heat (kj)
R	Gas constant (m^2/sec^2 C)
Re	Reynolds number $= D w \gamma/\mu$ (dimensionless)
S	Entropy (kj/C)
T	Absolute temperature (K)
W	Specific working fluid velocity, relative, in turbine blading (dimensionless)
X	Steam quality (dimensionless)
a	Specific available enthalpy (kj/kg)
b	Blade chord (m)
c	Working fluid velocity, absolute, in turbine blading (m/sec)
c_p	Specific heat at constant pressure (kj/kg C)
c_v	Specific heat at constant volume (kj/kg C)
d	Differential increment
f	Cross-sectional flow area (m^2)
h	Heat transfer coefficient (kj/m^2 C sec)
i	Specific enthalpy (kj/kg)
k	Overall heat transmission coefficient (kj/m^2 C sec)
l	Length (m)
m	Mass (kg) Also symbol for meter (m)
n	Polytropic exponent (dimensionless)
p	Pressure (kg/m sec^2, or ata — atmospheres, absolute)
q	Heat per unit mass (kj/kg)
r_k	Kinematic reaction (dimensionless)
s	Tube spacing, in diameters (dimensionless)
t	Temperature, Centigrade (C) Also specific entropy (kj/kg C
u	Wheel speed (m/sec)
v	Specific volume (m^3/kg)
w	Fluid velocity, relative (m/sec)
x	Percentage of combustion gas which consists of stoichiometric combustion products (dimensionless)
z	Number of tube rows or turbine stages (dimensionless)

Δ Increment in the quantity whose symbol follows

$\overline{\Delta t}$ Logarithmic mean temperature difference, $\frac{\Delta t_2 - \Delta t_1}{\ln \frac{\Delta t_1}{\Delta t_2}}$ (C)

Θ Temperature ratio, $\frac{t_1 - t_2}{\overline{\Delta t}}$ (dimensionless)

Λ $\frac{\mu^{0.39}}{\mathrm{Pr}^{0.68}\, T^{0.61}}$ (dimensionless)

Π Pressure ratio (dimensionless)

Σ Summation

Υ Ratio of blade perimeter to blade chord (dimensionless)

χ Fractional rise above hotwell enthalpy (dimensionless)

Ψ_e $1 - \left(\frac{1}{\Pi}\right)^{\frac{\kappa-1}{\kappa}}$ (dimensionless)

Ψ_K $\left(\frac{1}{\Pi}\right)^{\frac{\kappa-1}{\kappa}} - 1$ (dimensionless)

Ω $\Upsilon\left(\frac{b}{\tau} + \frac{b}{l}\sin\alpha_1\right) + 2\frac{\delta_a}{l}$ (dimensionless)

α Turbine working fluid absolute velocity direction, measured from axial (degrees)

β Turbine working fluid relative velocity direction, measured from axial (degrees)

γ Density (kg/m^3)

δ_a Axial clearance between turbine blade rows (m)

ϵ Ratio, gas side heat transfer coefficient to overall heat transmission coefficient (dimensionless)

ζ Friction factor in tube banks (dimensionless)
Loss coefficient (dimensionless)

η Efficiency (dimensionless)

ϑ Tube thickness (m)

κ Isentropic exponent (dimensionless)

λ Heat conductivity (kj/m C sec)

μ Viscosity (kg/m sec)

ν Turbine velocity ratio (dimensionless)

ξ Cooling loss factor (dimensionless)

π 3.14159

ρ Reheat number (dimensionless)

σ Tube bank arrangement factor (dimensionless)

τ Blade spacing (m)

ω Function of p and T in perfect vapor relationships (dimensionless)

APPENDIX C

References

Abbreviations:

ASME	= American Society of Mechanical Engineers
Inst Mech Engrs	= Institution of Mechanical Engineers, London
NACA	= National Advisory Committee on Aeronautics (USA)
p	= pages
Proc	= Proceedings
Trans	= Transactions
ZVDI	= Zeitschrift des Vereins Deutscher Ingenieure

The date of publication is in parentheses. The volume number of a periodical precedes the date; the issue number follows the date.

[1] *Atomic Energy Commission — Department of the Navy* — "Liquid Metals Handbook" Second edition, U. S. Government Printing Office, Washington, D. C. (June 1952).

[2] *Brown, T. W. F.* — "The Effect of the Radiation Correction on Cooling Loss in High-temperature Cooled Gas Turbines" Inst Mech Engrs — ASME General Discussion on Heat Transfer, London (11—13 Sept 1951), p 431—3, 466—7.

[3] *Buckland, B. O. and Berkey, D. C.* — "Design Features of a 5000 HP Gas Turbine" ASME Paper 51-A-113 (Nov 1951).

[4] *Cohen, H. and Bayley, F. J.* — "Heat Transfer Problems of Liquid-Cooled Gas-Turbine Blades" The Chartered Mechanical Engineer 2 (1955) 6, p 289—91.

[5] *Dollin, F.* — "Development of the Steam Turbine" The Engineer 198 (1954), p 623—8.

[6] *Dubbels, H.* — "Taschenbuch für den Maschinenbau" 11th edition, Volume II; Springer-Verlag, Berlin/Göttingen/Heidelberg (1953).

[7] *Eichelberg, C.* — "Die thermischen Eigenschaften des Wasserdampfes im technisch wichtigen Gebiet" Forschungsarbeiten auf dem Gebiete des Ingenieurwesens 220 (1920).

[8] *Ellerbrock, H. H., Jr.* — "Some NACA Investigations of Heat Transfer of Cooled Gas Turbine Blades" Inst Mech Engrs — ASME General Discussion on Heat Transfer, London (11—13 Sept 1951), p 410—20.

[9] *Elston, C. W. and Knowlton, P. H.* — "Comparative Efficiencies of Central Station Reheat and Nonreheat Steam Turbine-Generator Sets" Trans ASME 74 (1952), p 1389—99.

[10] *Erythropel, H.* — "Neue Wasserdampftafel bis 700 C" ZVDI 94 (1952) 31, p 1001—4.

[11] *Foster Wheeler Corporation* — Personal Communication (31 Jan 1955).

[12] *Gouy, M.* — "Sur les transformations et l'équilibre en thermodynamique" Comptes rendus de l'Académie des sciences (1889), p 507—9.

[13] *Grimison, E. D.* — "Correlation and Utilization of New Data on Flow Resistance and Heat Transfer for Cross Flow of Gases over Tube Banks" Trans ASME 59 (1937), p 583—94.

[14] *Gumz, W.* — "Brennstoffschwefel und Rauchgastaupunkt" Brennstoff, Wärme, Kraft 5 (1954) 8, p 264—9.

[15] *Hofmann, E.* — "Bestimmung der Wärmeübergangs und Druckverlustes in Rohren und an Rohrbündeln" ZVDI 84 (1940), p 759—60.

[16] *Hofmann, E.* — "Wärmeübergang und Druckverlust bei Querströmung durch Rohrbündel" ZVDI 84 (1940) 6, p 97—101.
[17] *Huge, E. C.* and *Piotter, E, C.* — "The Use of Additives for the Prevention of Low Temperature Corrosion in Oil-Fired Steam-Generating Units" Trans ASME 77 (1955) p 267—78.
[18] *Hütte* — "Des Ingenieurs Taschenbuch" 28th edition, Volume I, W. Ernst & Sohn, Berlin (1955).
[19] *Hütte* — "Des Ingenieurs Taschenbuch" 28th edition, Volume IIA, W. Ernst & Sohn, Berlin (1955).
[20] *Johnstone, H. F.* — "The Corrosion of Power Plant Equipment by Flue Gases" University of Illinois Engineering Experiment Station Bulletin No. 228 (June 1931).
[21] *Karlsson, H. and Hammond, W. E.* — "Air Preheater Design as Affected by Fuel Characteristics" Trans ASME 75 (1953), p 711—22.
[22] *Keenan, J. H.* — "Thermodynamics" John Wiley & Sons, New York, and Chapman & Hill, Ltd., London (1941).
[23] *Keenan, J. H. and Kaye, J.* — "Gas Tables" John Wiley & Sons, Inc., N. Y. (1948).
[24] *Keenan, J. H. and Keyes, F. C.* — "Thermodynamic Properties of Steam" John Wiley & Sons, Inc., N. Y. (1936).
[25] *Koch, W. and Schmidt, E.* — "VDI Wasserdampftafeln" Springer-Verlag, Berlin/Göttingen/Heidelberg (1952).
[26] *Labberton, J. M. and Marks, L. S.* — "Marine Engineers Handbook" McGraw-Hill Book Co., Inc., New York and London (1945).
[27] *McAdams, W. H.* — "Heat Transmission" McGraw-Hill Book Co., Inc., New York and London (1942).
[28] *Meyer, G. L.* — "Determination of Average Heat Transfer Coefficients for a Cascade of Symmetrical Impulse Turbine Blades: I. Heat Transfer from Blades to Cold Air" NACA Research Memorandum No. E8H12 (Nov 1948).
[29] *Mordell, D. L.* — "The Exhaust-Heated Gas-Turbine Cycle" Trans ASME 72 (1950), p 323—9.
[30] *Morosoff, D.* — "Gas Turbine-Steam Turbine for Ship Propulsion" Marine Engineering and Shipping Review 55 (1950), p 40—47; also Teknisk Tidskrift 21 (1949).
[31] *Mouravieff, M.* — "Mixed Gas and Steam Cycles for Power Generation" Revue Electricité et Mécanique, Alsthom (Apr-Jun 1948).
[32] *Profos, P.* — Personal Communication (31 Jan 1955).
[33] *Reeman, J., Buswell, R. W. A. and Ainley, D. G.* — "An Experimental Single Stage Air Cooled Turbine" Proc Inst Mech Engrs 167 (1953), p 341—70.
[34] *Reese, H. R. and Carlson, J. R.* — "Thermal Performance of Modern Turbines" Mechanical Engineering 74 (1952), p 205—11.
[35] *Rohsenow, W. M. and Bradley, C. H., Jr.* — "Combined Steam and Gas-Turbine Processes" ASME Paper No. 50-F-23 (1950).
[36] *Rothemich, E. F. and Parmikian, G.* — "Tubular Air Heater Problems" Trans ASME 75 (1953), p 723—28.
[37] *Salisbury, J. K.* — "The Steam-Turbine Regenerative Cycle — An Analytical Approach" Trans ASME 64 (1942), p 231—45.
[38] *Schack, A.* — "Der industrielle Wärmeübergang" 4th edition, Verlag Stahleisen m. b. H. Düsseldorf (1953).
[39] *Schäff, K.* — "Entwicklungen und Erfahrungen beim Bau von Dampfkraftwerken" ZVDI 98 (1956), p 1—9.
[40] *Schmidt, E. H. W.* — "Heat Transmission by Natural Convection at High Centrifugal Acceleration in Watercooled Gas Turbine Blades" Inst Mech Engrs — ASME

General Discussion on Heat Transfer, London (11—13 Sept 1951), p 361—3, 378—83, 388.

[41] *Short, B. E.* — "A Review of Heat Transfer Coefficients and Friction Factors for Tubular Heat Exchangers" Trans ASME 64 (1942), p 779—85.

[42] *Smith, A. G.* — "Heat Flow in the Gas Turbine" Proc Inst Mech Engrs 159 (1948), p 245—54.

[43] *Smith, A. G. and Pearson, R. D.* — "The Cooled Gas Turbine" Proc Inst Mech Engrs 163 (1950), p 221—34.

[44] *Soderberg, C. R.* — "Gas Turbines" Lectures, Massachusetts Institute of Technology (1947/1948).

[45] *Stodola, A.* — "Dampf- und Gasturbinen" 6th edition, Springer-Verlag, Berlin/Göttingen/Heidelberg (1925).

[46] *Traupel, W.* — "Ähnlichkeitstheorie der Wärmeaustauschapparate" Technische Rundschau Sulzer (1944), p 1—4.

[47] *Traupel, W.* — "Thermische Turbomaschinen" Lectures, Eidgenössische Technische Hochschule, Zürich (1954/1955).

[48] *Traupel, W.* — "Zur Dynamik realer Gase" Forschung 18 (1952) 1, p 3—9.

[49] *Ulsamer, J.* — "Die Wärmeabgabe eines Drahtes oder Rohres an einen senkrecht zur Achse strömenden Gas- oder Flüssigkeitsstrom" Forschung auf dem Gebiet des Ingenieurwesens 3 (1932), p 94—8.

[50] *Waeselynck, R.* — "L'Alliance de la Turbine à Gaz et de la Machine à Vapeur" Association Technique, Maritime et Aéronautique, Bulletin (1949), p 681—727.

[51] *Warren, C. B. and Knowlton, P. H.* — "Relative Engine Efficiencies Realizable from Large Modern Steam-Turbine Generator Units" Trans ASME 63 (1941)

Zusammenfassung

Beim Gasturbinen-Prozeß erfolgen die Wärmezufuhr und die Wärmeabgabe im allgemeinen bei hohen mittleren Temperaturen. Für den Dampfturbinen-Prozeß liegen die entsprechenden mittleren Temperaturen bedeutend niedriger. Eine Kombination dieser beiden Einzelprozesse ergibt einen Prozeß mit Wärmezufuhr bei hoher mittlerer Temperatur und Wärmeabgabe bei einer Temperatur wenig oberhalb der Umgebungstemperatur. Für diesen kombinierten Prozeß ergibt sich daher theoretisch die Möglichkeit, einen höheren Wirkungsgrad zu erreichen, als dies für die beiden Einzelprozesse allein möglich wäre. Bis zu welchem Grade diese Wirkungsgrad-Verbesserung in praktisch auszuführenden Anlagen verwirklicht werden könnte, kann nur durch eine sorgfältige, eingehende Untersuchung über die Einflüsse der Irreversibilitäten der zueinander in vernünftigem Größenverhältnis ausgelegten Einzelprozesse bestimmt werden.

Die Charakteristiken der Einzelprozesse werden durch detaillierte Untersuchungen ermittelt. Es wird eine Methode entwickelt zur Berechnung des Einflusses der Wasserkühlung in Gasturbinen hoher Temperatur. Für eine Standardreihe von Dampfturbinen werden die Charakteristiken berechnet. Für den Wärmeübergang in Dampferzeugern werden allgemeine Beziehungen entwickelt, welche in einer neuartigen Methode zur Analyse von Abwärme-Dampfprozessen verwendet werden. Die Einzelprozesse werden in verschiedenen Schaltungen miteinander kombiniert und die resultierenden Prozeß-Charakteristiken berechnet.

Obgleich der Wirkungsgrad-Gewinn von richtig ausgelegten Anlagen mit kombiniertem Prozeß gegenüber konventionellen Anlagen bestenfalls nur bescheiden ist, weist doch jeder der kombinierten Prozesse wichtige Vorteile auf. Wird ein Gasturbinen-Prozeß mit einem Niederdruck-Dampfprozeß ergänzt, der die Abwärme des Gasturbinen-Prozesses ausnützt, so ist mit einem kombinierten Prozeß relativ kleiner Leistung (10 000 kW bis 20 000 kW) derselbe Wirkungsgrad erreichbar, wie mit einer sehr großen (100 000 kW) Dampfturbinen-Anlage mit Zwischenüberhitzung.

Der Einbau von Verdampfer- und Überhitzerrohren in den Brennraum der Gasturbine ermöglicht eine äußerst kompakte Anlage hoher Leistung, deren Wirkungsgrad nur wenig tiefer liegt als derjenige einer sehr großen Dampfkraftanlage üblicher Bauart. Werden in den Abgasstrom der Gasturbine einer solchen Anlage Wärmeaustausch-Apparate eingeschaltet, so nimmt wohl die Größe der Anlage zu, aber zugleich wird ein wesentlicher Wirkungsgrad-Gewinn seitens des Dampfprozesses erreicht.

Abriß des Lebens- und Bildungsganges

Am 11. Februar 1919 wurde ich in Omaha, Nebraska, U.S.A., geboren. Dort habe ich die Primar- und Sekundarschulen besucht, und in 1938 bin ich in die U. S. Naval Academy, Annapolis, Maryland, U.S.A., eingetreten. Am Ende dieser Studien, im Dezember 1941, habe ich den Grad eines „Bachelor of Science" und ein Offizierspatent in der U. S. Navy erworben.

Während des zweiten Weltkrieges tat ich zuerst zweieinhalb Jahre Dienst auf einem Zerstörer im Pazifik und später ein Jahr als elektrotechnischer Offizier eines Schlachtschiffes. Von 1945 bis 1948 habe ich Schiffbau- und Marineingenieurwesen an dem Massachusetts Institute of Technology in Cambridge, Massachusetts, U.S.A., studiert und meine Studien mit dem Grad eines „Master of Science" abgeschlossen. Zu dieser Zeit wurde ich zum Mitglied der Honorary Research Fraternity „Sigma XI" gewählt.

Von 1948 bis 1950 hatte ich verschiedene Dienstposten in der Kriegsmarinewerft in Mare Island, Kalifornien, U.S.A. Chef der Konstruktionsabteilung der Kriegsmarinewerft in San Francisco, U.S.A., war meine Stellung von 1950 bis Ende 1952. Anschließend habe ich meine Doktorarbeit an der Eidgenössischen Technischen Hochschule in Zürich begonnen.